

Searches for supersymmetric particles at the Tevatron collider

M. Carena

Fermi National Accelerator Laboratory, Batavia, Illinois 60510-0500

R. Culbertson and H. Frisch

Enrico Fermi Institute, Chicago, Illinois 60637

S. Eno

Department of Physics, University of Maryland, College Park, Maryland 20742

S. Mrenna

Department of Physics, University of California, Davis, Davis, California 95616

The authors review the status of searches for supersymmetric particles at the Tevatron collider. After discussing the theoretical aspects relevant to the production and decay of supersymmetric particles at the Tevatron, the authors present the current results for runs Ia and Ib as of the summer of 1997. [S0034-6861(99)00404-3]

CONTENTS

I. Introduction	937
II. The Minimal Supersymmetric Extension of the Standard Model	938
A. Sparticle spectrum	939
B. Supergravity	941
C. Gauge-mediated supersymmetry breaking	944
D. R -parity violation	944
E. Run Ia parameter sets	945
III. The CDF and $D\bar{O}$ detectors	946
A. The CDF detector	946
B. The $D\bar{O}$ detector	947
C. Experimental realities	948
IV. The Present Status of Sparticle Searches	948
A. Charginos, neutralinos, and tripletons	949
Tripletons	952
B. Squarks and gluinos	954
1. Jets + E_T	954
2. Dileptons + E_T	956
C. Top squarks	959
1. Direct top-squark pair production	960
2. Top-squark production from top decays	962
D. Sleptons	963
E. Charged Higgs bosons	964
F. Neutral Higgs bosons	966
G. R -parity violation and a short-lived lightest superpartner	967
H. R -parity violation and long-lived heavy charged sparticles	968
I. Photon and E_T signatures	968
1. An unexpected turn: The CDF $ee\gamma\gamma E_T$ event	968
2. Gauge-mediated low-energy SUSY breaking: Gravitino lightest superpartner	969
3. Higgsino lightest superpartner	969
4. Inclusive two-photons-and- E_T signatures	970
5. Single photon, heavy flavor, and E_T	972
J. Other anomalies: Top dilepton events	973
V. Conclusions	976
Acknowledgments	977
Appendix: Decay modes and signatures of supersymmetry	977

I. INTRODUCTION

The Tevatron is a one-kilometer-radius superconducting accelerator ring, located at the Fermi National Accelerator Laboratory (Fermilab), in Batavia, Illinois. The ring is used in two modes: as a source of high-energy beams for fixed-target experiments and, in conjunction with the Antiproton Source, as a proton-antiproton collider, operating with a $p\bar{p}$ center-of-mass energy of $\sqrt{s}=1.8$ TeV. The Tevatron collider has been the world's accelerator-based high-energy frontier since it first began taking data in 1987 and has thus been a prime location to search for the final pieces of the standard model (Glashow, 1961; Weinberg, 1967; Salam, 1968) and new phenomena beyond.

With the discovery of the top quark at the Tevatron (Abe *et al.*, 1994a, 1995a; Abachi *et al.*, 1995a), the standard-model particle spectrum is almost complete, with only the Higgs boson (and, arguably, the tau neutrino) lacking direct experimental confirmation. If the interactions of the leptons, quarks, and gauge bosons of the standard model remain perturbative up to very high energies (as appears to be the case from the measured running of the gauge couplings), then the mechanism responsible for electroweak symmetry breaking (EWSB) is expected to contain one or more fundamental scalar Higgs bosons that are light, i.e., with masses of the order of the symmetry-breaking scale.

The Higgs mechanism (Higgs, 1964, 1966; see also Englert and Brout, 1964; Guralnik *et al.*, 1964) plays a crucial role in the standard model. The neutral component of the Higgs boson acquires a vacuum expectation value to give mass to the W and Z gauge bosons as well as to the standard-model fermions. In addition, the couplings of the Higgs boson to the gauge bosons and fermions are such as to cancel the infinities in the electroweak radiative corrections and prevent unitarity violation in the longitudinal scattering of the gauge bosons. However, if the standard model is valid up to an energy cutoff of $\Lambda_{\text{cutoff}} \approx M_{\text{Planck}}$ ($M_{\text{Planck}} = 1.22 \times 10^{19}$ GeV), the model

has a fundamental problem, the so-called *naturalness problem* (Wilson, 1979; Maiani, 1980; 't Hooft, 1980; Veltman, 1981).

The radiative corrections to the Higgs-boson mass squared calculated in the standard model are quadratically divergent (proportional to $\Lambda_{\text{cutoff}}^2$). A physical Higgs mass of the order of the electroweak scale requires a cancellation of one part in 10^{16} between these radiative corrections, which come from the interactions of the Higgs bosons with all other particles in the theory and the bare Higgs mass at the Planck scale:

$$m_H^2 \approx m_H^2(\Lambda_{\text{cutoff}}) - \alpha \Lambda_{\text{cutoff}}^2. \quad (1)$$

Either there is an extreme “fine tuning” necessary to have a cancellation of two independent effects (the naturalness problem), or there must be some new principle at work.

Supersymmetry (SUSY)¹ is a new symmetry which provides a well-motivated extension of the standard model with an elegant solution to the naturalness problem. Supersymmetric transformations relate fermionic and bosonic degrees of freedom. Each left-handed and right-handed fermion of the standard model is postulated to have its own bosonic superpartner with equal mass and coupling strengths. Similarly, each standard-model boson would have its own fermionic superpartner, again with equal mass and couplings. Because bosons and fermions induce radiative effects of opposite signs, SUSY naturally provides an exact cancellation of the otherwise quadratically divergent radiative corrections to the Higgs-boson mass (Ferrara *et al.*, 1974; Il-iopoulos and Zumino, 1974; Wess and Zumino, 1974b; Witten, 1981).

Given that no superparticles have been observed so far, it is assumed that SUSY is broken, and that in general the sparticles must be heavier than their partners. In order to break SUSY without spoiling the necessary cancellation of quadratic divergences, the splittings between the masses of the standard-model particles and their SUSY partners should not be much larger than a few TeV. If SUSY is a consistent description of Nature, then the lower range of sparticle masses can be within reach of the Tevatron (Ellis, Enqvist, *et al.*, 1986; Barbieri and Giudice, 1988; Anderson *et al.*, 1997), motivating a wide range of searches in a large number of channels (Dawson, 1985). The mass of the lightest neutral Higgs boson is strongly constrained within SUSY (Carena, Espinosa *et al.*, 1995; Carena, Quirós, and Wagner, 1996; Carena, Zerwas *et al.*, 1996; Haber *et al.*,

1997) and could be within reach of the upgraded Tevatron (Dai *et al.*, 1993; Mrenna and Kane, 1994; Stange *et al.*, 1994b; Amidei *et al.*, 1996b; Kim *et al.*, 1996; Yao, 1996; Mrenna, 1997b). In addition, the decay of the heavy top quark, pair produced in strong interactions with a cross section of ≈ 6 pb at the Tevatron, gives a unique mechanism for producing lighter supersymmetric particles which might not otherwise be produced at a large rate in proton-antiproton collisions.

Two experimental collaborations, CDF and DØ, have large, general-purpose detectors at Fermilab. The Tevatron had initial running periods in 1985 and 1987 with low luminosity.² In 1988–1989 (the “89 run”), the Tevatron operated at $\sqrt{s}=1.8$ TeV with an average instantaneous luminosity of $1.6 \times 10^{30} \text{ cm}^{-2} \text{ s}^{-1}$, and the CDF detector collected approximately 4.4 pb^{-1} of data. In 1992–1993 (Run Ia), CDF and DØ accumulated approximately 20 and 15 pb^{-1} , respectively, and in 1994–1995 (Run Ib), 90 and 108 pb^{-1} , for a total Run I integrated luminosity of more than 100 pb^{-1} per detector.³ The average instantaneous luminosity during Run I was approximately $1 \times 10^{31} \text{ cm}^{-2} \text{ s}^{-1}$. A new run (Run II) utilizing the new main injector and recycler rings and other major accelerator improvements is scheduled to begin around the year 2000, reaching an average instantaneous luminosity of $1 \times 10^{32} \text{ cm}^{-2} \text{ s}^{-1}$ and an expected integrated luminosity of 1000 pb^{-1} per year (Peoples, 1996). In addition, the energy of the machine will be increased to $\sqrt{s}=2$ TeV, substantially increasing the cross section for producing heavy particles (the top quark pair-production cross section, for example, increases by 40% from $\sqrt{s}=1.8$ –2 TeV). Run II, with an upgraded collider and detectors, holds a great deal of promise for Higgs-boson and sparticle searches.

II. THE MINIMAL SUPERSYMMETRIC EXTENSION OF THE STANDARD MODEL

In the past two decades, a detailed picture of the minimal supersymmetric extension of the standard model (MSSM) has emerged.⁴ In the MSSM, the particle

²The 1985 run produced the first detected luminosity, with 20 events recorded by CDF.

³The difference in integrated luminosities in Run Ib comes partly from the fact that DØ uses the 11.3 pb^{-1} from Run Ic while CDF ignores it, and the fact that the DØ experiment normalizes its luminosity (and hence all cross sections) to an inelastic cross section that is 2.4% smaller than that used by CDF. For the actual luminosities used in each analysis see Table I.

⁴For details see Dimopoulos and Georgi (1981), Dimopoulos, Raby, and Wilczek (1981), Ibáñez and Ross (1981), Amaldi *et al.* (1991), Anselmo *et al.* (1991), Ellis, Kelley, and Nanopoulos (1991), Langacker and Lou (1991), Langacker and Polonsky (1993), Carena, Pokorski, and Wagner (1993), Faraggi and Grinstein (1994), Bagger, Matchev, and Pierce (1995), Barbieri, Cigfaloni, and Strumia (1995), Bastero-Gil and Mercader (1995), Chankowski *et al.* (1995a, 1995b), and Langacker and Polonsky (1995).

¹Some fundamental SUSY papers are those of Gervais and Sakita (1971), Gol'fand and Likhtam (1971), Neveu and Schwarz (1971), Ramond (1971), Volkov and Akulov (1973), Wess and Zumino (1974a), Wess and Bagger (1983), Arnowitt *et al.* (1984), Nilles (1984), Haber and Kane (1985), Mohapatra (1986), West and (1986), and Barbieri (1988). For the reader just beginning on supersymmetry, we recommend Dawson (1996), and Tata (1996, 1997). Intended for theorists: Bagger (1996), Dine (1996), Lykken (1996).

spectrum is doubled by SUSY. Moreover, to generate masses for up- and down-type fermions while preserving SUSY and gauge invariance, the Higgs sector must contain two doublets (Fayet, 1975). After EWSB, there is a quintet of physical Higgs boson states: two CP -even scalar (h, H), one CP -odd pseudoscalar (A), and a pair of charged (H^\pm) Higgs bosons (Gunion, 1990). All the Higgs bosons and other standard-model particles have superpartners with the same quantum numbers under the standard-model gauge groups $SU(3)_C \times SU(2)_L \times U(1)_Y$, but with different spins (Wess and Bagger, 1983; Arnowitt *et al.*, 1984; Nilles, 1984; Haber and Kane, 1985; Mohapatra, 1986; West, 1986; Barbieri, 1988). The spin-1/2 partners of the gauge bosons (gauginos) are denoted as winos \tilde{W}^\pm , zinos \tilde{Z} , photinos⁵ $\tilde{\gamma}$, and gluinos \tilde{g} . The spin-1/2 partners of the Higgs bosons (Higgsinos) are \tilde{H}_1, \tilde{H}_2 , and \tilde{H}^\pm . Because of EWSB, the Higgsinos and $SU(2)_L \times U(1)_Y$ gauginos mix to give physical mass eigenstates consisting of two Dirac fermions of electric charge one, the charginos $\tilde{\chi}_{1,2}^\pm$, and four neutral Majorana fermions, the neutralinos $\tilde{\chi}_{1-4}^0$. The spin-0 partners of the fermions (sfermions)⁶ are squarks \tilde{Q} ,⁷ sleptons \tilde{L} , and sneutrinos $\tilde{\nu}$. Each charged lepton or quark has two scalar partners, one associated with each chirality. These are named “left-handed” squarks and sleptons, which belong to $SU(2)_L$ doublets, and “right-handed” squarks and sleptons, which are $SU(2)_L$ singlets. The neutrinos have only left-handed superpartners $\tilde{\nu}$, which belong to $SU(2)_L$ doublets. The gluino \tilde{g} and squarks \tilde{Q} carry color indices and are $SU(3)_C$ octets and triplets, respectively.

The MSSM Lagrangian contains interactions between particles and sparticles fixed by SUSY. There are also a number of soft SUSY-breaking mass parameters. “Soft” means that they break the mass degeneracy between standard-model particles and their SUSY partners without reintroducing quadratic divergences while respecting the gauge invariance of the theory. The soft SUSY-breaking parameters are extra mass terms for gauginos and scalar fermions, and trilinear scalar couplings. The exact number of extra parameters depends on the exact mechanism of SUSY breaking. In the remainder of this section, the MSSM particle spectrum and properties will be described in general, as well as with reference to specific SUSY-breaking scenarios and variations.

A. Sparticle spectrum

The chargino and neutralino masses and their mixing angles (that is, their gaugino and Higgsino composition) are determined by the standard-model gauge-boson

masses (M_W and M_Z), $\tan \beta$,⁸ two soft SUSY-breaking parameters [the $SU(2)_L$ gaugino mass M_2 and the $U(1)_Y$ gaugino mass M_1], and the SUSY Higgsino mass parameter μ , all evaluated at the electroweak scale M_{EW} .⁹ Explicit solutions are found by considering the 2×2 chargino \mathbf{M}_C and 4×4 neutralino \mathbf{M}_N mass matrices:¹⁰

$$\begin{aligned} \mathbf{M}_C &= \begin{pmatrix} M_2 & \sqrt{2}M_W s\beta \\ \sqrt{2}M_W c\beta & \mu \end{pmatrix}; & \mathbf{M}_N &= \begin{pmatrix} \mathbf{M}_i & \mathbf{Z} \\ \mathbf{Z}^T & \mathbf{M}_\mu \end{pmatrix}; \\ \mathbf{M}_i &= \begin{pmatrix} M_1 & 0 \\ 0 & M_2 \end{pmatrix}; & \mathbf{M}_\mu &= \begin{pmatrix} 0 & -\mu \\ -\mu & 0 \end{pmatrix}; \\ \mathbf{Z} &= \begin{pmatrix} -M_Z c\beta s_W & M_Z s\beta s_W \\ M_Z c\beta c_W & -M_Z s\beta c_W \end{pmatrix}. \end{aligned} \quad (2)$$

\mathbf{M}_C is written in the $\tilde{W}^+ - \tilde{H}^+$ basis, \mathbf{M}_N in the $\tilde{B} - \tilde{W}^3 - \tilde{H}_1 - \tilde{H}_2$ basis, with the notation $s\beta = \sin \beta$, $c\beta = \cos \beta$, $s_W = \sin \theta_W$, and $c_W = \cos \theta_W$. In general, the mass eigenstates are admixtures of the interaction states, but, for large values of $|\mu|$ or M_1 and M_2 , the limit is reached where the mass eigenstates are mostly pure gaugino or Higgsino states (independent of $\tan \beta$). In particular, if $|\mu| \gg M_Z$ and $M_1, M_2 \approx M_Z$, with $M_1 < M_2$, the lightest eigenstates are gaugino-like and the heaviest are Higgsino-like, leading to the following spectrum:

$$\begin{aligned} M_{\tilde{\chi}_1^\pm} &\approx M_2; & M_{\tilde{\chi}_2^\pm} &\approx |\mu|; \\ M_{\tilde{\chi}_1^0} &\approx M_1; & M_{\tilde{\chi}_2^0} &\approx M_2; & M_{\tilde{\chi}_3^0} &\approx M_{\tilde{\chi}_4^0} \approx |\mu|. \end{aligned} \quad (3)$$

Similarly, if $M_1, M_2 \gg M_Z$ and $|\mu| = M_Z$, the lightest eigenstates are Higgsino-like and the heaviest are gaugino-like:

$$\begin{aligned} M_{\tilde{\chi}_1^\pm} &\approx |\mu|; & M_{\tilde{\chi}_2^\pm} &\approx M_2; \\ M_{\tilde{\chi}_1^0} &\approx M_{\tilde{\chi}_2^0} \approx |\mu|; & M_{\tilde{\chi}_3^0} &\approx M_1; & M_{\tilde{\chi}_4^0} &\approx M_2. \end{aligned} \quad (4)$$

Another interesting example, where $\tilde{\chi}_1^0$ is Higgsino-like, $\tilde{\chi}_2^0$ is photino-like, and all other charginos and neutralinos are mixtures, occurs for $M_1 = M_2 \approx |\mu| \approx M_Z$ and $\tan \beta \approx 1$:

$$\begin{aligned} M_{\tilde{\chi}_{1,2}^\pm} &= \frac{1}{2} |M_2 + \mu \mp \sqrt{(M_2 - \mu)^2 + 4M_W^2}|; \\ M_{\tilde{\chi}_1^0} &= |\mu|; & M_{\tilde{\chi}_2^0} &= M_1; \\ M_{\tilde{\chi}_{3,4}^0} &= \frac{1}{2} |M_2 + \mu \mp \sqrt{(M_2 - \mu)^2 + 4M_Z^2}|. \end{aligned} \quad (5)$$

⁵The superpartners of the $U(1)_Y$ and $SU(2)_L$ gauge bosons (before EWSB) are the bino \tilde{B} , the unmixed neutral wino \tilde{W}_3 , and the unmixed charged winos \tilde{W}_1 and \tilde{W}_2 .

⁶Charge conjugate scalars are denoted by*, e.g., \tilde{Q}^* .

⁷To allow easier reading, we use the nonstandard symbol \tilde{Q} instead of \tilde{q} . This has no special significance.

⁸One Higgs doublet, H_2 , couples to u, c , and t , while the other, H_1 , couples to d, s, b, e, μ , and τ . The parameter $\tan \beta$ is the ratio of vacuum expectation values $\langle H_2 \rangle / \langle H_1 \rangle \equiv v_2 / v_1$, and $v^2 = v_1^2 + v_2^2$, where v is the order parameter of EWSB.

⁹The electroweak scale M_{EW} is roughly the scale of the sparticle masses themselves. Usually in the literature, for simplicity, $M_{EW} \approx M_Z$.

¹⁰Beware of different sign conventions for μ in the literature. Both PYTHIA and ISAJET use the convention used here.

Since the $SU(3)_C$ symmetry of the standard model is not broken, the gluinos have masses determined by the $SU(3)_C$ gaugino mass parameter M_3 .¹¹ The neutralinos and the gluinos are Majorana particles and do not distinguish between states and their charged conjugate. Depending on their Higgsino or gaugino composition, the $\tilde{\chi}$ couplings to gauge bosons and left- and right-handed sfermions will differ substantially, and the production and decay processes will strongly depend on that composition (see the discussion below).

The mass eigenstates of squarks and sleptons are, in principle, mixtures of their left- and right-handed components, given for the first generation by

$$\begin{aligned} m_{\tilde{u}_L}^2 &\approx m_{Q_1}^2 + m_u^2 + D_{\tilde{u}_L}, & m_{\tilde{u}_R}^2 &\approx m_{U_1}^2 + m_u^2 + D_{\tilde{u}_R}, \\ m_{\tilde{d}_L}^2 &\approx m_{Q_1}^2 + m_d^2 + D_{\tilde{d}_L}, & m_{\tilde{d}_R}^2 &\approx m_{D_1}^2 + m_d^2 + D_{\tilde{d}_R}, \\ m_{\tilde{e}_L}^2 &\approx m_{L_1}^2 + m_e^2 + D_{\tilde{e}_L}, & m_{\tilde{e}_R}^2 &\approx m_{E_1}^2 + m_e^2 + D_{\tilde{e}_R}, \\ m_{\tilde{\nu}_e}^2 &\approx m_{L_1}^2 + D_{\tilde{\nu}_e}, \end{aligned} \quad (6)$$

where $m_{Q_1}^2$, $m_{L_1}^2$, $m_{U_1}^2$, $m_{D_1}^2$, and $m_{E_1}^2$ are soft SUSY-breaking parameters and $D_{\tilde{f}_L} = M_Z^2 \cos(2\beta)(T_{3_f} - Q_f \sin^2 \theta_W)$ and $D_{\tilde{f}_R} = M_Z^2 \cos(2\beta)Q_f \sin^2 \theta_W$ are D terms¹² associated with EWSB (T_{3_f} is the weak-isospin eigenvalue of the fermion and Q_f the electric charge). A similar expression holds for the second (third) generation with the substitutions $u \rightarrow c(t)$, $d \rightarrow s(b)$, $e \rightarrow \mu(\tau)$, $1 \rightarrow 2(3)$. In most high-energy models, the soft SUSY-breaking sfermion mass parameters are taken to be equal at the high-energy scale, but, in principle, they can be different for each generation or even within a generation. However, the sfermion flavor dependence can have important effects on low-energy observables, and it is often strongly constrained. The suppression of flavor-changing neutral currents (FCNC's), such as $K_L \rightarrow \pi^0 \nu \bar{\nu}$, requires that either (i) the squark soft SUSY-breaking mass matrix be diagonal and degenerate, or (ii) the masses of the first- and second-generation sfermions be very large (Misiak *et al.*, 1997).

The left-right sfermion mixing is determined by the product of soft SUSY-breaking parameters and the mass of the corresponding fermion. Unless the soft SUSY-breaking parameters for the first two generations are orders of magnitude greater than for the third generation, the mixing in the first two generations can be neglected and $\tilde{Q}_{L,R}$, with $\tilde{Q} = \tilde{u}, \tilde{d}, \tilde{c}, \tilde{s}$, and $\tilde{\mathcal{Z}}_{L,R}, \tilde{\nu}_\ell$, with $\ell = e, \mu$, are the real mass eigenstates, with masses $m_{\tilde{Q}_{L,R}}$ and $m_{\tilde{\mathcal{Z}}_{L,R}}, m_{\tilde{\nu}_\ell}$, respectively. For the third-generation sfermions, the left-right mixing can be non-

trivial. The mass matrix for the top squarks (stops) in the $(\tilde{t}_L, \tilde{t}_R)$ basis is given by

$$M_{\tilde{t}}^2 = \begin{pmatrix} m_{Q_3}^2 + m_t^2 + D_{\tilde{t}_L} & m_t(A_t - \mu/\tan \beta) \\ m_t(A_t - \mu/\tan \beta) & m_{U_3}^2 + m_t^2 + D_{\tilde{t}_R} \end{pmatrix}, \quad (7)$$

where A_t is a soft SUSY-breaking parameter.¹³ Unless there is a cancellation between A_t and $\mu/\tan \beta$, left-right mixing occurs for the stop squarks because of the large top-quark mass. The stop mass eigenstates are then given by

$$\begin{aligned} \tilde{t}_1 &= \cos \theta_{\tilde{t}} \tilde{t}_L + \sin \theta_{\tilde{t}} \tilde{t}_R, \\ \tilde{t}_2 &= -\sin \theta_{\tilde{t}} \tilde{t}_L + \cos \theta_{\tilde{t}} \tilde{t}_R, \end{aligned} \quad (8)$$

where the masses and mixing angle $\theta_{\tilde{t}}$ are fixed by diagonalizing the squared-mass matrix, Eq. (7). Because of the large mixing, the lightest stop \tilde{t}_1 can be one of the lightest sparticles. For the sbottom, an analogous formula for the mass matrix holds, with $m_{U_3} \rightarrow m_{D_3}$, $A_t \rightarrow A_b$, $D_{\tilde{t}_{L,R}} \rightarrow D_{\tilde{b}_{L,R}}$, $m_t \rightarrow m_b$, and $\tan \beta \rightarrow 1/\tan \beta$. For the stau, substitute $m_{Q_3} \rightarrow m_{L_3}$, $m_{U_3} \rightarrow m_{E_3}$, $A_t \rightarrow A_\tau$, $D_{\tilde{t}_{L,R}} \rightarrow D_{\tilde{\tau}_{L,R}}$, $m_t \rightarrow m_\tau$, and $\tan \beta \rightarrow 1/\tan \beta$. The parameters A_t , A_b , and A_τ can be independent soft SUSY-breaking parameters, or they might be related by some underlying principle. When $m_b \tan \beta$ or $m_\tau \tan \beta$ is large [$\mathcal{O}(m_t)$], left-right mixing can also become relevant for the sbottom and stau. It will become clear below that A_b and A_τ do not contribute in a major way to left-right mixing, since they do not have a $\tan \beta$ enhancement.

The Higgs-boson spectrum at tree level can be expressed in terms of the weak gauge-boson masses, the CP -odd Higgs-boson mass M_A , and $\tan \beta$:¹⁴

$$\begin{aligned} M_{h,H}^2 &= (1/2)[M_A^2 + M_Z^2 \\ &\quad \mp \sqrt{(M_A^2 + M_Z^2)^2 - 4M_Z^2 M_A^2 \cos^2 2\beta}], \\ M_{H^\pm}^2 &= M_A^2 + M_W^2. \end{aligned} \quad (9)$$

These relations yield $M_h \lesssim M_Z$, but this result is strongly modified by radiative corrections that depend on other MSSM parameters (Brignole *et al.*, 1991; Ellis, Ridolfi, and Zwirner, 1991a and 1991b; Haber and Hempfling, 1991; Okada *et al.*, 1991a, 1991b; Drees and Nojiri, 1992; Hempfling and Hoang, 1994; Kodaira *et al.*, 1994; Casas *et al.*, 1995). The dominant radiative corrections to M_h grow as m_t^4 and are logarithmically dependent on the third-generation squark masses. The heavy CP -even and charged Higgs-boson masses, M_H and M_{H^\pm} , respectively, are directly controlled by M_A . If all SUSY particles were heavy, but M_A were small, then the low-

¹¹The physical gluino mass is shifted from the value of the gluino mass parameter M_3 because of radiative corrections. As a result, there is an indirect dependence on the squark masses.

¹² D terms are terms in the scalar potential which are quartic in the fields and are proportional to the gauge couplings squared.

¹³Beware also of different sign conventions for A_t . Both PYTHIA and ISAJET use the convention used here.

¹⁴In the MSSM, M_A is related to the values of the Higgs soft SUSY-breaking parameters m_{H_1} and m_{H_2} and the Higgsino mass parameter μ through $M_A^2 = m_{H_1}^2 + m_{H_2}^2 + 2\mu^2$.

energy theory would look like a two-Higgs-doublet model. For sufficiently large M_A , the heavy Higgs doublet decouples, and the effective low-energy theory has only one light Higgs doublet with standard-model-like couplings to gauge bosons and fermions.

Within the MSSM, a general upper bound on M_h can be determined by a careful evaluation of the one-loop and dominant two-loop radiative corrections (Carena *et al.*, 1995; Carena, Quiros, and Wagner, 1996; Carena, Zerwas, *et al.*, 1996; Haber *et al.*, 1997). For $m_t = 175$ GeV and an extremely conservative set of assumptions,¹⁵ the upper bound on the lightest Higgs mass is maximized, yielding $M_h \leq 130$ GeV. For more moderate values of the MSSM parameters, the upper bound on M_h becomes smaller. Most importantly, given the general upper bound on M_h of about 130 GeV, the upgraded Tevatron has the potential to provide a crucial test of the minimal supersymmetric extension of the standard model (Dai *et al.*, 1993; Mrenna and Kane, 1994; Stange *et al.*, 1994; Amidei *et al.*, 1996b; Kim *et al.*, 1996; Yao, 1996; Mrenna, 1997b).

R -parity, defined as $R = (-1)^{2S+3B+L}$ (Farrar and Fayet, 1978), is a discrete multiplicative symmetry where S is the particle spin, B is the baryon number, and L is the lepton number. All standard-model particles have $R=1$, while all superpartners have $R=-1$, so a single SUSY particle cannot decay into only standard-model particles if R -parity is conserved. In this case, the lightest superpartner is absolutely stable. Astrophysical considerations imply that a stable lightest superpartner should be electrically neutral (Ellis, Hagelin, *et al.*, 1984). The best candidates, then, are the lightest neutralino $\tilde{\chi}_1^0$ and the sneutrino $\tilde{\nu}$, or alternatively the gravitino \tilde{G} (see below). Since the lightest superpartner can carry away energy without interacting in a detector, the apparent violation of momentum conservation is an important part of SUSY phenomenology (Farrar and Fayet, 1978). Additionally, when R -parity is conserved, superpartners must be produced in pairs from a standard-model initial state. The breaking of the R -parity symmetry would result in lepton- and/or baryon-number-violating processes. While there are strong experimental constraints on some classes of R -parity-violating interactions, others are hardly constrained at all. Unless it is explicitly stated otherwise, R -parity conservation is assumed below.

Quite generally, the dependence of the SUSY spectrum on $\tan\beta$ can be very strong, and it is necessary to determine the possible range of values for this essential parameter of the theory. The fermion masses, which are not fixed by SUSY, are a function of $\tan\beta$ and the standard-model Yukawa couplings. For the up- and down-quark and lepton masses, it follows that $m_u = h_u v \sin\beta$, $m_d = h_d v \cos\beta$, and $m_\ell = h_\ell v \cos\beta$, where

$h_{f=u,d,\ell}$ is the corresponding Yukawa coupling and $v = 174$ GeV is the order parameter of EWSB. Equivalently, $m_u = h_u v_2$, $m_d = h_d v_1$, and $m_\ell = h_\ell v_1$, where $v_2 = v \sin\beta$ and $v_1 = v \cos\beta$. The value of $\tan\beta$ and the Yukawa couplings can vary in a range consistent with the experimental values of the fermion masses. However, for the theory to remain perturbatively well defined up to a given cutoff scale, the Yukawa couplings should remain finite up to this cutoff scale. Whether this is the case can be determined by studying the renormalization-group evolution of each Yukawa coupling from low- to high-energy scales. In particular, the large value of the top-quark mass is associated with a large value of the top Yukawa coupling at low energies, which, depending on $\tan\beta$, may become too large to be compatible with a perturbative description of the theory (Alvarez-Guamé *et al.*, 1983; Bagger *et al.*, 1985; Bardeen *et al.*, 1992, 1994; Barger *et al.*, 1993; Carena, Pokorski, and Wagner, 1993; Langacker and Polonsky, 1994). The measured value of the top-quark mass, $m_t \approx 175$ GeV, defines a lower bound on $\tan\beta$ of about 1.2, provided that the top Yukawa coupling remains finite up to a scale of the order of 10^{16} GeV. If, instead, the top Yukawa coupling should remain finite only up to scales of the order of a TeV, values of $\tan\beta$ as low as 0.5 are still possible.¹⁶ A similar situation occurs when $\tan\beta$ is large, but now the crucial role is played by the bottom Yukawa coupling. If $\tan\beta$ becomes too large, large values of the bottom Yukawa coupling are necessary to obtain values of the bottom mass compatible with experiment. The exact bound on $\tan\beta$ depends on the SUSY spectrum, since there are radiative corrections to the bottom mass coming from sparticle exchange loops (Carena *et al.*, 1994b; Hall *et al.*, 1994; Hempfling, 1994). Generically, it can be shown that values of $\tan\beta \geq 60$ are difficult to obtain if the MSSM is expected to remain a valid theory up to scales of order 10^{16} GeV.

B. Supergravity

At present, the exact mechanism of SUSY breaking is unknown. Supergravity (SUGRA) models assume the existence of extra superfields (the so-called “hidden sector”) which couple to the MSSM particles only through gravitational-like interactions. When SUSY is spontaneously or dynamically broken in the hidden sector, some of the components of the hidden sector acquire vacuum expectation values. Interaction terms between those components of the hidden sector and the MSSM superfields give rise to the effective soft SUSY-breaking terms of the MSSM, which are proportional to vacuum expectation values of the hidden sector divided by powers of M_{Planck} . The low-energy Lagrangian then looks like a SUSY-conserving MSSM with a number of extra terms that break supersymmetry. Although low-energy gravi-

¹⁵To produce this bound, the masses of all SUSY particles and M_A are chosen to be around one TeV, $\tan\beta > 20$, and the stop mixing parameters are varied to give the largest possible effect.

¹⁶This implies that a perturbative description of the MSSM would only be valid up to the weak scale, which is, of course, not a very interesting possibility.

tational interactions depend only on mass and spin, the general supergravity Lagrangian may contain higher-dimensional interactions between the hidden sector and MSSM superfields that are flavor dependent.

The number of possible SUSY-breaking terms is over one hundred. In the minimal supergravity scenario, however, the MSSM sparticles couple universally to the hidden sector, and the number of terms is greatly reduced. Using this guiding principle, at a scale of order M_{Planck} (or, approximately, M_{GUT} , the scale where the gauge couplings unify), all scalars (Higgs bosons, sleptons, and squarks) are assumed to have a common squared mass m_0^2 , all gauginos (bino, wino, and gluino) have a common mass $m_{1/2}$, and all trilinear couplings have the value A_0 . After specifying $\tan\beta$, all that remains is to relate the values of the soft SUSY-breaking parameters specified at M_{GUT} to their values at M_{EW} . This is accomplished using renormalization-group (RG) equations (Martin, 1997). The physical sparticle masses are then determined using relations like Eq. (6), or by diagonalizing mass matrices like those in Eqs. (2) and (7). Finally, the Higgsino mass parameter is determined (up to a sign) by demanding the correct radiative EWSB. At the tree level, this requires

$$\tan^2\beta = \frac{\mu^2 + m_{H_1}^2 + M_Z^2/2}{\mu^2 + m_{H_2}^2 + M_Z^2/2}, \quad (10)$$

where m_{H_1} and m_{H_2} are soft SUSY-breaking mass parameters for the two Higgs doublets evaluated at M_{EW} .

Not surprisingly, the masses of the gluinos, charginos, and neutralinos are strongly correlated. The gaugino mass parameters M_i at the electroweak scale depend mainly on the running of the gauge couplings between M_{GUT} and M_{EW} :

$$\begin{aligned} M_3 &= \frac{\alpha_3(M_3)}{\alpha_{GUT}} m_{1/2} \approx 2.6m_{1/2}, \\ M_2 &= \frac{\alpha_2(M_2)}{\alpha_{GUT}} m_{1/2} \approx 0.8m_{1/2}, \\ M_1 &= \frac{\alpha_1(M_1)}{\alpha_{GUT}} m_{1/2} \approx 0.4m_{1/2} \end{aligned} \quad (11)$$

(where we consider $m_{1/2} \sim M_{EW}$). As will be shown below, once the RG evolution of the Higgs mass parameters is included in Eq. (10), it follows that the Higgsino mass term μ tends to be larger than the bino and wino masses M_1 and M_2 , becoming the largest for values of $\tan\beta$ closest to 1. As a result, the lightest two neutralinos and the lightest chargino tend to be gaugino-like. This is similar to the example presented in Eq. (3) with the approximate mass hierarchy

$$M_{\tilde{\chi}_2^0} \approx 2M_{\tilde{\chi}_1^0} \approx M_{\tilde{\chi}_1^\pm} \approx 1/3M_{\tilde{g}}. \quad (12)$$

The lightest neutralino $\tilde{\chi}_1^0$ can be the lightest superpartner.

Because sleptons have only electroweak quantum numbers and the lepton Yukawa couplings are small, the slepton mass parameters do not evolve much from M_{GUT} to M_{EW} . The left- and right-handed soft SUSY-breaking parameters at the scale M_{EW} which determine the mass eigenstates through Eq. (6) are given by

$$\begin{aligned} m_{L_{1,2}}^2 &\approx m_{L_3}^2 \approx m_0^2 + 0.5m_{1/2}^2; \\ m_{E_{1,2}}^2 &\approx m_{E_3}^2 \approx m_0^2 + 0.15m_{1/2}^2. \end{aligned} \quad (13)$$

For $\tan\beta \geq 40$, the third-generation mass parameters also receive non-negligible contributions from the τ Yukawa coupling in their running, which can modify these expressions. The different coefficients of $m_{1/2}$ in Eq. (13) arise from the different electroweak quantum numbers for sleptons in $SU(2)_L$ doublets and singlets. If m_0 and $m_{1/2}$ are of the same order of magnitude, physical slepton masses are dominated by m_0 . When m_0 is small, the sneutrino can be the lightest superpartner instead of the $\tilde{\chi}_1^0$. The $\tilde{\nu}$ mass is fixed by the sum rule $m_{\tilde{\nu}_\ell}^2 = m_{\ell}^2 + M_W^2 \cos 2\beta$.

The squark mass parameters evolve mainly through the strong coupling to the gluino, so their dependence on the common gaugino mass is stronger than for sleptons. For the first and second generation, the left- and right-handed soft SUSY-breaking parameters at M_{EW} are given approximately by

$$m_{Q_{1,2}}^2 \approx m_0^2 + 6.3m_{1/2}^2; \quad m_{U_{1,2}}^2 \approx m_{D_{1,2}}^2 \approx m_0^2 + 5.8m_{1/2}^2. \quad (14)$$

In general, the squarks are heavier than the sleptons or the lightest neutralino and chargino. Since first- and second-generation squark soft SUSY-breaking parameters are the same for squarks with the same quantum numbers, flavor-changing neutral currents are suppressed.

For the third-generation squarks, the large top and bottom Yukawa couplings play a crucial role in the evolution of the RG equation. As mentioned generically in Sec. II.A, the top Yukawa coupling h_t is related to the top-quark mass by $m_t = (246/\sqrt{2})h_t \sin\beta \text{ GeV}$ and the bottom Yukawa coupling h_b is given by $m_b = (246/\sqrt{2})h_b \cos\beta \text{ GeV}$, so that h_b is large (of order h_t) when $\tan\beta$ is about 40 or larger. When h_t at M_{GUT} is sufficiently large, its low-energy value is independent of its exact value at M_{GUT} . This behavior is known as the *infrared fixed-point* solution of the top-quark mass (Hill, 1981; Alvarez-Guamé *et al.*, 1983; Bagger *et al.*, 1985; Hill *et al.*, 1985; Bardeen *et al.*, 1992, 1994; Barger, Berger, and Ohmann, 1993; Langacker and Polonsky, 1994). With the definition $Y_t \equiv h_t^2/(4\pi)$, the infrared fixed-point value of Y_t at the scale m_t is $Y_t^{ir} \approx 8\alpha_3/9$. Within the one-loop approximation, the effects of the top Yukawa coupling on the evolution of the RG equa-

tion can be parametrized in terms of the ratio Y_t/Y_t^{ir} . For small and moderate values of $\tan\beta$, the left- and right-handed soft SUSY-breaking parameters which determine the stop and sbottom masses are then given by (Carena, Olechowski, *et al.*, 1994a; Carena and Wagner, 1994a, 1995; Drees and Martin, 1996; Carena, Chankowski, *et al.*, 1997)

$$m_{Q_3}^2 \approx m_0^2 \left(1 - \frac{1}{2} \frac{Y_t}{Y_t^{ir}} \right) + m_{1/2}^2 \left[6.3 + \frac{Y_t}{Y_t^{ir}} \left(-\frac{7}{3} + \frac{Y_t}{Y_t^{ir}} \right) \right],$$

$$m_{U_3}^2 \approx m_0^2 \left(1 - \frac{Y_t}{Y_t^{ir}} \right) + m_{1/2}^2 \left[5.8 + \frac{Y_t}{Y_t^{ir}} \left(-\frac{14}{3} + 2 \frac{Y_t}{Y_t^{ir}} \right) \right], \quad (15)$$

and $m_{D_3} \approx m_{D_{1,2}}$. For large $\tan\beta$, assuming t - b Yukawa coupling unification at high energies [$Y_b = Y_t$ at M_{GUT} , which is a generic prediction of $SO(10)$ GUT models], the expressions for the third-generation soft SUSY-breaking parameters are (Carena, Olechowski, *et al.*, 1994b):

$$m_{Q_3}^2 \approx m_0^2 \left(1 - \frac{6}{7} \frac{Y_t}{Y_t^{ir}} \right) + m_{1/2}^2 \left[6.3 + \frac{Y_t}{Y_t^{ir}} \left(-4 + \frac{12}{7} \frac{Y_t}{Y_t^{ir}} \right) \right],$$

$$m_{U_3}^2 \approx m_{D_3}^2 \approx m_0^2 \left(1 - \frac{6}{7} \frac{Y_t}{Y_t^{ir}} \right) + m_{1/2}^2 \left[5.8 - \frac{Y_t}{Y_t^{ir}} \left(-4 + \frac{12}{7} \frac{Y_t}{Y_t^{ir}} \right) \right]. \quad (16)$$

Contributions proportional to A_0^2 and $A_0 m_{1/2}$ with a prefactor proportional to $(1 - Y_t/Y_t^{ir})$ are also present in Eqs. (15) and (16). For $m_t \approx 175$ GeV, the value of the ratio Y_t/Y_t^{ir} varies from 3/4 to 1 depending on $\tan\beta$, with $Y_t/Y_t^{ir} \rightarrow 1$ as $\tan\beta \rightarrow 1$, and $Y_t/Y_t^{ir} \approx 0.85$ for $\tan\beta = 40$. The value of A_t is governed by $m_{1/2}$, and, for large values of the top Yukawa coupling, depends weakly on its initial value and $\tan\beta$ (Carena, Olechowski, *et al.*, 1994a; Carena, Chankowski, *et al.*, 1997),

$$A_t \approx \left(1 - \frac{Y_t}{Y_t^{ir}} \right) A_0 - 2m_{1/2}. \quad (17)$$

The exact values of A_b and A_τ are not important, since the mixing in the stau and sbottom sectors is governed by the terms $m_b \mu \tan\beta$ and $m_\tau \mu \tan\beta$, respectively. In supergravity models, the above relations between the mass parameters lead to the general prediction $m_{\tilde{Q}} \geq 0.85 M_{\tilde{g}}$ (for the five lightest squarks and small or moderate $\tan\beta$).

The soft SUSY-breaking parameters in the Higgs sector also have simple expressions. For small and moderate $\tan\beta$ (Carena, Olechowski, *et al.*, 1994a; Carena and Wagner, 1994a; Drees and Martin, 1996; Carena, Chankowski, *et al.*, 1997),

$$m_{H_1}^2 \approx m_0^2 + 0.5m_{1/2}^2,$$

$$m_{H_2}^2 \approx m_0^2 \left(1 - \frac{3}{2} \frac{Y_t}{Y_t^{ir}} \right) + m_{1/2}^2 \left[0.5 + \frac{Y_t}{Y_t^{ir}} \left(-7 + 3 \frac{Y_t}{Y_t^{ir}} \right) \right]. \quad (18)$$

Substituting these relations back into Eq. (10) yields the result

$$\mu^2 + M_Z^2/2 \approx m_0^2 \left[1 + \left(\frac{3}{2} \frac{Y_t}{Y_t^{ir}} - 1 \right) \tan^2 \beta \right] \frac{1}{\tan^2 \beta - 1} + m_{1/2}^2 \left\{ 0.5 - \left[0.5 + \frac{Y_t}{Y_t^{ir}} \times \left(-7 + 3 \frac{Y_t}{Y_t^{ir}} \right) \right] \tan^2 \beta \right\} \frac{1}{\tan^2 \beta - 1}. \quad (19)$$

Note in Eq. (18) that $m_{H_2}^2 < 0$, which is usually a sufficient condition to induce EWSB. For large $\tan\beta$, the Higgs mass parameters are more complicated. In the limit of t - b Yukawa unification, they simplify to (Carena, Olechowski, *et al.*, 1994b)

$$m_{H_1}^2 \approx m_{H_2}^2 \approx m_0^2 \left(1 - \frac{9}{7} \frac{Y_t}{Y_t^{ir}} \right) + m_{1/2}^2 \left[0.5 + \frac{Y_t}{Y_t^{ir}} \left(-6 + \frac{18}{7} \frac{Y_t}{Y_t^{ir}} \right) \right] \quad (20)$$

and Eq. (19) must be modified accordingly. All of these relations are only approximate: the coefficients of $m_{1/2}$ depend on the exact values of α_s and the scale of the sparticle masses, while the coefficients of m_0 and A_0 depend mainly on $\tan\beta$.

The supergravity model presented here is minimal (mSUGRA) in the sense that it is defined in terms of only five parameters at a high scale: m_0 , $m_{1/2}$, A_0 , $\tan\beta$, and the sign of μ . It is natural to question the exact universality of the soft SUSY-breaking parameters (Carena and Wagner, 1994b; Pomarol and Polonsky, 1994; Matalliotakis and Nilles, 1995; Olechowski and Pokorski, 1995). For example, in a $SU(5)$ SUSY GUT model, the left-handed sleptons and right-handed down-type squarks reside in the same 5 multiplet of $SU(5)$ and naturally have the common mass parameter $m_0^{(5)}$ at the GUT scale. Similarly, \tilde{u}_L , \tilde{d}_L , \tilde{u}_R , and \tilde{e}_R , which reside in the same 10 multiplet, have a common mass $m_0^{(10)}$. The two Higgs-boson doublets reside in different 5 and $\bar{5}$ multiplets, with masses $m_0^{(5')}$ and $m_0^{(\bar{5}')}$. There is no symmetry principle that demands that all these mass parameters be the same. The most naive breakdown of exact universality is to consider different values for $m_0^{(5')}$ and $m_0^{(\bar{5}')}$, taking m_0 as the common mass for sleptons and squarks.

Depending on the exact mechanism of SUSY breaking, it may occur that $m_{1/2} \approx 0$. Low-energy gaugino masses are then dominated by contributions of stop-top and Higgs-Higgsino loops (Barbieri *et al.*, 1983; Barbieri and Maiani, 1989). In this case, the gluino could be the lightest superpartner with a mass of $M_{\tilde{g}} \approx$ a few GeV and the lightest neutralino may be somewhat heavier

due to contributions from electroweak loops (Farrar and Masiero, 1994; Farrar, 1995). Light-gluino scenarios are being explored by many experiments (Barate *et al.*, 1997; Farrar, 1997).

C. Gauge-mediated supersymmetry breaking

In supergravity, gravitational interactions generate the soft SUSY-breaking terms in the MSSM Lagrangian. Alternatively, soft SUSY-breaking terms can be generated through gauge interactions. This has the feature that mass degeneracies between sfermions with the same quantum numbers (and, hence, the same gauge couplings) occur naturally, which suppresses flavor-changing neutral currents. Also, in gauge-mediated models, the scale of the SUSY breaking is much smaller than the scale where gravity becomes relevant, so there is no possibility of Planck-scale corrections to these degeneracies (as there can be between the GUT and Planck scales in supergravity; Kolda, 1998). In simple models (Dine *et al.*, 1995a, 1995b), the existence of heavy messenger superfields ψ with standard-model quantum numbers is postulated. Supersymmetry is broken in a hidden sector, which also couples to the messengers, so that the ψ fermion components have mass M , while the scalar components have masses $M\sqrt{1 \pm x}$, where x is a dimensionless parameter that controls the size of SUSY breaking. The MSSM gauginos and sfermions acquire masses different from their standard-model partners because of the radiative effects generated by the messenger fields. It is more convenient to define $\Lambda \equiv xM$, which fixes Λ as the overall mass scale of the MSSM sparticles. The gaugino masses at a low-energy scale μ are

$$M_i(\mu) = \frac{\alpha_i(\mu)}{4\pi} g(x)(b_i - b'_i)\Lambda, \quad (21)$$

where i specifies the gauge group, b_i is the MSSM coefficient of the beta function for the running of α_i , b'_i includes the additional effect of the messenger fields in the running, and $g(x) \approx 1 + x^2/6$. The scalar soft SUSY-breaking parameters acquire values

$$m_i^2(\mu) = 2\Lambda^2 \sum_i \left(\frac{\alpha_i(M)}{4\pi} \right)^2 C_i \{ f(x)(b_i - b'_i) + g(x)^2 [(b_i - b'_i)^2/b_i] [\alpha_i^2(\mu)/\alpha_i^2(M) - 1] \}, \quad (22)$$

where $C_1 = 5/3Y^2$, $C_2 = 3/4$, and $C_3 = 4/3$ (Y is the weak hypercharge), and $f(x) \approx 1 + x^2/36$. The formula in Eq. (22) ignores Yukawa couplings and will be modified for the stop and possibly sbottom and stau (Carena, Chankowski *et al.*, 1998; Wagner, 1998). By comparing the previous two equations, one can see that the gaugino and scalar masses are roughly of the same order of magnitude. Even after evolving these mass parameters to M_{EW} (ignoring the effects of Yukawa couplings), sfermions with the same quantum numbers acquire the same masses, yielding a natural mass hierarchy between

weakly and strongly interacting sfermions; the hierarchy of the gaugino masses is fixed by the gauge couplings (as in supergravity models). If the superfields ψ reside in a complete representation of $SU(5)$ or $SO(10)$, then unification of the gauge couplings at a high scale is not compromised, though the unification will occur at stronger values of the couplings and at a slightly different scale from the naive GUT scale. One distinctive feature of these models is that the spin-3/2 superpartner of the graviton, the gravitino \tilde{G} , can play a crucial role in the phenomenology. Since the gravitino mass is given by the relation $M_{\tilde{G}} = M\Lambda/M_{\text{Planck}}$, the gravitino can be very light (depending only on the value of M), in contrast to supergravity, where the gravitino has a mass on the order of M_W . As a result, in gauge-mediated supersymmetry breaking, the gravitino can be the lightest superpartner.

In the above discussion, it is assumed that the messengers ψ form a complete GUT multiplet. However, if the messengers were neutral under some gauge group, then the associated gauginos would be massless at one-loop order because of gauge invariance. In particular, it is possible to construct a model in which the gluino is a stable lightest superpartner with a mass of a few tens of GeV (Raby, 1997). In this case, the missing energy signal for SUSY disappears, since a stable lightest superpartner gluino will form stable hadrons.

D. R -parity violation

One simple extension of the MSSM is to break the multiplicative R -parity symmetry. At present, neither experiment nor any theoretical argument demands R -parity conservation, so it is natural to consider the most general case of R -parity breaking. It is convenient to introduce a function of superfields called the superpotential, from which the Feynman rules for R -parity-violating processes can be derived. The R -parity-violating (RPV) terms which can contribute to the superpotential¹⁷ are

$$W_{RPV} = \lambda_{ijk} L^i L^j \bar{E}^k + \lambda'_{ijk} L^i Q^j \bar{D}^k + \lambda''_{ijk} \bar{U}^i \bar{D}^j \bar{D}^k, \quad (23)$$

where i, j, k are generation indices (1,2,3), $L_1^i \equiv \nu_L^i$, $L_2^i = \ell_L^i$ and $Q_1^i = u_L^i$, $Q_2^i = d_L^i$ are lepton and quark components of $SU(2)_L$ doublet superfields; $E^i = e_R^i$, $D^i = d_R^i$, and $U^i = u_R^i$ are lepton, down-, and up-quark $SU(2)_L$ singlet superfields, respectively. The unwritten $SU(2)_L$ and $SU(3)_C$ indices imply that the first term is antisymmetric under $i \leftrightarrow j$, and the third term is antisymmetric under $j \leftrightarrow k$. Therefore $i \neq j$ in $L^i L^j \bar{E}^k$, and $j \neq k$ in $\bar{U}^i \bar{D}^j \bar{D}^k$. The coefficients λ_{ijk} , λ'_{ijk} , and λ''_{ijk} are Yukawa couplings, and there is no *a priori* generic pre-

¹⁷In Eq. (23) bilinear terms are ignored. A discussion of the phenomenological implications of such terms can be found in the literature (Diaz, 1997b, 1997a; Carena, Pokoski, and Wagner, 1998).

diction for their values. In principle, W_{RPV} contains 45 extra parameters over the R -parity-conserving MSSM case.

Expanding Eq. (23) as a function of the superfield components, we derive the interaction Lagrangian from the first term,

$$\mathcal{L}_{LLE} = \lambda_{ijk} \{ \bar{\nu}_L^i e_L^j \bar{e}_R^k + \bar{e}_L^i \nu_L^j \bar{e}_R^k + (\bar{e}_R^k)^* \nu_L^i e_L^j + \text{H.c.} \}, \quad (24)$$

and from the second term,

$$\mathcal{L}_{LQD} = \lambda'_{ijk} \{ \bar{\nu}_L^i d_L^j \bar{d}_R^k - \bar{e}_L^i u_L^j \bar{d}_R^k + \bar{d}_L^j \nu_L^i \bar{d}_R^k - \bar{u}_L^j e_L^i \bar{d}_R^k + (\bar{d}_R^k)^* \nu_L^i d_L^j - (\bar{d}_R^k)^* e_L^i u_L^j + \text{H.c.} \}. \quad (25)$$

Both of these sets of interactions violate lepton number. The $\bar{U}\bar{D}\bar{D}$ term, instead, violates baryon number. In principle, all types of R -parity-violating terms may coexist, but this can lead to a proton with a lifetime shorter than the present experimental limits. The simplest way to avoid this is to allow only operators that conserve baryon number but violate lepton number or vice versa.

These new couplings have several effects on the SUSY phenomenology: (1) lepton- or baryon-number-violating processes are allowed, including the production of single sparticles (instead of pair-production); (2) the lightest superpartner is no longer stable, but can decay to standard-model particles within a collider detector; (3) because it is unstable, the lightest superpartner need not be the neutralino or sneutrino, but can be charged or colored.

Present data are in remarkable agreement with the standard-model predictions, and very strong bounds on the R -parity-breaking operators can be derived from the following processes: (a) charged-current universality, (b) $\Gamma(\tau \rightarrow e \nu \bar{\nu}) / \Gamma(\tau \rightarrow \mu \nu \bar{\nu})$, (c) the bound on the mass of ν_e , (d) neutrinoless double-beta decay, (e) atomic parity violation, (f) $D^0 - \bar{D}^0$ mixing, (g) $R_\ell = \Gamma_{had}(Z^0) / \Gamma_\ell(Z^0)$, (h) $\Gamma(\pi \rightarrow e \bar{\nu}) / \Gamma(\pi \rightarrow \mu \bar{\nu})$, (i) $BR(D^+ \rightarrow \bar{K}^{0*} \mu^+ \nu_\mu) / BR(D^+ \rightarrow \bar{K}^{0*} e^+ \nu_e)$, (j) ν_μ deep-inelastic scattering, (k) $BR(\tau \rightarrow \pi \nu_\tau)$, (l) heavy-nucleon decay, and (m) $n - \bar{n}$ oscillations. Additional limits can be derived from deep-inelastic experiments at HERA (Bhattacharyya, 1997; Dreiner, 1998). On the other hand, within the allowed values of the R -parity-violating couplings, $\lambda_{ijk}, \lambda'_{ijk}$, a whole new world opens up for SUSY searches.

E. Run-Ia parameter sets

Some CDF and DØ SUSY searches are analyzed in the framework of the so-called ‘‘SUGRA-inspired models.’’ Since these analyses have been made for a very specific choice of parameters, they do not generically represent supergravity scenarios. To avoid any misunderstanding, we refer to these models as Run-Ia parameter sets, or RIPS. To understand the limits that appear in many published analyses, it is necessary to state explicitly the framework behind RIPS.

First, there are five main input parameters: $M_{\tilde{g}}, m_{\tilde{Q}}, M_A, \tan \beta$, and the magnitude and sign of μ . The gluino mass $M_{\tilde{g}}$ is defined to be M_3 , which is equivalent to specifying $m_{1/2}$ and hence M_1 and M_2 using the unification relations, Eq. (11). The chargino and neutralino properties are then fixed by $M_1, M_2, \tan \beta$, and μ . In practice, the value of μ is set much larger than M_1 and M_2 , so the properties of the neutralinos, charginos, and gluino are similar to those in a pure supergravity model.

Next, all squark soft SUSY-breaking mass parameters are set to $m_{\tilde{Q}}$, and the D terms are neglected. The result is that the first five squarks are degenerate in mass. This may be unrealistic if $\tan \beta$ is large, since the sbottom mass can be naturally lighter because of non-negligible off-diagonal elements in the sbottom mass matrix. The stop squarks are made heavier than the other squarks by fixing $A_t = \mu / \tan \beta$ [see Eq. (7)], which tunes away the mixing between \tilde{t}_L and \tilde{t}_R . The resulting stop masses are $m_{\tilde{t}_1} = m_{\tilde{t}_2} = \sqrt{m_{\tilde{Q}}^2 + m_t^2}$. Therefore experimental limits placed on RIPS show no sensitivity to the stop squarks. Note that, in supergravity models, the stop soft SUSY-breaking parameters $m_{\tilde{Q}_3}^2$ and $m_{\tilde{U}_3}^2$ are generally not equal and are smaller than the other squark parameters at M_{EW} , so that one stop squark is lighter than the other squarks.

Giving the other five squarks a common value at the weak scale ignores the details of running from the GUT scale [see Eq. (14)] and the different D terms. However, if we use an average of the two formulas in Eq. (14), a specific $m_{1/2}$ and $m_{\tilde{Q}}$ roughly determine a value of m_0^2 . Whenever there is a solution with $m_0^2 > 0$ (which implies $m_{\tilde{Q}} > 0.85 M_{\tilde{g}}$), RIPS has many features of a supergravity model. Indeed, when $m_{\tilde{Q}} > M_{\tilde{g}}$, the approximate supergravity relations $m_{\tilde{L}}^2 = m_{\tilde{Q}}^2 - 0.73 M_{\tilde{g}}^2 - 0.27 M_Z^2 \cos 2\beta$, $m_{\tilde{R}}^2 = m_{\tilde{Q}}^2 - 0.78 M_{\tilde{g}}^2 + 0.23 M_Z^2 \cos 2\beta$, and $m_{\tilde{\nu}}^2 = m_{\tilde{Q}}^2 - 0.73 M_{\tilde{g}}^2 + 0.5 M_Z^2 \cos 2\beta$ are used to fix the slepton masses.¹⁸ The region $m_{\tilde{Q}} < M_{\tilde{g}}$ is very hard to realize in supergravity models, but is also worth investigating. In this case, for some analyses, a constant value of 350 GeV is set by hand for $m_{\tilde{L}}, m_{\tilde{R}}$, and $m_{\tilde{\nu}}$. Accordingly, experimental limits placed on RIPS when $m_{\tilde{Q}} < M_{\tilde{g}}$ show little sensitivity to the sleptons.

Finally, the Higgs mass M_A is used to determine the Higgs-boson sector. This is equivalent to considering partial nonuniversality for the scalar sfermion and Higgs-boson soft SUSY-breaking mass parameters at high energies, i.e., $m_0 \neq m_0^{(5')} \neq m_0^{(\bar{5}')}$ (see the discussion near the end of Sec. II.B). In practice, the CP -odd Higgs-boson mass M_A is set to a large value, so that the lightest neutral Higgs boson h has standard-model-like

¹⁸Observe that the D terms for the sleptons, although correct, are negligible in comparison with the approximation made in defining a common $m_{\tilde{Q}}$. However, D terms are included to assure the correct splittings between the \tilde{Z}_L and $\tilde{\nu}$ masses.

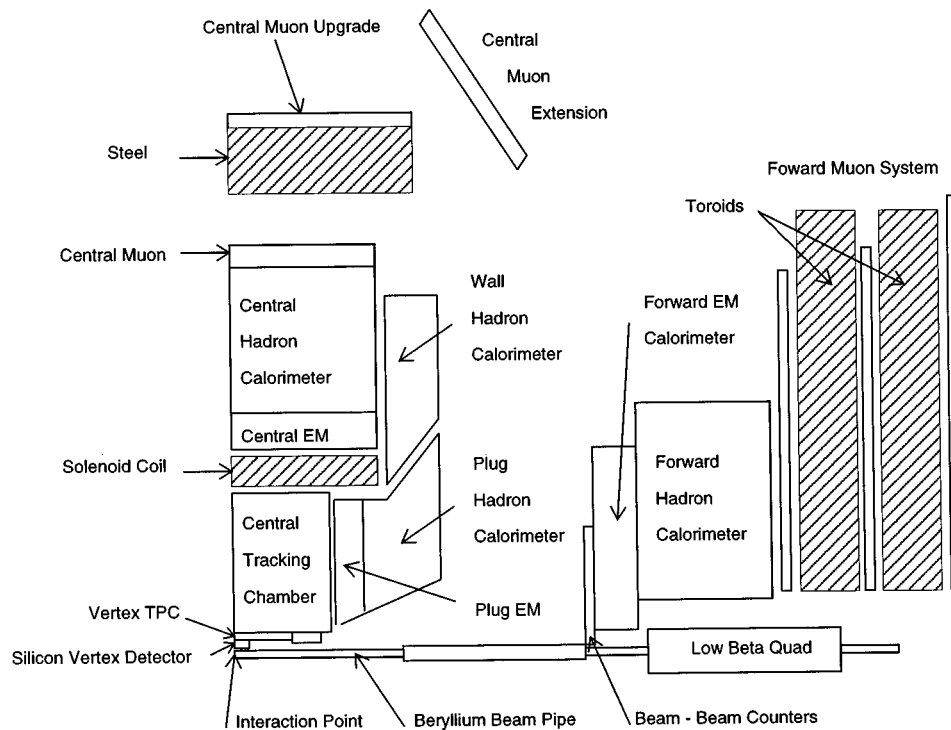


FIG. 1. A one-quarter-cross-section view of the CDF detector.

couplings to gauge bosons and fermions, and all other Higgs bosons are so heavy they are not kinematically accessible at the Tevatron.

III. THE CDF AND DØ DETECTORS

The CDF (Abe *et al.*, 1988) and DØ (Abachi *et al.*, 1994) detectors are located at the interaction regions B0 and D0 in the accelerator ring.¹⁹ Both detectors feature particle-tracking detectors close to the interaction region, surrounded by quasihermetic calorimetry covering the region of pseudorapidity²⁰ of approximately $|\eta| < 4$. Muon detection systems are located outside the calorimeters for both detectors.

A. The CDF detector

The CDF detector (see Fig. 1) is distinguished by its magnetic spectrometer: a 3-m-diameter, 5-m-long superconducting solenoidal magnet, which creates a 1.4-T field uniform at the 0.1% level and contains the particle-tracking detectors. A four-layer silicon-microstrip vertex detector (SVX; Amidei *et al.*, 1994), located directly outside the beampipe, tracks charged particles in the $r-\phi$ plane. The SVX measures the impact parameter of

tracks coming from secondary vertices of bottom and charm decays with a typical resolution of $30 \mu\text{m}$, providing heavy-flavor tagging for jets. A set of vertex time projection chambers (VTX) surrounding the SVX provides tracking in the radial and z directions and is used to find the z position of the $\bar{p}p$ interaction. Outside the VTX, from a radius of 30–150 cm, the 3.2-m-long central tracking chamber is used to measure the momentum of charged particles, with up to 84 measurements per track.

The calorimeter is divided into a central barrel ($|\eta| < 1.1$), end plugs²¹ ($1.1 < |\eta| < 2.4$), and forward/backward modules ($2.4 < |\eta| < 4.2$). Each of these is segmented into projective²² electromagnetic and hadronic towers subtending 0.1 in η by 15° in ϕ in the central calorimeter and 5° elsewhere. Wire chambers with cathode-strip readout give information on electromagnetic shower profiles in the central and plug calorimeters. A system of drift chambers outside the magnet coil and in front of the electromagnetic calorimeters serves as a “preradiator,” allowing additional photon/ π^0 discrimination on a statistical basis. Muons are identified with the central muon chambers, situated outside the calorimeters in the region where $|\eta| < 1.1$.

The magnetic spectrometer measures muon and other charged-particle transverse momenta with a resolution $\sigma_{p_T}/p_T < 0.001 p_T$ (p_T in GeV) and allows a precision

¹⁹The Tevatron ring has sixfold symmetry, with the centers of the straight sections labeled as A0, B0, C0, D0, E0, and F0.

²⁰The pseudorapidity η is defined as $-\ln(\tan(\theta/2))$. In the CDF and DØ coordinate systems, θ and ϕ are the polar and azimuthal angles, respectively, with respect to the proton-beam direction z .

²¹“End plugs” because they plug into the ends of the solenoid and central calorimeter.

²²Projective means pointing approximately at the interaction region.

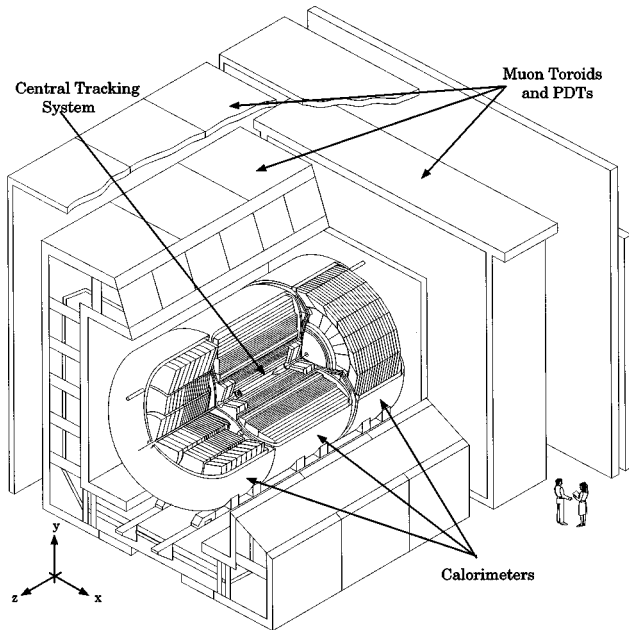


FIG. 2. The DØ detector.

calibration of the electromagnetic calorimeters by comparing the measured calorimeter response to the measured momentum from high-energy electrons from W decays (Abe *et al.*, 1994b). Electron energies are measured with a resolution $\sigma_E/E = 0.135/\sqrt{E_T} \oplus 0.01$ (E_T in GeV).²³ Jets are reconstructed as energy clusters in the calorimeter, using a cone algorithm (Flaucher and Meier, 1990) with a cone radius of either $R=0.7$ (Abe *et al.*, 1992) or $R=0.4$ (Abe *et al.*, 1994c) in $\Delta\eta \times \Delta\phi$ space. The jet energy resolution in the central region is approximately $\sigma_E/E = 0.80/\sqrt{E} \oplus 0.04$ (E in GeV).

Missing transverse energy,²⁴ (\cancel{E}_T), a key quantity in SUSY searches, is calculated as $\sum E^{\text{tower}} (\hat{\mathbf{n}} \cdot \hat{\mathbf{r}}) \hat{\mathbf{r}}$, where the sum is over both electromagnetic and hadronic calorimeter towers²⁵ in $|\eta| < 3.6$, E^{tower} is the energy measured in the tower, $\hat{\mathbf{n}}$ is the unit vector pointing in the direction of the center of the tower from the event vertex, and $\hat{\mathbf{r}}$ is the unit vector in the radial direction. The \cancel{E}_T is always corrected for the momentum of muons; for many SUSY analyses, it is also corrected for the calorimeter response to jets. The typical resolution on a component of \cancel{E}_T is 5.7 GeV in $Z^0 \rightarrow e^+e^-$ events.

B. The DØ detector

The DØ detector (see Fig. 2) consists of three major components: a nonmagnetic central tracking system,

²³The symbol \oplus denotes addition in quadrature, e.g., $a \oplus b = \sqrt{a^2 + b^2}$. The total resolution can be parametrized this way when there are two or more independent components of resolution.

²⁴The transverse momentum of a particle with momentum p is $p_T = p \sin \theta$. The analogous quantity using energy, defined as $E_T = E \sin \theta$, is called transverse energy.

²⁵A tower is a cell in $\eta - \phi$ space.

central and forward liquid-argon sampling calorimeters, and a toroidal muon spectrometer. The central tracking system consists of four detector subsystems: a vertex drift chamber, a transition radiation detector, a central drift chamber, and two forward drift chambers. Its outer radius is 76 cm. The system provides identification of charged tracks in the pseudorapidity range $|\eta| \leq 3.5$. It measures the trajectories of charged particles with a resolution of 2.5 mrad in ϕ and 28 mrad in θ . Using the reconstructed charged tracks, one can reconstruct the position of the primary interaction along the beamline direction with a resolution of 8 mm. The central tracking system also measures the ionization of tracks to allow single charged particles to be distinguished from e^+e^- pairs from photon conversion. The transition radiation detector aids in distinguishing electrons from charged pions.

The calorimeter is transversely segmented into pseudoprojective towers with $\Delta\eta \times \Delta\phi = 0.1 \times 0.1$ and provides full coverage to $|\eta| \leq 4.2$. The calorimeter is divided into three parts, a central calorimeter and two end calorimeters. These are further segmented into an inner electromagnetic section, followed by a fine hadronic section, and then a coarse hadronic section. Between the central and end-cap calorimeters, a set of scintillator tiles provides improved energy resolution for jets that straddle the two detectors. The electromagnetic calorimeter is divided into 32 modules in ϕ , each of which has 22 layers, each approximately 1 radiation length²⁶ thick, with liquid argon as the active element and ^{238}U plates as the passive element. These layers are arranged into four longitudinal segments per tower, called cells. The first cell contains two layers, the second cell contains two more layers, the third cell is finely segmented, with $\Delta\eta \times \Delta\phi = 0.05 \times 0.05$, and contains seven layers, and the last cell contains ten layers. The fine hadronic calorimeter uses a uranium-niobium alloy as its passive element, and the coarse hadronic uses copper. The electron energy resolutions, as measured in the electromagnetic calorimeter, are $\sigma_E/E = 0.130/\sqrt{E_T} \oplus 0.0115 \oplus 0.4/E$ for $|\eta| < 1.1$, and $\sigma_E/E = 0.157/\sqrt{E} \oplus 0.010 \oplus 0.4/E$ for $1.4 \leq |\eta| \leq 3.0$ (Zhu, 1994). The azimuthal position resolution for electrons above 50 GeV as measured by the calorimeter is 2.5 mm. The muon spectrometer provides muon detection in the range $|\eta| \leq 3.3$. The total thickness of the calorimeter plus the toroid varies from 13 to 19 interaction lengths, making hadronic punchthrough backgrounds negligible. The muon momentum resolution is $\sigma_p/p = 0.18(p - p_0)/p \oplus 0.008p$ (p in GeV/c, $p_0 = 2$ GeV/c). The DØ detector has a compact tracking volume which helps control backgrounds to prompt muons from in-flight decays of π and K mesons. Jets are reconstructed as energy clusters in the calorimeter, using a cone algorithm with a cone radius of $R=0.5$ or $R=0.7$ in $\Delta\eta \times \Delta\phi$ (Abachi *et al.*,

²⁶The radiation length is the mean distance traversed by an electron in a given material during which it radiates a fraction $1 - e^{-1}$ of its energy via bremsstrahlung.

1995). The jet energy resolution is approximately $\sigma_E/E = 0.8/\sqrt{E}$ (E in GeV; Abachi *et al.*, 1995c).

Missing E_T is calculated using the vector sum of energy deposited in all calorimeter cells, over the full calorimeter coverage for $|\eta| \leq 4.2$, with corrections applied to clustered cells to take account of the jet energy scale, and to unclustered cells as determined from studies of E_T balance in $Z^0 \rightarrow e^+e^-$ events that do not contain hadronic calorimeter clusters. The resolution on a component of \vec{E}_T in “minimum-bias” events²⁷ is $1.1 \text{ GeV} + 0.02 \Sigma E_T$, where ΣE_T is the scalar sum of transverse energies in all calorimeter cells. For some analyses, the \vec{E}_T is corrected for the presence of muons, which leave only a small fraction of their energy in the calorimeter.

C. Experimental realities

There are potentially two types of backgrounds to any experimental signature, physics and instrumental. Physics backgrounds mimic the event signature even in an ideal detector, while instrumental backgrounds arise because of detector flaws. Experimental signatures—SUSY or otherwise—are identified from “objects,” the building blocks of the event. Examples of objects that CDF and/or DØ use are electrons, muons, taus, \vec{E}_T , so-called “generic jets” (presumably from quarks and/or gluons, but without flavor identification), c 's, b 's, photons, and, using another level of kinematic reconstruction, W 's, Z 's, and t 's. The selection of each of these objects carries with it an efficiency and also a “fake rate,” a probability that the object is actually a different object which has been misidentified. The description of an object as an “electron,” for example, more precisely means an “electron candidate that passes the electron cuts,” no more and no less.

For the majority of searches, the signal and its physics backgrounds can be estimated using Monte Carlo simulation. The output of an event generator such as ISAJET (Paige and Protopopescu, 1986; Baer, Paige, *et al.*, 1986) or PYTHIA (Sjöstrand, 1994; Mrenna, 1997a) can be folded with relatively simple parametrizations of the detector response to give a good description of the data. A typical simple simulation transforms the final-state partons from a Monte Carlo into jets, using a clustering algorithm similar to the one used for the data. It then convolutes the momenta of the electrons, photons, muons, and jets with the appropriate experimental resolutions, generating “smeared” momenta. Missing E_T is calculated by first summing the smeared visible momenta, and then adding the effects of additional minimum-bias events in the same beam crossing. When calculating the geometric acceptance of the detector, it is necessary to include the distribution for the interaction

vertex position in z , which is Gaussian with an RMS of approximately 30 cm. Finally, the detection efficiencies are applied for electrons, photons, b quarks, τ 's, and muons (jets above 20 GeV are usually found with good efficiency). Initial- and final-state gluon radiation values need to be included, since they can affect the efficiency by adding extra jets which can modify the event signature or promote backgrounds into the signature.

In order to make even rough predictions of instrumental backgrounds, imperfections in the detectors must be taken into account. Two effects make these difficult to estimate: fakes and tails on jet energy resolution distributions. Because of the very large multijet production rate at the Tevatron, there can be significant fake backgrounds, even if the fake probability is very small. Fakes are very complicated, and the fake rate must be evaluated for each analysis using the appropriate data. In general, the efficiency for properly identifying an object and the probability that another object fakes it are complementary. For signatures dominated by instrumental backgrounds, tighter selection criteria (“cuts”) make for a purer sample, but reduce efficiency. For signatures dominated by physics backgrounds, looser cuts are preferred because they produce a higher efficiency for the same ratio of signal to background. Fakes are an especially serious problem for signatures involving photons and taus, b - and c -quark tagging, and \vec{E}_T in events with jets. Although jet energy resolutions are roughly Gaussian, even small non-Gaussian tails, convoluted with the large jet cross section, can lead to significant numbers of events with large fake \vec{E}_T . In addition, there are some other factors that contribute to fakes and that are unique to working at the Tevatron, such as the long interaction region, the existence of multiple collisions in a single event, the presence of the main ring in the same tunnel as the beam, and larger cosmic-ray backgrounds than found at detectors that are deeper underground (such as the LEP experiments). Even a full detector simulation cannot correctly model all detector imperfections and these other effects.

IV. THE PRESENT STATUS OF SPARTICLE SEARCHES

Most previous Tevatron searches have been made under very specific assumptions. Several of the classic signatures, such as “jets+ \vec{E}_T ” (Baer, Tata, and Woodside, 1989, 1990, 1991), “trileptons” (Baer, Hagiwara, and Tata, 1987; Nath and Arnowitt, 1987; Barbieri, Caravaglios, *et al.*, 1991; Baer, Kao, and Tata, 1993b, Lopez *et al.*, 1993, 1994, 1995; Kamon *et al.*, 1994; Diehl *et al.*, 1995), and “same-sign dileptons” (Barger *et al.*, 1985; Baer, Kao, and Tata, 1993a; Barnett *et al.*, 1993) are likely to be fruitful in many models; others may be specific to a certain model. We advocate a signature-based approach, in which a broad range of channels are studied for departures from standard model expectations, without engineering the analysis for a specific class of models (see Appendix). While this may sound obvious, it is a large task with no well-defined beginning. With the experience of several years of data-taking, however,

²⁷These events are defined by the requirement that a beam-beam collision take place as measured by arrays of scintillation counters forward and backward near the beampipe, and therefore they have a smaller selection bias than events selected with more selective triggers.

experimentalists now have an idea of what they can do well. Signatures involving high- p_T isolated electrons, muons, and photons, b quarks, c quarks, τ leptons, and/or E_T can be measured accurately and have understandable backgrounds. Such signatures, then, are a practical starting point for the new generation of searches. In addition, there are motivations that are more general than the predictions of specific models for studying samples of (i) high-mass, high- E_T events to probe gluino and squark production, (ii) inclusive leptons, lepton pairs, and gauge bosons (γ , W , and Z) to probe both direct and cascade production of charginos and neutralinos, and (iii) third-generation fermions (t , b , and τ) to probe decays of light squarks and sleptons, as well as decays of Higgs bosons and Higgsinos. When setting limits, it is convenient to use specific models (such as SUGRA or RIPS), which reduce the number of free parameters but the quoted limits are valid only in that context and are not general limits. New physics may appear where we do not expect it.

In the sections below we discuss the status of SUSY searches at the Tevatron as of the summer of 1997.²⁸ We also discuss the phenomenology behind these searches and comment on possible improvements. Table I summarizes those CDF and DØ analyses that have been published or presented at conferences. The pace and scope, as well as the sophistication, of supersymmetry searches at the Tevatron have grown enormously in the last several years as the emphasis has shifted beyond the top quark and more data have become available; there are many analyses currently in progress. A much broader picture of the Tevatron's capabilities should emerge as these results become available.

A. Charginos, neutralinos, and trileptons

In supergravity models, the light neutralinos and charginos are much lighter than the gluino or squarks, and may be the only sparticles directly accessible at the Tevatron. In general, the lightest neutralino is a good lightest-superpartner candidate, so, assuming all charginos and neutralinos are relatively light, a discussion of their phenomenology is a good starting point for an overview of Tevatron searches.

Chargino and neutralino pairs would be produced directly²⁹ at hadron colliders through their electroweak couplings to squarks and the vector bosons γ , W , and Z . The production cross sections are not a simple function of chargino and neutralino masses, but also depend on

their (model-dependent) mixings and the squark masses. Quite generally, there are three contributions to $\tilde{\chi}\tilde{\chi}$ production: (i) s -channel gauge-boson production, (ii) t -channel squark exchange, and (iii) interference. For type (i), the reactions $q\bar{q}' \rightarrow W^* \rightarrow \tilde{\chi}_i^\pm \tilde{\chi}_j^0$ and $q\bar{q} \rightarrow \gamma^*/Z^* \rightarrow \tilde{\chi}_i^+ \tilde{\chi}_j^-$ occur through wino and Higgsino components, and $q\bar{q} \rightarrow Z^* \rightarrow \tilde{\chi}_i^0 \tilde{\chi}_j^0$ through Higgsino components of the neutralinos and charginos, respectively.³⁰ In type (ii), the scattering quarks and antiquarks exchange squarks subject to the constraint that \tilde{Q}_R couples only to the bino component of neutralinos, and \tilde{Q}_L to bino and wino components of the neutralinos and to charginos. Any \tilde{Q}_R or \tilde{Q}_L coupling to Higgsino components is proportional to the corresponding quark mass and can be ignored for chargino and neutralino pair production (even though \tilde{b} and \tilde{t} have large couplings, the contribution of b and t initial states from hadrons is small). Hence, in chargino pair production (e.g., $\tilde{\chi}_1^+ \tilde{\chi}_1^-$), only \tilde{Q}_L exchange is important, since \tilde{Q}_R only couples to the charged Higgsino. In the case when all squarks are heavy, type-(i) contributions dominate. When the squarks are sufficiently light, both types (ii) and (iii) can be important. For example, if $|\mu| \gg M_1, M_2$ [see Eq. (3)], then $\tilde{\chi}_1^0$, $\tilde{\chi}_2^0$, and $\tilde{\chi}_1^\pm$ are mostly gaugino-like, and both \tilde{Q}_L and \tilde{Q}_R can have electroweak strength couplings to them. If, on the other hand, $|\mu| \ll M_1, M_2$ [see Eq. (4)], \tilde{Q} exchange is only important for the heavier states, which might not be kinematically accessible.

Figure 3 shows the production cross sections of various chargino and neutralino pairs at the Tevatron for the limiting cases considered earlier in Eqs. (3) and (4). In this figure, $\tan\beta=2$, $m_{\tilde{Q}}=500$ GeV, and the gauginos obey the unification relations [see Eq. (11)]. The left figure is generated by fixing $\mu=-1$ TeV and varying $m_{1/2}$, the right figure by fixing $m_{1/2}=1$ TeV and varying μ . For reference, the standard-model $W^\pm h$ production cross section is shown as a function of M_h . The example of Eq. (3) is most like a pure supergravity model, in which the couplings of $W\tilde{\chi}_1^\pm \tilde{\chi}_2^0$ and $Z\tilde{\chi}_1^+ \tilde{\chi}_1^-$ are large, so the $\tilde{\chi}_1^\pm \tilde{\chi}_2^0$ and $\tilde{\chi}_1^+ \tilde{\chi}_1^-$ production cross sections are the largest.

Charginos and neutralinos can also be produced in associated production: $\tilde{Q}\tilde{\chi}$ and $\tilde{g}\tilde{\chi}$. This is discussed further in Sec. IV.B.

The decay patterns for the charginos and neutralinos are also very model dependent. When kinematically allowed, a tree-level two-body decay dominates over a tree-level three-body decay, because the latter has an extra factor of $g^2/(4\pi^2)$ in the decay rate. Possible two-body decays of the chargino are to $W^\pm \tilde{\chi}_1^0$, $H^\pm \tilde{\chi}_1^0$, $Z_{L,R}\nu$, $\tilde{\nu}/\ell$, and $\tilde{Q}q'$. The heavier chargino $\tilde{\chi}_2^\pm$ can also decay to $Z\tilde{\chi}_1^\pm$ and $h\tilde{\chi}_1^\pm$ (when Higgs bosons are part of the event signature, the final states can contain heavy-flavor

²⁸The Large Electron-Positron Collider (LEP) is also sensitive to SUSY production and, in many cases, its sensitivity is comparable to or exceeds the sensitivity of the Tevatron. The set of analyses performed at LEP is too extensive to report in this review, so only the most relevant results will be mentioned, with references to recent reviews and summaries (Janot, 1997; Grivaz, 1998; Hinchliffe, 1998; Schmitt, 1998).

²⁹They may also be produced indirectly in the decays of heavier sparticles.

³⁰An asterisk superscript on a gauge boson refers to a resonance off the mass shell.

TABLE I. A compilation of results from Run-I Tevatron SUSY searches as of the summer of 1997. The symbol b denotes an additional b -tagged jet. Also listed are the references and the section of this paper where each analysis is discussed. More information is available for DØ at http://www-d0.fnal.gov/public/new/new_public.html, and for CDF at <http://www-cdf.fnal.gov/>

Sparticle	Signature	Expt.	Run	$\int \mathcal{L} dt (\text{pb}^{-1})$	Ref.	Sec.
Charginos	$\mathbf{E}_T + \text{trilepton}$	CDF	Ia	19	Abe <i>et al.</i> (1996a)	IV.A
and	$\mathbf{E}_T + \text{trilepton}$	CDF	Iab	107	Bevensee (1997)	"
neutralinos	$\mathbf{E}_T + \text{trilepton}$	DØ	Ia	12.5	Abachi <i>et al.</i> (1996a)	"
	$\mathbf{E}_T + \text{trilepton}$	DØ	Ib	95	Abbott <i>et al.</i> (1997a)	"
	$\gamma\gamma + \mathbf{E}_T$ or jets	CDF	Ib	85	Culbertson (1998)	IV.I
	$\gamma\gamma + \mathbf{E}_T$	DØ	Iab	106	Abachi <i>et al.</i> (1997e)	"
Squarks	$\mathbf{E}_T + \geq 3,4$ jets	CDF	Ia	19	Abe <i>et al.</i> (1997a)	IV.B
and	$\mathbf{E}_T + \geq 3,4$ jets	DØ	Ia	13.5	Abachi <i>et al.</i> (1995d)	"
gluinos	$\mathbf{E}_T + \geq 3$ jets	DØ	Ib	79.2	Abachi <i>et al.</i> (1997a)	"
	dilepton + ≥ 2 jets	CDF	Ia	19	Abe <i>et al.</i> (1996b)	"
	$\mathbf{E}_T + \text{dilepton} + \geq 2$ jets	CDF	Ib	81	Done (1996)	"
	$\mathbf{E}_T + \text{dilepton}$	DØ	Ib	92.9	Abachi <i>et al.</i> (1997b)	"
Stop	$\mathbf{E}_T + \ell + \geq 2$ jets + b	CDF	Ib	90	Azzi (1997)	IV.C
	$\mathbf{E}_T + \ell + \geq 3$ jets + b	CDF	Iab	110	Wilson (1997)	"
	dilepton + jets	DØ	Ib	74.5	Abachi <i>et al.</i> (1996c)	"
	$\mathbf{E}_T + 2$ jets	DØ	Ia	7.4	Abachi <i>et al.</i> (1996b)	"
	$\mathbf{E}_T + \gamma + b$	CDF	Ib	85	Culbertson (1998)	IV.I
Sleptons	$\gamma\gamma \mathbf{E}_T$	DØ	Iab	106	Abachi <i>et al.</i> (1997e)	IV.I
Charged	dilepton + \mathbf{E}_T	CDF	Ia	19	Abe <i>et al.</i> (1994e), Wang (1994) ¹	IV.E
Higgs	$\tau + 2$ jets + \mathbf{E}_T	CDF	Ia	19	Abe <i>et al.</i> (1996c) ²	"
	$\tau + b + \mathbf{E}_T + (\ell, \tau, \text{jet})$	CDF	Iab	91	Abe <i>et al.</i> (1997b)	"
	$\tau + b + \mathbf{E}_T + (\ell, \tau, \text{jet})$	DØ	Iab	125	Abachi <i>et al.</i> (1997c)	"
Neutral	$WH \rightarrow \ell + \mathbf{E}_T + b + \text{jet}$	CDF	Iab	109	Abe <i>et al.</i> (1997c)	IV.F
Higgs	$WH \rightarrow \ell + \mathbf{E}_T + b + \text{jet}$	DØ	Ib	100	Abachi <i>et al.</i> (1997b)	"
	$WH, ZH \rightarrow \gamma\gamma + 2$ jets	DØ	Ib	101.2	Abachi <i>et al.</i> (1997d)	"
	$ZH \rightarrow b + \text{jet} + \mathbf{E}_T$	DØ	Ib	20	Abachi <i>et al.</i> (1997d)	"
	$WH, ZH \rightarrow 2$ jets + $2b$'s	CDF	Ib	91	Valls (1997)	"
R violating	dilepton + ≥ 2 jets	CDF	Iab	105	Chertok (1998)	IV.G
Charged lightest superpartner	slow, long-lived particle	CDF	Ib	90	Maeshima (1997)	IV.H

¹This analysis uses 18.7 pb^{-1} from Run Ia and a signature of a hadronically decaying $\tau + \geq 1 \text{ jet} + \mathbf{E}_T$.

²This analysis uses 19.3 pb^{-1} from Run Ia and a signature of two leptons + \mathbf{E}_T .

quarks or tau leptons). When no two-body final states are kinematically allowed, the chargino will decay to a three-body final state with contributions similar to those for chargino production (described previously): (i) virtual gauge-boson decays, (ii) virtual sfermion decays, and (iii) interference. A common decay is $\tilde{\chi}^\pm \rightarrow \tilde{\chi}^0 f\bar{f}'$. If sfermions are much heavier than a chargino, then type (i) dominates, and the decays proceed through W^* with branching ratios similar to those of the on-shell W boson. Virtual squarks and sleptons can significantly alter the branching ratios to a specific $f\bar{f}'$ final state depending on the squark and slepton masses, so that a 100%

branching ratio to $\ell\nu\tilde{\chi}_1^0$ or $jj\tilde{\chi}_1^0$ final states is possible. A three-body decay $\tilde{\chi}_j^\pm \rightarrow \tilde{g}q\bar{q}'$ can occur through virtual squark decays, provided the gluino is light enough (see Appendix).

Similarly, for neutralinos, the two-body decays to $Z\tilde{\chi}^0$, $h\tilde{\chi}^0$, $W^\pm\tilde{\chi}^\pm$, $H^\pm\tilde{\chi}^\pm$, $\tilde{\nu}_{L,R}\ell$, $\tilde{\nu}\nu$, or $\tilde{Q}q$ will dominate when kinematically allowed. When this is not the case, the three-body decay $\tilde{\chi}_i^0 \rightarrow \tilde{\chi}_j^0 f\bar{f}'$ (or $\tilde{\chi}^0 \rightarrow \tilde{g}q\bar{q}$) can occur through virtual Z bosons, squarks, or sleptons. Three-body decays can also be in competition with a loop decay, so that $\tilde{\chi}_2^0 \rightarrow \tilde{\chi}_1^0 \gamma$, since the same factor of $g^2/(4\pi)^2$ coming from a loop integral for a two-body

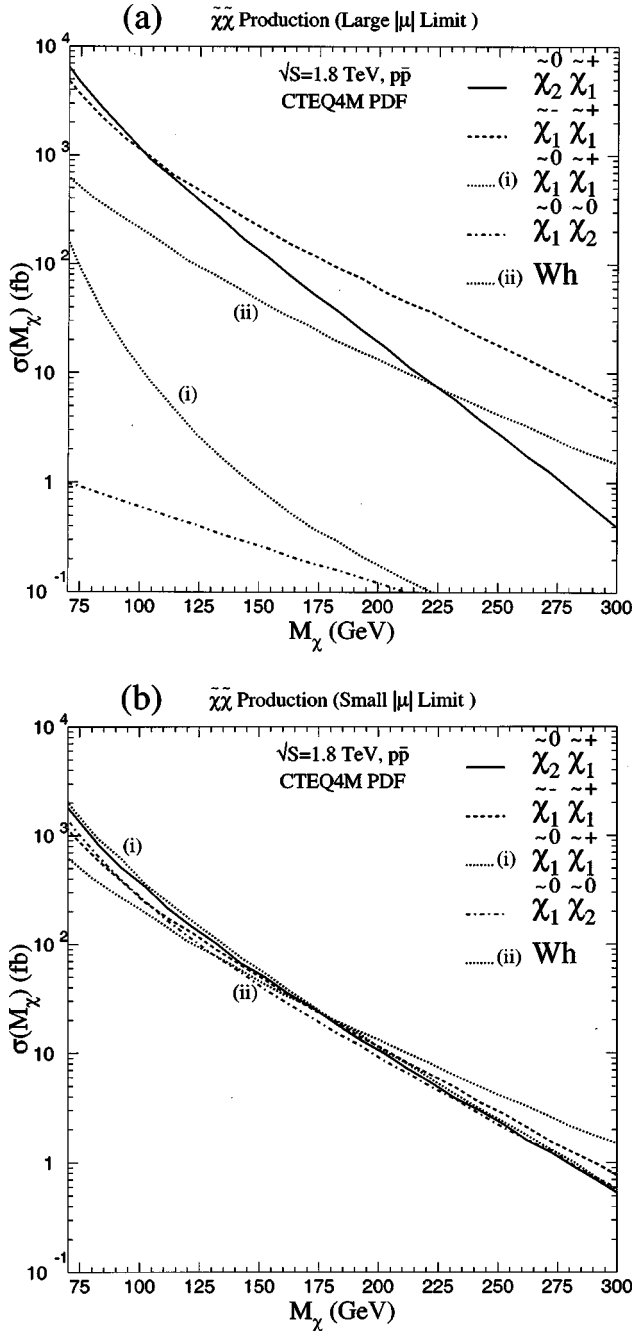


FIG. 3. Production cross sections at the Tevatron for chargino and neutralino pair production vs the lightest chargino mass for two limiting models discussed in the text: large $|\mu|$ (a) and small $|\mu|$ (b). The Wh cross section (curve ii) is shown for reference as a function of M_h .

decay also appears in the three-body decay rate. Such a decay is important when the $\tilde{\chi}_1^0$ is Higgsino-like and $\tilde{\chi}_2^0$ is gaugino-like, or vice versa.

It should be noted that the lightest stau mass eigenstate $\tilde{\tau}_1$ can be significantly lighter than the selectron or smuon. This arises naturally for large $\tan\beta$ when the tau Yukawa coupling becomes of $\mathcal{O}(1)$ and the left-right mixing becomes sizable. In this case, neutralinos and charginos may decay preferentially to τ leptons.

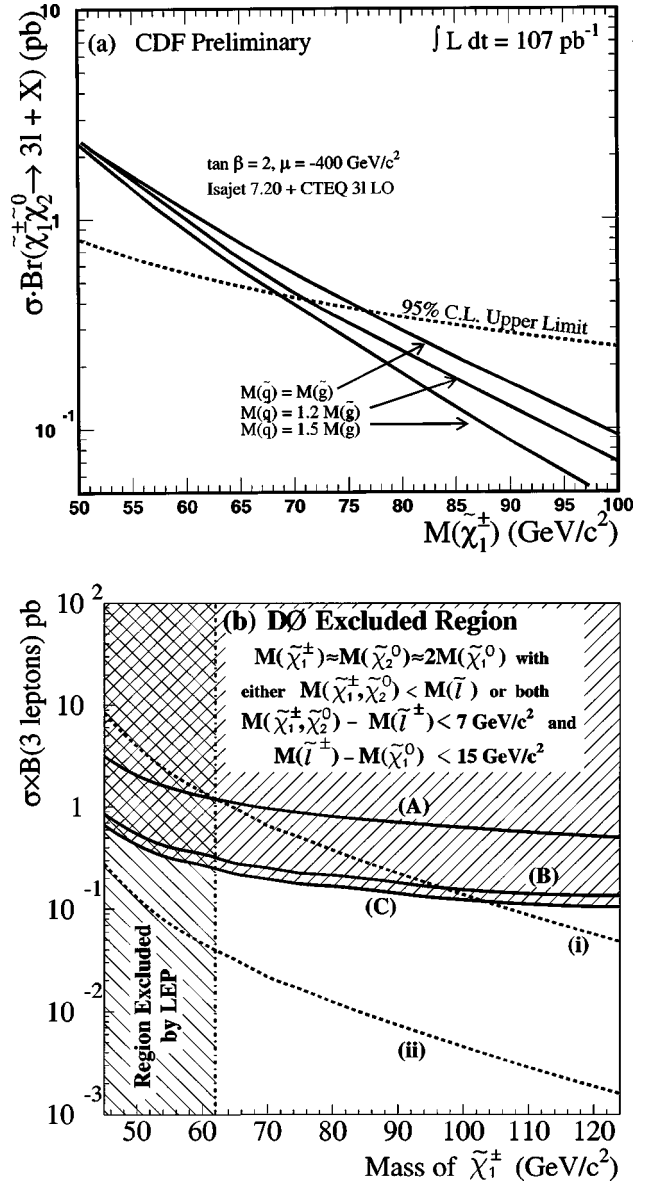


FIG. 4. Limits on the cross-section \times branching ratio of $\tilde{\chi}_1^\pm - \tilde{\chi}_2^0$ production in the trilepton mode vs chargino mass. Typically, $M_{\tilde{\chi}_2^0} \approx M_{\tilde{\chi}_1^\pm} \approx 2M_{\tilde{\chi}_1^0}$. (a) The CDF 95% C.L. limits in 107 pb^{-1} of data. The limit is on the sum of the signals for eee , $ee\mu$, $\mu\mu\mu$, and $\mu\mu e$ when $\tilde{\chi}_1^\pm \rightarrow \ell \nu \tilde{\chi}_1^0$ and $\tilde{\chi}_2^0 \rightarrow \ell \ell \tilde{\chi}_1^0$. The signals expected for three different Run-Ia parameter sets scenarios are shown for comparison (Baer and Tata, 1993); (b) similar limits from $D\emptyset$, but for the average of all four channels (to compare to the CDF limit, multiply by 4). The curves (A), (B), and (C) show the Run Ia, Run Ib, and combined limits. Curve (i) shows the predicted cross section \times branching ratio assuming $\text{BR}(\tilde{\chi}_1^\pm \rightarrow \ell \nu \tilde{\chi}_1^0) = \text{BR}(\tilde{\chi}_2^0 \rightarrow \ell \ell \tilde{\chi}_1^0) = 1/3$ ($\ell = e, \mu, \tau$). Curve (ii) assumes $\text{BR}(\tilde{\chi}_1^\pm \rightarrow \ell \nu \tilde{\chi}_1^0) = 0.1$ and $\text{BR}(\tilde{\chi}_2^0 \rightarrow \ell \ell \tilde{\chi}_1^0) = 0.033$. For both CDF and $D\emptyset$, kinematic efficiencies are calculated using the production cross section from ISAJET. The region excluded by LEP now extends up to a chargino mass of about 85 GeV and should restrict both CDF and $D\emptyset$ analyses.

In general, for $\tilde{\chi}_2^0 \tilde{\chi}_1^\pm$ production, the final states are (i) four leptons and \vec{E}_T , or (ii) two leptons, two jets, and \vec{E}_T , or (iii) four jets and \vec{E}_T . Some of the leptons can be

TABLE II. Selection criteria and results for the CDF trilepton gaugino search. The “very loose” muon category refers to isolated stiff tracks that leave only small amounts of energy in the calorimeters, but do not have a corresponding track in a muon chamber (this substantially increases the acceptance).

Quantity	Criteria/cut value
Lepton ID categories	1 tight+2 loose, $ \Sigma Q \neq 3$
Lepton isolation	$\Sigma E_T < 2$ GeV in a cone $R=0.4$
Tight E_T^e , η range	> 11 GeV, $ \eta < 1.0$
Loose E_T^e , η range	> 5 GeV, $ \eta < 2.4$
Tight p_T^μ , η range	> 11 GeV, $ \eta < 0.6$
Loose p_T^μ , η range	> 4 GeV, $ \eta < 1.0$
Very loose muon p_T^μ , η range	> 10 GeV, $ \eta < 1.0$
Z, Y, J/ ψ mass window cuts	75–105, 9–11, 2.9–3.1 GeV
$\Delta\phi$ between highest $2E_T$ leptons	$< 170^\circ$
ΔR between any 2 leptons	> 0.4
E_T	> 15 GeV
$\int \mathcal{L} dt$	107 pb $^{-1}$
Expected background	1.2 events
Observed events	0 events

neutrinos. For $\tilde{\chi}_1^+ \tilde{\chi}_1^-$ production, the final states are (i) two acollinear charged leptons and E_T , or (ii) one charged lepton, two jets, and E_T , or (iii) four jets and E_T . A wide variety of signatures is possible from the production of other chargino and neutralino combinations.

Trileptons

The production of $\tilde{\chi}_1^\pm \tilde{\chi}_2^0$, followed by the decays $\tilde{\chi}_1^\pm \rightarrow \tilde{\chi}_1^0 \ell \nu$ and $\tilde{\chi}_2^0 \rightarrow \ell^+ \ell^- \tilde{\chi}_1^0$, is a source of three charged leptons (e or μ) and E_T , called trilepton events (the E_T is silent). The trilepton signal has small standard-model backgrounds and is consequently one of the “golden” SUSY signatures (Baer, Hagiwara, and Tata, 1987; Nath and Arnowitt, 1987; Barbieri, Caravaglios *et al.*, 1991; Baer, Kao, and Tata, 1993b; Baer and Tata, 1993; Lopez *et al.*, 1993, 1994, 1995; Kamon *et al.*, 1994; Baer, Chen, *et al.*, 1995, 1996; Diehl *et al.*, 1995).

The overall efficiency for $\tilde{\chi}_1^\pm \tilde{\chi}_2^0$ production with decays into three detected leptons is set mainly by the branching ratio for the trilepton final state, which is highly model dependent. The efficiency also depends on mass splittings between the $\tilde{\chi}_1^\pm$ and $\tilde{\chi}_2^0$ and the $\tilde{\chi}_1^0$. For example, if the two-body decay chain $\tilde{\chi}_2^0 \rightarrow \tilde{\chi} \ell$ and $\tilde{\chi} \rightarrow \ell \tilde{\chi}_1^0$ occurs, and the mass splitting between $\tilde{\chi}_2^0$ and $\tilde{\chi}$ or between $\tilde{\chi}$ and $\tilde{\chi}_1^0$ is small, one of the leptons can be too soft to detect. In addition, if the mass splitting between $\tilde{\chi}_1^0$ and $\tilde{\chi}_2^0$ is large, decays to real Z or h bosons are possible. Real Z bosons have a small branching ratio to e^+e^- and $\mu^+\mu^-$ and are a standard-model background, and h will decay mainly to $b\bar{b}$, decreasing the trilepton rate. A similar discussion holds for the decays of the $\tilde{\chi}_1^\pm$, especially in supergravity since $M_{\tilde{\chi}_1^\pm} \approx M_{\tilde{\chi}_2^0}$.

For example, in SUGRA models, the branching ratios can be $\text{BR}(\tilde{\chi}_1^\pm \rightarrow \ell \nu \tilde{\chi}_1^0) = 0.22$, $\text{BR}(\tilde{\chi}_2^0 \rightarrow \ell^+ \ell^- \tilde{\chi}_1^0) = 0.32$ when the sleptons are off-shell but lighter than the squarks, or $\text{BR}(\tilde{\chi}_1^\pm \rightarrow \ell \nu \tilde{\chi}_1^0) = 0.66$, $\text{BR}(\tilde{\chi}_2^0 \rightarrow \ell^+ \ell^- \tilde{\chi}_1^0) = 0$ when the sneutrinos are light enough to allow $\tilde{\chi}_2^0 \rightarrow \tilde{\nu} \nu$ on-shell. The branching fractions also depend on $\tan\beta$, and, for large $\tan\beta$, decays to b’s and τ ’s are enhanced. The decays of $\tilde{\chi}_2^0$ to e^+e^- and $\mu^+\mu^-$ are strongly suppressed for large $\tan\beta$, falling a factor of about 5 between $\tan\beta=2$ and $\tan\beta=20$ if the squarks are much heavier than the sleptons (Baer, Chen *et al.*, 1997).

The results of the CDF (Abe *et al.*, 1996a; Bevensee, 1997) and D \bar{O} searches (Abachi *et al.*, 1996a; Abbott *et al.*, 1997a) are shown in Fig. 4 analyzed using Run-Ia parameter sets (RIPS; see Sec. II.E). The searches include four channels: $e^+e^-e^\pm$, $e^+e^-\mu^\pm$, $e^\pm\mu^+\mu^-$, and $\mu^\pm\mu^+\mu^-$. The CDF analysis is based on the cuts listed in Table II and requires one lepton with $E_T > 11$ GeV, passing tight identification cuts, and two other leptons with $E_T > 5$ GeV (electrons) or $p_T > 4$ GeV (muons), passing loose identification cuts. All leptons must be isolated, meaning there is little excess E_T in a cone of size $R=0.4$ in $\eta-\phi$ space centered on the lepton. The event must have two leptons with the same flavor and opposite sign. If two leptons of the same flavor and opposite charge have a mass consistent with the J/ Ψ , Y, or Z boson, the event is rejected. The detection efficiency for an event that decayed to three leptons is on the order of 5% (the branching ratios are discussed above). After this selection, six events remain in the data set, while the expected background, dominated by Drell-Yan pair production plus a fake lepton, is eight events. After demanding $E_T > 15$ GeV, no events remain, while 1.2 are expected from standard-model sources.

TABLE III. Selection criteria and results for the $D\bar{O}$ run-Ib trilepton search.

	eee		Channel and trigger					
		Trigger	$ee\mu$	Trigger	$e\mu\mu$	Trigger	$\mu\mu\mu$	Trigger
Energy ordered	$>22,5,5$	eE_T	$>22(e),5,5$	eE_T	$>9(e),10,5$	$e\mu$	$>17,5,5$	μ
E_T (GeV)	$>14,9,5$	$2eE_T$	$>14,9,5(\mu)$	$2eE_T$	$>17(\mu),5,5$	μ	$>5,5,5$	$\mu\mu$
			$>9(e),10(\mu),5$	$e\mu$	$>5,5,5$	$\mu\mu$		
Mass window cut	80–100 GeV		None		0–5 GeV		0–5 GeV	
E_T	>15 GeV		>10 GeV		>10 GeV		>10 GeV	
$\Delta\phi$	$ \pi - \Delta\phi_{e,e} > 0.2$		None		$ \pi - \Delta\phi_{\mu,\mu} > 0.1$		$ \pi - \Delta\phi_{\mu,\mu} > 0.1$	
cuts	2 leading e 's						all combinations	
$\int \mathcal{L} dt$	94.9 pb^{-1}		94.9 pb^{-1}		89.5 pb^{-1}		75.3 pb^{-1}	
Background	0.34 ± 0.07		0.61 ± 0.36		0.11 ± 0.04		0.20 ± 0.04	
Observed	0		0		0		0	

The $D\bar{O}$ analysis requires leptons with $E_T > 5$ GeV satisfying the selection criteria of Table III. However, several different triggers are used, and some lepton categories are required to have a larger E_T to pass the various trigger thresholds. All leptons are required to be isolated. To reduce events with mismeasured E_T , the E_T must not be along or opposite a muon. Additional cuts are tuned for each topology. For example, the background from Drell-Yan pair production plus a fake lepton is highest in the eee channel, so these events are rejected if an electron pair is back to back. The E_T cut is 15 GeV for eee , and 10 GeV for the other three topologies. The detection efficiency for an event that decayed to three leptons ranges from 1% for the $\mu\mu\mu$ mode to 5% for the eee mode. No events are observed in any channel, with a total of 1.26 events expected from (i) Drell-Yan production plus a fake lepton and (ii) heavy-flavor production.

To compare the $D\bar{O}$ and CDF 95%-C.L. results, note that the two experiments present different quantities: the $D\bar{O}$ limit is the average of the results from the four modes (eee , $ee\mu$, $e\mu\mu$, and $\mu\mu\mu$), while the CDF limit is on the sum. After accounting for this difference, the CDF limit is twice as sensitive at a given $\tilde{\chi}_1^\pm$ mass. The CDF limit shown is compared to three RIPS, which have different ratios of $m_{\tilde{Q}} to $M_{\tilde{g}}$. The $D\bar{O}$ limit is compared to a wide variety of possible branching ratios. Curve (i) assumes $\text{BR}(\tilde{\chi}_1^\pm \rightarrow \nu \tilde{\chi}_1^0) = \text{BR}(\tilde{\chi}_2^0 \rightarrow \ell \tilde{\chi}_1^0) = 1/3$ (no hadronic decays), while curve (ii) assumes $\text{BR}(\tilde{\chi}_1^\pm \rightarrow \nu \tilde{\chi}_1^0) = 0.1$, and $\text{BR}(\tilde{\chi}_2^0 \rightarrow \ell \tilde{\chi}_1^0) = 0.033$ (gauge-boson-like decays). The $D\bar{O}$ theory curve assumes heavy squarks, suppressing the squark exchange diagram, but the CDF curves do not. The wide differences in the theory curves in Fig. 4 show the dangers of quoting a mass limit rather than a cross section \times branching ratio limit.$

The experimental limit on the cross section (times branching ratio) depends on the kinematics of the decays, mostly through the mass splitting between $\tilde{\chi}_1^\pm$, $\tilde{\chi}_2^0$, and the lightest superpartner. For $\mu > 0$, the mass splitting $M_{\tilde{\chi}_1^\pm} - M_{\tilde{\chi}_1^0}$ is smaller, and the lepton p_T cuts are less efficient. As long as the sleptons are heavier than $\tilde{\chi}_1^\pm$

and $\tilde{\chi}_2^0$, the leptonic decays of $\tilde{\chi}_1^\pm$ and $\tilde{\chi}_2^0$ through virtual W and Z bosons and sleptons have similar kinematics, since the decays are dominated by phase space. However, when the experimental result is presented as a limit on the mass of the lightest chargino rather than as a cross-section limit, the result is highly model dependent. The theoretical cross section and branching ratios are strongly affected by the SUSY parameters. If sleptons and squarks are both heavy, the decays of $\tilde{\chi}_1^\pm$ and $\tilde{\chi}_2^0$ to leptons follow the pattern of the standard-model gauge particles. If the sleptons are light and the squarks

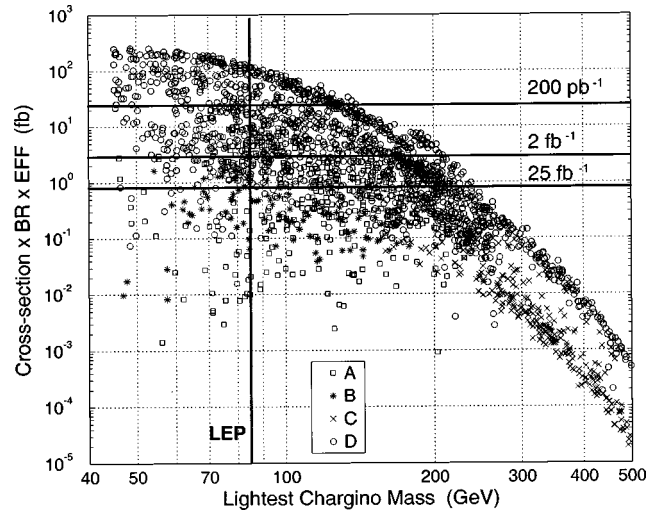


FIG. 5. The overall trilepton signal rate (Mrenna *et al.*, 1996) for an ensemble of minimal supergravity models as a function of the lightest chargino mass $M_{\tilde{\chi}_1^\pm}$. The kinematics cuts are different from those used in the present experimental analyses. The different symbols refer to solutions showing interesting behavior where $\tilde{\chi}_2^0$ has (A) a neutral “invisible” branching ratio (generally $\tilde{\chi}_2^0 \rightarrow \bar{\nu} \bar{\nu}$) $> 90\%$, (B) a large destructive interference in three-body leptonic decays, (C) a branching ratio to Higgs of $> 50\%$, or (D) all other solutions. The horizontal lines represent the 5σ discovery reach for various integrated luminosities. Generically, the present LEP limit on the chargino mass is about 85 GeV with some dependence on the MSSM parameter space (vertical line).

are heavy, decays to trileptons are enhanced.

Figure 5 shows the wide variation in total kinematic efficiency \times cross section \times branching ratio at a given chargino mass for the trilepton signature by sampling a large ensemble of minimal supergravity (mSUGRA) models (Mrenna *et al.*, 1996). The horizontal lines represent the 5σ discovery reach for various integrated luminosities. While the Tevatron reach can be quite good for sufficiently high luminosities, no absolute lower limit on the chargino mass is possible even in the restrictive mSUGRA framework.

To recapitulate, Tevatron data on the trilepton signature bounds the product of cross section and branching ratio for $\tilde{\chi}_2^0\tilde{\chi}_1^\pm$ production below about 25 fb for chargino masses below about 100 GeV. This limit assumes unification relations between the neutralino and chargino masses. It can be interpreted to exclude chargino masses below about 68–78 GeV for some limited choices of RIPS. Generically, LEP data have the potential to exclude chargino masses close to the kinematic limit. At present, this implies a limit of about 85 GeV. For the details of the variation of this limit as a function of the MSSM parameters, see Schmitt (1998).

B. Squarks and gluinos

Since the Tevatron is a hadron collider, it can produce gluinos and squarks through their $SU(3)_C$ couplings to quarks and gluons. The dominant production mechanisms are $gg, q\bar{q} \rightarrow \tilde{g}\tilde{g}$ or $\tilde{Q}\tilde{Q}^*$, $qq \rightarrow \tilde{Q}\tilde{Q}$, and $qg \rightarrow \tilde{Q}\tilde{g}, \bar{q}g \rightarrow \tilde{Q}^*\tilde{g}$. Because QCD is unbroken,³¹ the production cross sections of gluinos and squarks can be calculated as a function of only the squark and gluino masses (ignoring electroweak radiative corrections). Figure 6 shows the production cross sections for squarks and gluinos as a function of the sparticle masses at $\sqrt{s} = 1.8$ TeV (a) and 2 TeV (b), where next-to-leading-order (NLO) supersymmetric QCD corrections have been included (Beenakker, Hopker, and Spira, 1996; Beenakker, Hopker *et al.*, 1996a, 1996b, 1996c). The total cross sections can be of the order of a few picobarns for squark and gluino masses up to 400 GeV. The NLO corrections are in general significant and positive (evaluated at the scale³² $Q = \bar{m}$, the average mass of the two produced particles), and are much less sensitive to the

³¹The strong couplings of gluinos and squarks are the same as those of gluons and quarks, so that the production cross sections are the usual strong-interaction cross sections.

³²In the perturbative calculation of scattering probabilities in field theory, two scales appear: a factorization scale, where the parton distribution functions are evaluated, and a renormalization scale, where the running coupling is evaluated. In practice, these scales are chosen to be the same. This scale should be representative of the typical momentum flowing through a Feynman diagram. In Drell-Yan production, for example, the scale is the invariant mass of the Drell-Yan pair. The higher the order of a perturbative calculation, the less the dependence on this scale.

choice of scale than a leading-order calculation. In Fig. 6, five degenerate squark flavors are assumed,³³ which is one way to suppress flavor-changing neutral currents.

The ultimate detectability of squarks and gluinos depends upon their decays, which, in turn, depends on the electroweak couplings of the squarks and the mixings in the neutralino and chargino sector. Since squarks and gluinos decay into charginos and neutralinos, their signatures can be similar to $\tilde{\chi}\tilde{\chi}$ production, but with accompanying jets. If $m_{\tilde{Q}} > M_{\tilde{g}}$, then the squark has the two-body decay $\tilde{Q} \rightarrow \tilde{g}q$. The gluino has then the possible decays $\tilde{g} \rightarrow q\bar{q}\tilde{\chi}_i^0$ or $\tilde{g} \rightarrow q\bar{q}'\tilde{\chi}_i^\pm$, where q can stand for t or b as well, or even $\tilde{g} \rightarrow t\bar{t}^*$ or $\bar{t}\bar{t}$ if kinematically allowed. The gluino can also decay via one-loop diagrams, as in $\tilde{g} \rightarrow g\tilde{\chi}_i^0$. If, instead, $m_{\tilde{Q}} < M_{\tilde{g}}$, then the gluino has the two-body decay $\tilde{g} \rightarrow \tilde{Q}q$. The squarks can then decay as $\tilde{Q}_{L,R} \rightarrow q\tilde{\chi}_i^0$, $\tilde{u}_L \rightarrow d\tilde{\chi}_i^+$, and $\tilde{d}_L \rightarrow u\tilde{\chi}_i^-$. The final event signatures depend on the decay channels of the charginos and neutralinos, but typically involve E_T and a multiplicity of jets and/or leptons. The three-body or top-stop decay modes of the gluino can produce a higher multiplicity of standard-model particles in their decays than the squark two-body decays to neutralinos or charginos, particularly if $\tilde{Q} \rightarrow q\tilde{\chi}_1^0$ is the dominant squark decay. On the other hand, the lightest superpartner in gluino decays must share energy with more particles, producing less E_T on the average (see Fig. 7).

Gluinos and squarks may also be produced at the Tevatron in association with charginos or neutralinos (analogous to W and Z +jet production). These processes can be more important than pair production of gluinos and squarks if the latter are kinematically limited. Event signatures are similar to those from \tilde{Q} and \tilde{g} production, but possibly with fewer jets, though the events may still pass the selection criteria for the squark and gluino searches. For example, $\tilde{Q}\tilde{\chi}_1^\pm$ production will result in one less jet than $\tilde{Q}\tilde{Q}$ production, assuming the decay $\tilde{Q} \rightarrow q'\tilde{\chi}_1^\pm$ or $\tilde{Q} \rightarrow q\tilde{\chi}_1^0$.

Promising signatures for squark and gluino production are (i) multiple jets and E_T (Baer, Tata, and Woodside, 1989, 1990, 1991) and (ii) isolated leptons and jets and E_T (Baer, Kao, and Tata, 1993a; Barnett *et al.*, 1993; Barger *et al.*, 1985).

1. Jets + E_T

Both CDF and DØ have performed searches for events with jets and E_T . This signature has significant physics and instrumental backgrounds. The three dominant physics backgrounds are (i) $Z \rightarrow \nu\bar{\nu}$ plus jets, (ii) $W \rightarrow \tau\nu$ plus jets, where the τ decays hadronically, and (iii) $t\bar{t} \rightarrow \tau$ plus jets, where the τ decays hadronically. The E_T in leptonic W decays peaks at $M_W/2 \approx 40$ GeV, with a long tail at high E_T due to off-shell or high- p_T W 's and

³³Assuming the same mass for the bottom squark is a simplification that becomes questionable in the large- $\tan\beta$ region.

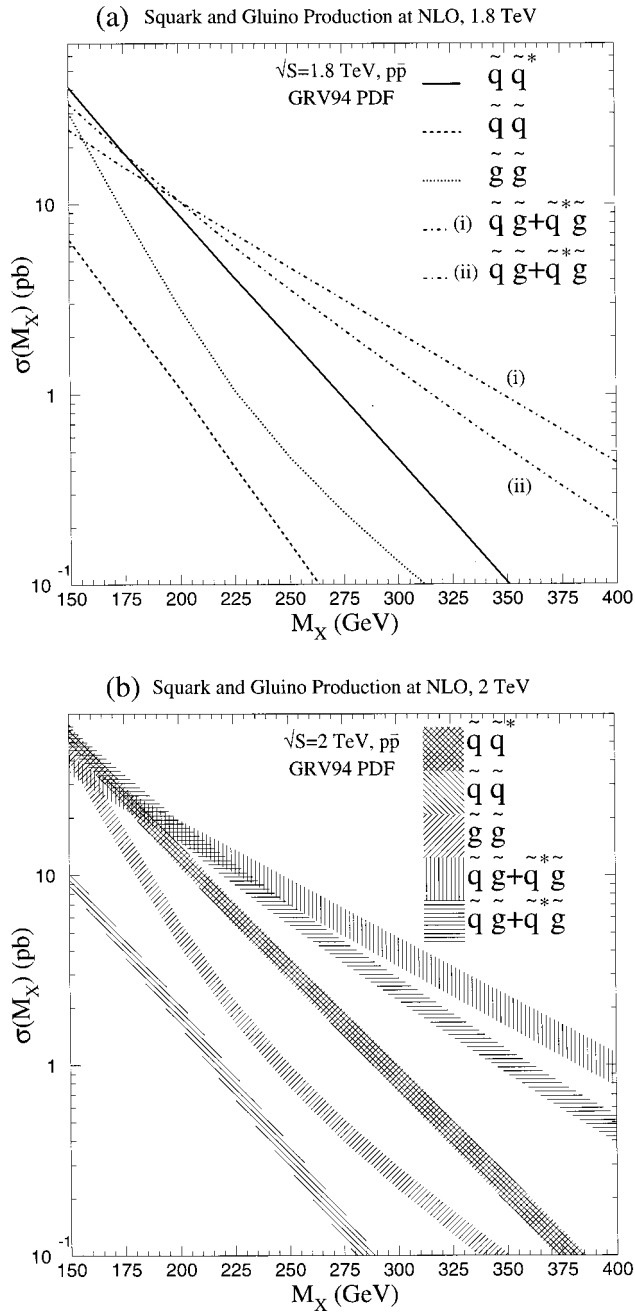


FIG. 6. Production cross sections for gluinos and squarks at the Tevatron vs sparticle mass M_X : (a) Predictions for Run I ($\sqrt{s}=1.8$ TeV) assuming degenerate masses for five flavors of squarks. For $\bar{Q}Q^*$ and $\bar{Q}Q$ production, M_X is the squark mass and $M_{\tilde{g}}=200$ GeV. For $\tilde{g}\tilde{g}$ production, M_X is the gluino mass and $M_{\tilde{Q}}=200$ GeV. For $\bar{Q}\tilde{g}$ production (i), M_X is the squark mass and $M_{\tilde{g}}=200$ GeV; for (ii), M_X is the gluino mass and $M_{\tilde{Q}}=200$ GeV. The scale is the average mass of the two produced sparticles. (b) The same curves with $\sqrt{s}=2$ TeV. The bands show the change in rate caused varying the scale from 1/2 to 2 times the average mass of the produced particles.

energy mismeasurements, so a cut at a large value of E_T is needed to remove these events. Instrumental backgrounds come from mismeasured vector-boson, top, and QCD multijet events. Backgrounds from vector-boson production occur for $W \rightarrow e\nu, \mu\nu$ plus jets events when

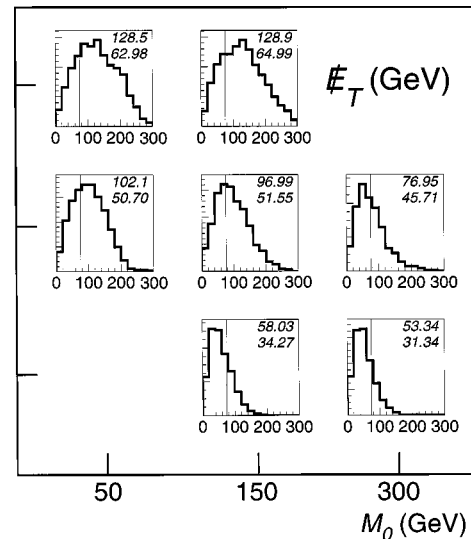


FIG. 7. The E_T distribution from simulations of squark/gluino events in the $D\bar{O}$ detector based on ISAJET and GEANT. The simulation used minimal supergravity mass relations assuming $\tan\beta=2$, $A_0=0$, and $\mu<0$ and seven values of m_0 and $m_{1/2}$. The numbers in the upper-right-hand corner of each plot are the mean and RMS of the distribution. The normalization is arbitrary.

the lepton is lost in a crack or is misidentified as a jet. The same problem can occur when the W is produced in a $t\bar{t}$ event. QCD multijet production is a background when jet energy mismeasurements cause false E_T .

The $D\bar{O}$ Run-Ia analysis (Abachi *et al.*, 1995d) searches for events with three or more jets and E_T and, separately, for events with four or more jets and E_T . The analysis is described in Table IV. The resulting mass limits on squarks and gluinos are shown in the right-hand figure in Fig. 8 (the plot containing the CDF results also shows the $D\bar{O}$ Ia results) and were set using a RIPS model with the following parameters: $M_{H^\pm}=500$ GeV, $\tan\beta=2$, $\mu=-250$ GeV, and $M_{\tilde{\gamma}}=m_{\tilde{Q}}$. The efficiency, branching ratios, and theoretical cross sections were calculated using ISAJET and a detector simulation, assuming five flavors of squarks with the same mass and neglecting top-squark production.

$D\bar{O}$ also has a three-jet analysis (Abachi *et al.*, 1997a) based on 79.2pb^{-1} of Run-Ib data. The basic requirements are three jets with $E_T>25$ GeV and a central leading jet ($|\eta|<1.1$). The E_T may be significantly overestimated if the wrong interaction vertex is used;³⁴ to reduce this effect, the tracks in the leading jet are required to point back to the primary vertex. The E_T is required to be uncorrelated in ϕ with any jet. A cut on the scalar sum of the E_T of the nonleading jets, called H_T , effectively reduces events from vector-boson backgrounds. The leading jet is also required to have $E_T>115$ GeV because the only available unbiased sample

³⁴The calculation of E_T uses the event vertex to calculate E_T for all objects.

TABLE IV. Selection criteria for Tevatron squark and gluino searches in the three or four jets + E_T channels. Cuts specific to the $D\bar{O}$ four-jet analysis are in parentheses.

Quantity	Experiment	
	$D\bar{O}$	CDF
Trigger	$E_T > 40$ GeV	$E_T > 35$ GeV
E_T	$> 75-100, (65)$ GeV	1 jet with $E_T^j > 50$ GeV
E_T^j	$> 25, (20)$ GeV	> 60 GeV with $S > 2.2 \text{ GeV}^{1/2}$
Leading E_T^j	> 115 GeV $ \eta < 1.1, (N.A.)$	> 50 GeV
$\Delta\phi_i$ between	$5.7^\circ < \Delta\phi_i < 174.3^\circ$	$\Delta\phi_i > 30^\circ$
E_T and jet i ; $i=1$ is the leading jet	$\sqrt{(\Delta\phi_1 - 180^\circ)^2 + \Delta\phi_2^2} > 28.6^\circ$	$\Delta\phi_1 < 160^\circ$
Leptons	Veto all (N.A.)	Veto all
Vertices	Confirmed (only one)	Any number

to study the QCD multijet background had this requirement. These cuts are summarized in Table IV. Vector-boson backgrounds are estimated using VECBOS (Berends *et al.*, 1991), while the $t\bar{t}$ background uses HERWIG (Marchesini and Webber, 1988a, 1988b) normalized to the $D\bar{O}$ -measured $t\bar{t}$ cross section. The detector simulation is based on the GEANT (Brun and Carminati, 1993) program. Two techniques were used to calculate the QCD multijet background. One compares the opening angle between the two leading jets and the E_T in the signal sample to the distribution in a generic multijet sample. The other selects events from a single jet trigger which pass all the selection criteria except for the E_T requirement. The E_T distribution is fit in the low- E_T region and extrapolated into the signal region. The complete set of background estimates can be found in Table V.

The $D\bar{O}$ data have been analyzed in the context of a minimal supergravity model. For fixed $\tan\beta$, A_0 , and sign of μ , exclusion curves are plotted in the $m_0 - m_{1/2}$ plane, Fig. 8(a). The limits are from the three-jet, 79.2-pb^{-1} analysis only. Efficiencies and branching ratios are calculated using ISAJET for production of gluinos and five flavors of squarks with the same mass, neglecting the top squark. For each point in the $m_0 - m_{1/2}$ plane, the E_T and H_T cuts are reoptimized based on the predicted background and SUSY signal. The total efficiency \times branching ratio is in the range 5–8%. Figure 7 shows the E_T as a function of m_0 and $m_{1/2}$ for $\tan\beta = 2$, $A_0 = 0$, and $\mu < 0$. When $m_0 \gg m_{1/2}$, the E_T signature is degraded, because $m_{\tilde{Q}} \gg M_{\tilde{g}}$ and thus higher-multiplicity $\tilde{g}\tilde{g}$ events dominate. Since higher multiplicity also means higher H_T , varying the cuts can maintain sensitivity. These results are robust within the mSUGRA framework (Abachi *et al.*, 1997a).

The CDF analysis of the Run Ib data set is not yet complete, but the Run-Ia result based on 19pb^{-1} has been published (Abe *et al.*, 1997a). The basic requirements are three or four jets and $E_T > 60$ GeV. The full set of cuts is listed in Table IV. As in the $D\bar{O}$ search, the

direction of the E_T is not allowed to coincide with that of a jet, and events with leptons are rejected to reduce the background from W and top events. The variable S , which indicates the significance of the E_T , is used to reduce fake E_T measurements; S is calculated by dividing the E_T by the square root of the scalar sum of the E_T in the calorimeters. The total efficiency \times branching ratio is in the range 2–15%. The vector-boson backgrounds are estimated using VECBOS normalized to the CDF Wjj data. Top backgrounds are determined using ISAJET normalized to the CDF-measured top cross section. The QCD background is estimated using an independent data sample based on a trigger that required one jet with $E_T > 50$ GeV. First all analysis cuts (Table IV) are applied to this sample except for the S cut, the E_T cut, and the three- or four-jets cut. Next the E_T distribution is fit and the number of events expected to pass the E_T cut is derived. Finally the efficiency of the last three cuts is applied to arrive at the final background estimate, shown in Table V.

The limits derived from the CDF analysis are shown in Fig. 8(b) within the RIPS framework (see Sec. II.E). In RIPS, a heavy gluino implies a heavy $\tilde{\chi}_1^0$, so a light squark ($m_{\tilde{Q}} \approx M_{\tilde{\chi}_1^0}$) decay will not produce much E_T . The consequence is an apparent hole in the CDF limit for small $m_{\tilde{Q}}$ and large $M_{\tilde{g}}$. However, lighter gluinos always produce a large E_T because of the enforced mass splitting between $M_{\tilde{g}}$ and $M_{\tilde{\chi}_1^0}$. The branching ratios are calculated within the model. The results of this analysis do not change substantially as parameters are varied within the RIPS framework (Abe *et al.*, 1997a).

The results summarized in Fig. 6 are complemented by the dilepton + E_T analysis shown in Figs. 7 and 9. The limits on the gluino and squark masses in each scenario (minimal SUGRA and RIPS) will be discussed below.

2. Dileptons + E_T

If, in the cascade decay chain of the \tilde{Q} 's and \tilde{g} 's, two charginos decay $\tilde{\chi}_1^\pm \rightarrow \ell \nu \tilde{\chi}_1^0$, or one neutralino decays

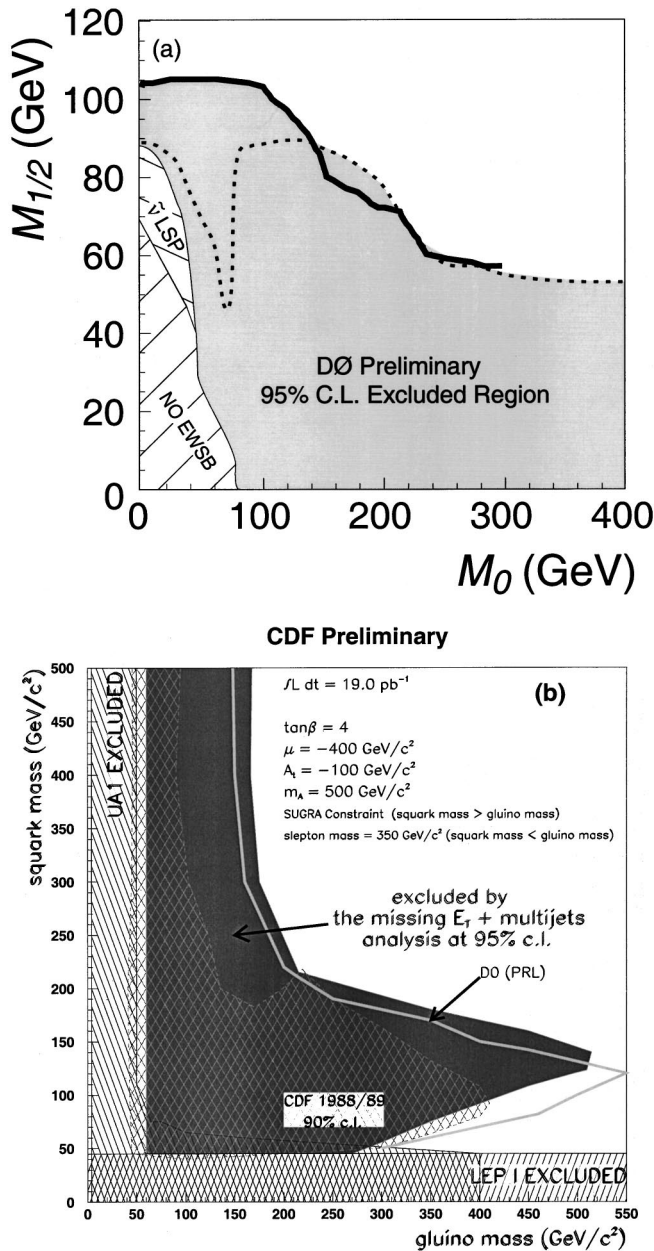


FIG. 8. Limits from jets+ E_T searches: (a) The DØ excluded region in the m_0 – $m_{1/2}$ plane with fixed parameters $\tan\beta=2$, $A_0=0$, and $\mu<0$. The heavy solid line is the limit contour of the DØ jets and missing transverse energy analysis. The dashed line is the limit contour of the DØ dielectron analysis. The lower hatched area is a region where minimal supergravity is not compatible with electroweak symmetry breaking. The upper hatched region shows where the sneutrino is the lightest superpartner. (b) The CDF mass limits on squarks and gluinos from the search in jets and E_T (Abe *et al.*, 1997a), using 19 pb^{-1} of data and the ISAJET 7.06 Run-I parameter set (RIPS) with $\tan\beta=4$, $\mu=-400 \text{ GeV}$, $A_t=-100 \text{ GeV}$, and $m_A=500 \text{ GeV}$. For $m_{\tilde{Q}}<M_{\tilde{g}}$, the cross section used is leading order, and three or more jets are required. For $M_{\tilde{g}}<m_{\tilde{Q}}$, the cross section is NLO (Beenakker *et al.*, 1996a; 1996b; 1996c; Beenakker, Hopker, and Spira, 1996a) and four jets are required. The line labeled “DØ PRL” is the DØ result from Run Ia using 13.5 pb^{-1} of data (Abachi *et al.*, 1995d).

$\tilde{\chi}_2^0 \rightarrow \ell^+ \ell^- \tilde{\chi}_1^0$, the final state can contain two leptons, jets, and E_T (Barger *et al.*, 1985; Baer, Kao, and Tata, 1993a; Barnett *et al.*, 1993). This channel has the advantage of being relatively clean experimentally. The requirement of two leptons significantly reduces jet backgrounds and removes most of the W backgrounds. Requiring that the mass of the two leptons be inconsistent with the Z mass removes most of the remaining vector-boson backgrounds. If the leptons are required to have $p_T > 20 \text{ GeV}$, the major background from physics processes is $t\bar{t} \rightarrow bW^+ \bar{b}W^- \rightarrow b\bar{b}\ell^+\ell^- E_T$. As the cut on lepton p_T is lowered, $Z \rightarrow \tau^+\tau^-$, where the τ 's decay semileptonically, also becomes an important background. The instrumental backgrounds are small. The spectacular signature of like-sign, isolated dileptons, which is difficult to produce in the standard model, can occur whenever a gluino is produced directly or in a cascade decay, since the gluino is a Majorana particle (neutralinos are also Majorana particles and can produce the same signature). This property is exploited in the CDF dilepton searches, but not the DØ searches, since the DØ detector cannot determine the sign of a particle's charge. Nonetheless, the DØ analysis achieves a similar sensitivity to that of the CDF analysis by using higher p_T thresholds. The kinematic efficiency for these searches ranges from 5–10%. Due to the small branching ratio to leptons, the overall efficiency varies from 0.1–0.2% for the models considered.

Figures 9 and 10 show the DØ (Abachi *et al.*, 1997b) and CDF (Abe *et al.*, 1996b; Done, 1996) results from run Ib, once again compared to mSUGRA and RIPS, respectively. The CDF limit is based on NLO cross sections (Beenakker, Hopker, *et al.*, 1996a, 1996b, 1996c; Beenakker, Hopker, and Spira, 1996), which tend to improve the limit by 10–30 GeV, and the DØ limit is based on leading-order cross sections. The DØ limits on m_0 and $m_{1/2}$ are calculated including contributions from the production of all sparticles (for instance, associated production of neutralinos or charginos with squarks or gluinos), while the CDF result only considers \tilde{Q} and \tilde{g} production. Table VI gives the selection criteria for the two analyses. The experimental cuts are chosen to identify two high- p_T leptons, which come predominantly from \tilde{Q} and \tilde{g} decays into charginos or neutralinos which in turn decay into real or virtual W or Z bosons. In both analyses, the branching ratios for dilepton production are computed as defined in the given RIPS or mSUGRA framework.

DØ has also presented an experimental limit in the $M_{\tilde{g}}-m_{\tilde{Q}}$ plane (Fig. 11), which allows a comparison with the CDF limit (Fig. 10). For $m_{\tilde{Q}} \gg M_{\tilde{g}}$ or, equivalently, for $m_0 \gg m_{1/2}$, $\tilde{g}\tilde{g}$ pair production is the dominant SUSY process. As $m_0(m_{\tilde{Q}})$ is varied with the other parameters fixed, the branching ratios for the three-body gluino decays to charginos or neutralinos and jets become fairly constant, so the production rate of leptonic final states becomes constant; the experimental limit consequently approaches a constant value asymptotically, as can be seen in both the DØ and CDF plots.

TABLE V. The number of expected and observed events for Tevatron squark and gluino searches in the jets+ E_T channel after performing the cuts in Table IV.

Analysis	DØ		CDF	
	3 jets	4 jets	3 or 4 jets	4 jets
$\int \mathcal{L} dt (\text{pb}^{-1})$	79.2	13.5	19	19
W^\pm	$1.56 \pm 0.67 \pm 0.42$	4.2 ± 1.2	$13.9 \pm 2.1 \pm 6.0$	$2.6 \pm 0.9 \pm 1.7$
$Z \rightarrow \ell\bar{\ell}, \nu\bar{\nu}$	$1.11 \pm 0.83 \pm 0.36$	1.0 ± 0.4	$5.0 \pm 0.9 \pm 2.7$	$0.4 \pm 0.2 \pm 0.4$
$t\bar{t}$	$3.11 \pm 0.17 \pm 1.35$	–	$4.2 \pm 0.3 \pm 0.5$	$2.2 \pm 0.2 \pm 0.4$
QCD multijets	3.54 ± 2.64	1.6 ± 0.9	$10.2 \pm 10.7 \pm 4.2$	$3.2 \pm 3.8 \pm 1.3$
Total background	$9.3 \pm 0.8 \pm 3.3$	6.8 ± 2.4	$33.5 \pm 11 \pm 16$	$8 \pm 4 \pm 4$
Events observed	15	5	24	6

Observe that, for large enough values of the gluino mass, the leptons easily pass the experimental cuts, so the experimental efficiency also becomes constant.

The relation $m_{\tilde{Q}} \ll M_{\tilde{g}}$ is not possible in minimal supergravity, and is treated in an *ad hoc* manner in RIPS. There is no limit in this region for either opposite- or like-sign dilepton pairs because the large, fixed slepton masses limit the branching ratios to leptonic final states. The possibility of like-sign dilepton pairs is further reduced because both the $\tilde{g}\tilde{g}$ and $\tilde{g}\tilde{Q}$ cross sections (which produce like-sign leptons because the gluino is a Majorana particle) and the $\tilde{Q}\tilde{Q}$ cross section (which produces like-sign leptons because the squarks have the same charge) are small in this region. It is very difficult for $\tilde{Q}\tilde{Q}^*$ production to yield like-sign leptons in general.

When $m_{\tilde{Q}} \approx M_{\tilde{g}}$, the $\tilde{g}\tilde{g}$ cross section is supplemented by the $\tilde{g}\tilde{Q}$ cross section. Just above the diagonal line at $M_{\tilde{g}} = m_{\tilde{Q}}$ (i.e., $m_{\tilde{Q}}$ just larger than $M_{\tilde{g}}$) in Figs. 10 and 11, there are “noses” in the limit plots, with the limit becoming stronger close to the diagonal.

The limits in Figs. 10 and 11 are for a specific choice of parameters within the RIPS or mSUGRA framework. If μ , A_t , and $\tan\beta$ are varied, the branching ratios into charginos or neutralinos can vary strongly. The sensitive dependence on the parameters can be seen within minimal supergravity models from the DØ limits in Fig. 9. The dip in the $\tan\beta=2$ limit (a), around $m_0=70$ GeV, is a point where $m_{\tilde{\nu}} > M_{\tilde{\chi}_2^0} > m_{\tilde{\nu}}$ and $\text{BR}(\tilde{\chi}_2^0 \rightarrow \nu\bar{\nu}\tilde{\chi}_1^0) \approx 1$, so the detection efficiency is very sensitive to the choice of high-energy parameters m_0 and $m_{1/2}$. In Fig. 9(b), with $\tan\beta=6$, the limits are severely reduced compared to Fig. 9(a), with $\tan\beta=2$, in the region where the squark mass is large compared to the gluino mass. For large $\tan\beta$, the mass splitting $M_{\tilde{\chi}_1^\pm, \tilde{\chi}_2^0} - M_{\tilde{\chi}_1^0}$ is reduced, so that the leptons from the $\tilde{\chi}_1^\pm$ and $\tilde{\chi}_2^0$ decays are softer. The nontrivial shape of the limit curves results from an interplay between the cross section's being larger when m_0 and $m_{1/2}$ are smaller (sparticle masses are smaller) and the mass splittings being smaller. Consequently, although the dileptons+jets+ E_T signature is an excellent discovery channel with little standard model background, it is hard to set significant parameter limits even using minimal supergravity models.

From the present analyses in the E_T +jets and dileptons+ E_T channels, some preliminary conclusions can be drawn on the squark and gluino masses. These depend, however, on the assumed SUSY parameters. The DØ limit on the gluino mass effectively develops a plateau for large m_0 at 185 GeV for $\tan\beta=2$, and at 134 GeV for $\tan\beta=6$. The CDF limit on the gluino mass is 180 GeV for $\tan\beta=4$ for large $m_{\tilde{Q}}$. Instead, for equal squark and gluino masses, the DØ mass limit for $\tan\beta=2$ is 267 GeV, using all SUSY production and decay modes in the model. From the CDF analyses and $m_{\tilde{Q}} \approx M_{\tilde{g}}$, the limit is about 220 GeV for $\tan\beta=4$. A direct comparison of all the above results is rather difficult since DØ and CDF have done analyses assuming different sets of MSSM parameters (see Figs. 8–11). Moreover, CDF considers only squark and gluino production, while DØ considers all possible sparticle production, and the associated production of neutralinos or charginos with squarks or gluinos can have an impact on the experimental limits.

It would be very useful for purposes of comparing and combining the two experimental limits to have both collaborations use at least one common model (such as mSUGRA) and agree on several values of the parameters to do the searches. For example, the two collaborations could present their limits in the $m_{1/2}$ - $\tan\beta$ plane (for large m_0). Second, they could move (partially) towards more experimentally based quantities by plotting contours of cross-section limit and also contours of acceptance \times efficiency in the m_0 - $m_{1/2}$ plane. This would eliminate the strong model dependence on the branching ratios. The experimental acceptance for the signature of two leptons+jets is much less model dependent, since it simply reflects the hard kinematics from the decays of two heavy objects. A presentation of cross section \times branching ratio limits, in addition to the mass limits, would be of more general use to model builders.

In summary, the Tevatron data exclude gluinos with masses below about 180–185 GeV (and above 50 GeV) for any squark mass, and can probe squark masses in the range 220–267 GeV for gluino masses larger than the squark masses. However, the exact limits are model dependent and assume that five flavors of squarks have the same mass. Top squarks are not included in the analysis,

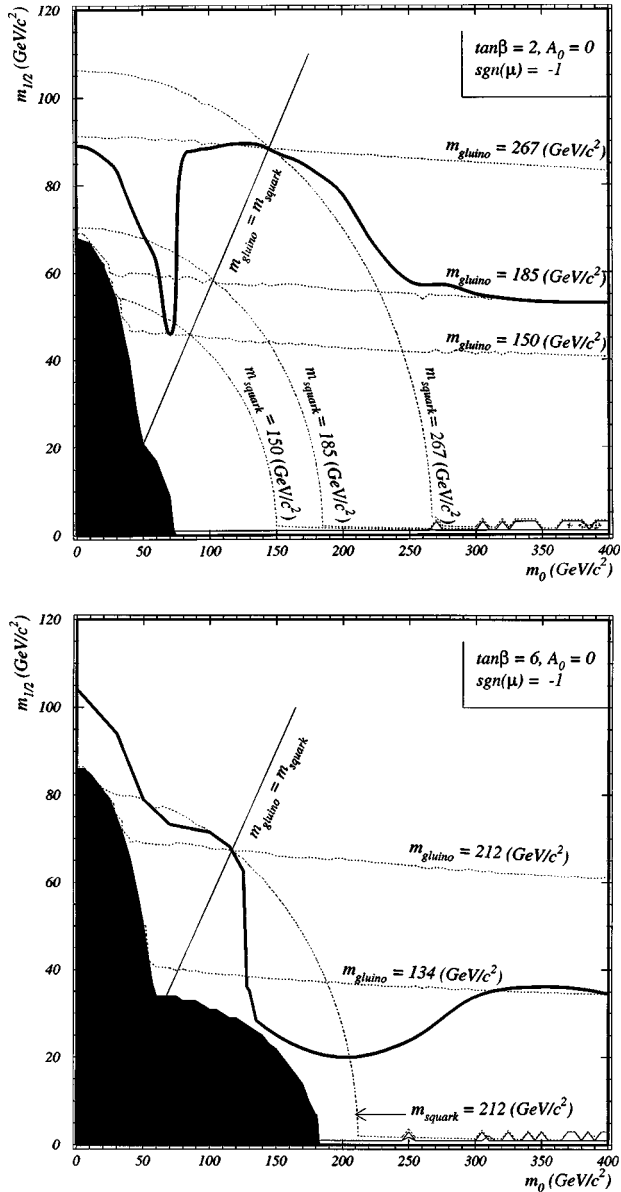


FIG. 9. The DØ limits on the minimal supergravity parameters m_0 and $m_{1/2}$ from the two leptons, two jets, and E_T search (Abachi *et al.*, 1997b): (a) the limits for $\tan\beta=2$, $A_0=0$, and $\mu<0$; (b) the same plot for $\tan\beta=6$, $A_0=0$, and $\mu<0$. In both plots, the dark shaded area is the region in which minimal supergravity is not compatible with electroweak symmetry breaking. Selected contours of squark and gluino masses are also shown.

but are studied separately. For comparison, LEP data exclude bottom squarks with masses below about 53–78 GeV, depending on the left-right mixing and the mass splittings (Schmitt, 1998).

C. Top squarks

The top squark (stop) is a special case worth a separate discussion. The mass degeneracy in the stop sector is expected to be strongly broken, and, for sufficiently large left-right mixing, the lightest stop can be rather

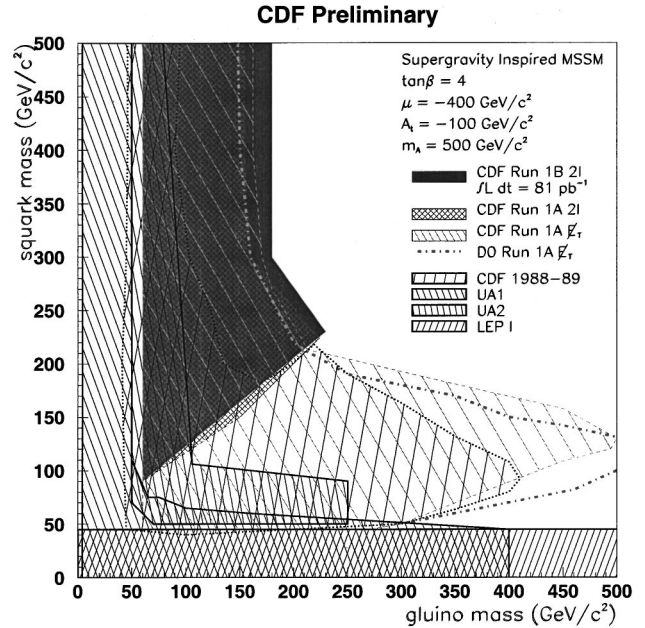


FIG. 10. CDF limits on the squark and gluino masses from the two like-sign leptons, two jets, and E_T search in 81 pb^{-1} . The limits were set using the ISAJET 7.06 Run-I parameter set (RIPS) with $\tan\beta=4$, $\mu=-400\text{ GeV}$, $A_t=-100\text{ GeV}$, and $m_A=500\text{ GeV}$.

light, possibly lighter than the lightest chargino. The lightest stop has about a tenth the production cross section of a top quark of the same mass, because the threshold behavior is β^3 (compared to β for fermion pairs) and only half the scalar partners are being considered. At leading order, the cross section is independent of the gluino mass and depends only on the stop mass.³⁵ Due to the large left-right mixing, the NLO supersymmetry QCD corrections must deal with different left- and right-handed couplings of the quarks to squarks and gluinos. The results for the stop pair-production cross section as a function of the stop mass are plotted in Fig. 12 (Beenakker, Kramer *et al.*, 1998).

The stop can be produced directly as $\tilde{t}\tilde{t}^*$ pairs or, depending on the stop mass, indirectly (Baer, Drees *et al.*, 1991) in decays of the top $t\rightarrow\tilde{\chi}_1^0$, or sparticles, such as $\tilde{\chi}_i^\pm\rightarrow b\tilde{t}$. Also depending on the stop mass, one of three decay modes is expected to dominate. If (a) $m_{\tilde{t}_1} > m_{\tilde{\chi}_1^0} + m_b$, then \tilde{t}_1 can decay into $b\tilde{\chi}_1^0$, followed by the decay of the chargino. This can look similar to the top decay $t\rightarrow bW$, but with different kinematics and branching ratios for the final state. Instead, if the stop is the lightest charged SUSY particle, it is expected to de-

³⁵Since the incoming partons are not tops, if flavor-changing neutral currents are suppressed by a supersymmetric GIM mechanism, stop production via gluino interchange is not allowed. After including the NLO supersymmetry QCD corrections, the dependence on $m_{\tilde{g}}$ and stop mixing becomes explicit, but, in practice, numerical results are insensitive to the exact gluino mass and the mixing.

TABLE VI. Selection criteria for Tevatron searches for squarks or gluinos in the dileptons, two jets, and E_T channel.

Quantity	Experiment	
	DØ	CDF
$\int \mathcal{L} dt (\text{pb}^{-1})$	92.9	81
$E_T^{e_1}, E_T^{e_2}$	$> 15, 15 \text{ GeV}$	$> 11, 5 \text{ GeV}$
$p_T^{\mu_1}, p_T^{\mu_2}$	N.A.	$> 11, 5 \text{ GeV}$
$E_T^{j_1, j_2}$	$> 20 \text{ GeV}$	$> 15 \text{ GeV}$
Mass window cut	$M_Z \pm 12 \text{ GeV}$	N.A.
ΔR between leptons and jets	N.A.	> 0.7
E_T	$> 25 \text{ GeV}$	$> 25 \text{ GeV}$
Like-sign dileptons	No requirement	Yes

cay exclusively through a chargino-bottom loop as (b) $\tilde{t}_1 \rightarrow c \tilde{\chi}_1^0$, which looks quite different from standard-model top decays. Finally, the stop can decay (c) $\tilde{t} \rightarrow b W \tilde{\chi}_1^0$ through a real or virtual top quark.

The possible signals from $\tilde{t}\tilde{t}^*$ production, with decay (a) and depending on the chargino decay modes, are (i) $b\bar{b}\ell^+\ell^-E_T$, (ii) $b\bar{b}\ell^\pm jjE_T$, or (iii) $b\bar{b}jjjjE_T$. These are similar to $t\bar{t}$ final states, except that (iii) has real E_T . If decay (b) dominates, this yields a signature of two acollinear charm jets and E_T . Finally, if decay (c) occurs, the events are similar to $t\bar{t}$ events, except that the kinematics of the individual t and \bar{t} are altered and there can be much more E_T .

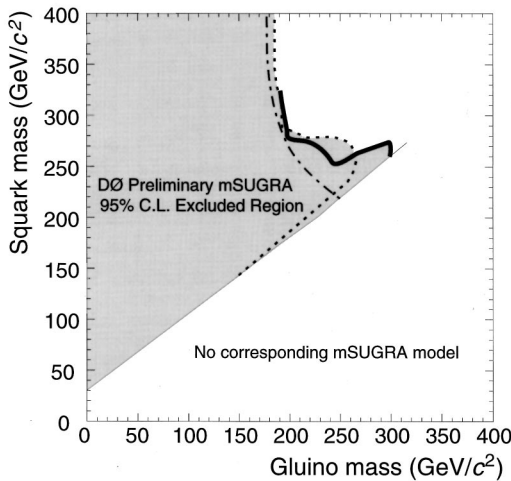


FIG. 11. Excluded region from various DØ analyses in the $m_{\tilde{Q}}-M_{\tilde{g}}$ plane with fixed minimal supergravity (mSUGRA) parameters $\tan\beta=2$, $A_0=0$, and $\mu<0$. Note that there are no mSUGRA models in the region to the right of the diagonal thin line. The heavy solid line is the limit contour of the DØ Run-Ib three jets+missing transverse energy analysis. The dashed line is the limit contour of the DØ Run-Ib dielectron analysis. The dot-dashed line is the limit contour of the DØ Run-Ia three and four jets and missing transverse energy analysis shown only in the region with valid minimal supergravity models.

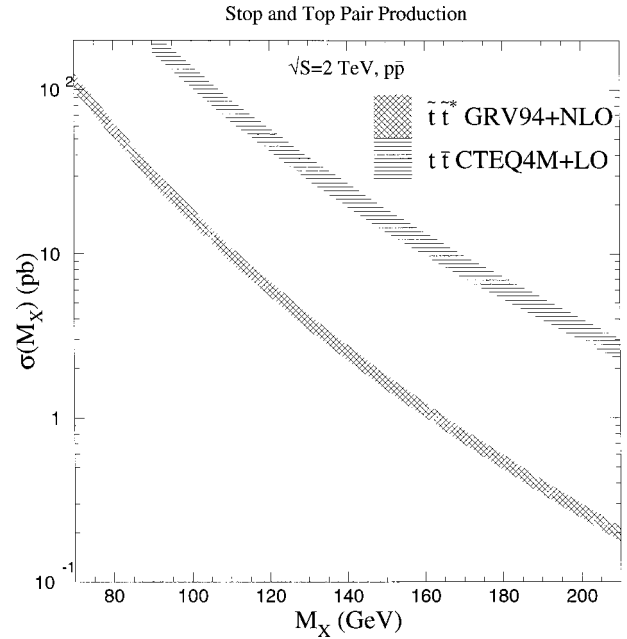


FIG. 12. The cross section for pair production of one stop quark vs the stop mass at the Tevatron, calculated to next-to-leading order. The band represents the variation of the scale from 1/2 to 2 times the stop mass. The top pair-production cross section vs the top mass is shown for reference, calculated only at leading order. The band represents the variation of the scale from 1/2 to 2 times the transverse mass $p_{T\oplus}m_t$, where $p_{T\oplus}$ is the transverse momentum of the top quark.

If the stop mass is in the range 100–150 GeV, $\tilde{t}\tilde{t}^*$ production may be too small to observe and it might be easier to observe a light stop in top-quark decays $t \rightarrow \tilde{t}\tilde{\chi}_1^0$. If $\tilde{\chi}_1^0$ is Higgsino-like, then the BR($t \rightarrow \tilde{t}\tilde{\chi}_1^0$) can be 50%. If decay (a) occurs, then top-quark events have the same signatures as in the standard model but have more E_T and softer jets and leptons. In case (b), fewer leptons and jets are produced and the E_T distribution is affected. If there is one standard-model top decay and one SUSY top decay, the final state can be $b\ell^\pm cE_T$, which would appear at a small rate in the Wjj sample, but not in the standard-model $t\bar{t}$ event sample.

An indirect limit can also be set on the decay (b). Such decays would not fall in the standard-model $t\bar{t}$ dilepton or lepton+jets samples, but instead would deplete them. Given a theoretical prediction for the $t\bar{t}$ production cross section, the branching ratio for decays which deplete the standard-model $t\bar{t}$ samples can be bounded in a straightforward manner. If decay (a) occurs, the analysis is more involved, since the kinematic acceptance for the stop decays must be calculated for many different choices of MSSM parameters. Also in case (a), some $\tilde{t}\tilde{t}^*$ events will feed into the top-quark event samples.

1. Direct top-squark pair production

DØ has searched for $\tilde{t}\tilde{t}^*$ production with $\tilde{t} \rightarrow c \tilde{\chi}_1^0$ using 7.4 pb^{-1} of Run Ia data (Abachi *et al.*, 1996b). The

TABLE VII. Selection criteria for the $D\bar{O}$ 2 jet+ E_T hadronic direct stop pair-production search. j_1 and j_2 are the leading and subleading jets ranked by E_T .

Quantity	$D\bar{O}$
$E_T^{j_1}, E_T^{j_2}$	>30 GeV
$\Delta\phi_{j_1-j_2}$	$90^\circ < \Delta\phi < 165^\circ$
$\Delta\phi_{j_1-E_T}$	$10^\circ < \Delta\phi < 125^\circ$
$\Delta\phi_{j_2-E_T}$	$10^\circ < \Delta\phi$
Lepton veto	e and μ
E_T	>40 GeV

signature is two acollinear jets and E_T , satisfying the selection criteria in Table VII. The dijet cross section at the Tevatron is large, and thus this signature has large instrumental backgrounds (without c -quark tagging). It also has backgrounds from vector-boson production. The QCD and vector-boson backgrounds would, naively, be a factor of $1/\alpha_s$ larger than for the hadronic squark/gluino search, as this search requires only two jets while the latter searches require at least three or four jets. This is not the case, since the multijet backgrounds can be controlled by requiring that $\Delta\phi > 45^\circ$ between the E_T and each jet, and that the jets not be back to back. The vector-boson backgrounds are controlled by requiring that the two leading jets be sepa-

TABLE VIII. Selection criteria for the CDF lepton+jets + b -tag direct stop pair-production search. $\ell=e$ or μ .

Quantity	CDF cuts
E_T^ℓ	>20 GeV
E_T	>20 GeV
$E_T^{j_1}, \eta$ range	>15 GeV, $ \eta < 2.0$
$E_T^{j_2}, \eta$ range	>8 GeV, $ \eta < 2.4$
Jets	$\leq 4, E_T^j > 8$ GeV
SVX b tag	$1, E_T^j > 8$ GeV

rated by at least $\Delta\phi > 90^\circ$. After these cuts, the dominant backgrounds are from W and Z boson production and decay, with the largest being $W \rightarrow \tau\nu$. If the τ decays hadronically, only one additional jet is necessary to fake the signature. Top-quark production is not as important a background for the light stop search as for the conventional hadronic squark search because of the lower jet-multiplicity requirement. As with the hadronic squark/gluino searches, the cuts are not very efficient for signal events. The efficiency is largest when the stop is heavy compared to the $\tilde{\chi}_1^0$ (near the kinematic boundary for the decay $\tilde{t}_1 \rightarrow t\tilde{\chi}_1^0$), reaching a maximum value of only 4%. The mass difference $m_{\tilde{t}_1} - M_{\tilde{\chi}_1^0}$ determines the E_T of the charm jet and rapidly limits this search mode as the charm jets become soft (see Fig. 13).

With the assumption that $\text{BR}(\tilde{t}_1 \rightarrow c\tilde{\chi}_1^0) = 1$, the predicted SUSY final state depends only on $M_{\tilde{\chi}_1^0}$ and $m_{\tilde{t}_1}$. The result of this search is a 95%-C.L. exclusion limit on a region in the $M_{\tilde{\chi}_1^0} - m_{\tilde{t}_1}$ plane, shown in Fig. 13. The production rate has been calculated using only leading-order production cross sections evaluated at the scale $Q^2 = 2stu/(s^2 + t^2 + u^2)$ from ISAJET, so the limit will change somewhat if reevaluated with NLO production cross sections.

CDF and $D\bar{O}$ have also presented results from a search for $\tilde{t}_1\tilde{t}_1^*$ production, with $\tilde{t}_1 \rightarrow b\tilde{\chi}_1^\pm$ (Baer, Sender, and Tata, 1994) followed by $\tilde{\chi}_1^\pm \rightarrow W^*\tilde{\chi}_1^0$. The two-body decay of the stop is dominant if kinematically allowed. The three-body decay of the chargino through a virtual W boson dominates as long as the sleptons and squarks are heavy enough. The analysis assumes branching ratios of unity for both of these decays. The CDF search is in the lepton+jets channel and uses a shape analysis of the transverse mass³⁶ of the lepton and E_T (Azzi, 1997). The selection criteria are given in Table VIII. For both searches, the detection efficiency is smaller than for $t\bar{t}$ production with a top quark of the same mass because of the softer leptons from the three-body decay $\tilde{\chi}_1^\pm \rightarrow \ell\nu\tilde{\chi}_1^0$. The mass splitting $M_{\tilde{t}_1} - M_{\tilde{\chi}_1^\pm}$ sets the efficiency for detecting the jets. The results of the CDF search are

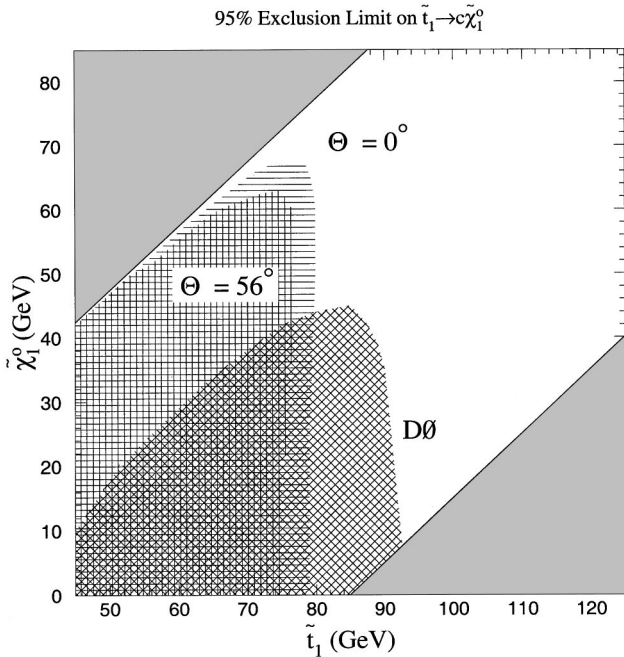


FIG. 13. Mass limits from the $D\bar{O}$ search for $\tilde{t}\tilde{t}^*$ production with the decay $\tilde{t} \rightarrow c\tilde{\chi}_1^0$ at the Tevatron (Abachi *et al.*, 1996b). The decay is kinematically forbidden in the two solid gray regions. The hatched regions marked $\Theta_{\tilde{t}}$ show the LEP excluded regions as a function of the stop mixing angle, which determines the strength of the stop coupling to the Z boson. The mixing does not affect the tree-level process at hadron colliders.

³⁶Transverse mass squared is $M_T^2 = (|\vec{p}_T^\ell| + |\vec{E}_T|)^2 - (\vec{p}_T^\ell + \vec{E}_T)^2$ and is a useful experimental quantity when information about the longitudinal component of momentum is missing.

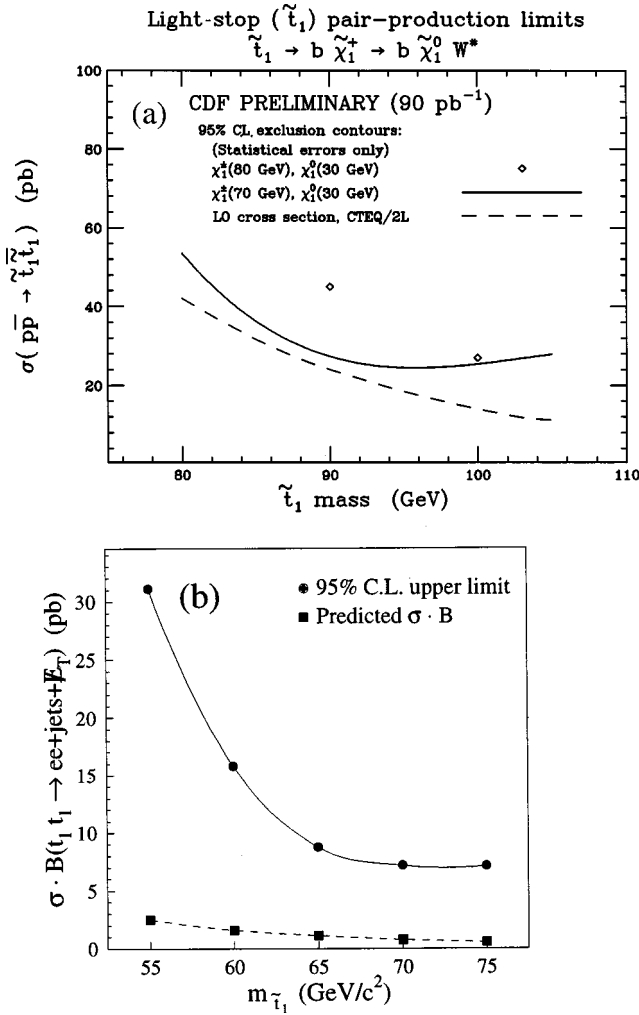


FIG. 14. Limits on cross section \times branching-ratio for direct stop production vs the stop mass: (a) The CDF limit from 90 pb^{-1} of data assuming the decay mode $\tilde{t}_1 \rightarrow b\tilde{\chi}_1^+ (\rightarrow W^* \tilde{\chi}_1^0)$ for two choices of chargino mass: 80 GeV (symbols) and 70 GeV (solid line). The lightest-superpartner mass is fixed at 30 GeV. One W must decay semileptonically, giving a signature of a lepton, E_T , and jets. The theoretical cross section (dashed line) is from ISAJET 7.06. (b) The DØ 95% C.L. limit for a final state containing two electrons, E_T , and jets (solid line; see Abachi *et al.*, 1996c). The mass of the lightest chargino is assumed to be 47 GeV. The predicted cross section \times branching ratio from ISAJET is also shown (dashed line).

shown in Fig. 14(a). The decay $\tilde{\chi}_1^\pm \rightarrow W^* \tilde{\chi}_1^0$ is assumed using the masses (i) $M_{\tilde{\chi}_1^\pm} = 80 \text{ GeV}$ and $M_{\tilde{\chi}_1^0} = 30 \text{ GeV}$ and (ii) $M_{\tilde{\chi}_1^\pm} = 70 \text{ GeV}$ and $M_{\tilde{\chi}_1^0} = 30 \text{ GeV}$. Given these mass choices, there is little other parameter dependence. Presently, the cross-section limits are above the predicted cross sections due to the high E_T cuts.

DØ searches in the dilepton channel (Abachi *et al.*, 1996c) using the cuts listed in Table IX. The signature is similar to the squark and top-dilepton searches. The results are shown in Fig. 14(b), assuming $M_{\tilde{\chi}_1^\pm} = 47 \text{ GeV}$ and $M_{\tilde{\chi}_1^0} = 28.5 \text{ GeV}$. A substantial background comes from $Z \rightarrow \tau^+ \tau^-$, again requiring a high threshold for the

TABLE IX. Selection criteria for the DØ dielectron+jets + E_T direct stop pair-production search.

Quantity	DØ cuts
$E_T^{e_1}, E_T^{e_2}$	$> 16,8 \text{ GeV}$
E_T^j	$> 30 \text{ GeV}$
$E_T^{e_1} + E_T^{e_2} + E_T $	$< 90 \text{ GeV}$
M_{ee}	$< 60 \text{ GeV}$
E_T	$> 22 \text{ GeV}$

E_T cuts, and no limit can be set.

The above analyses were done in regions of SUSY parameters that have been excluded by LEP. They show, however, the procedures to be followed in redoing these studies for other regions of the MSSM parameter space.

2. Top-squark production from top decays

CDF has presented another analysis using the silicon-vertex-tagged lepton+jets sample to search for the decay $t \rightarrow \tilde{t}_1 \tilde{\chi}_1^0$, with $\tilde{t}_1 \rightarrow b \tilde{\chi}_1^\pm$ (Wilson, 1997). If one of the top quarks in a $t\bar{t}$ event decays $t \rightarrow bW (\rightarrow \ell \nu)$ and the other $t \rightarrow \tilde{t}_1 \tilde{\chi}_1^0$ followed by $\tilde{t}_1 \rightarrow b \tilde{\chi}_1^\pm (\rightarrow jj \tilde{\chi}_1^0)$ or $t \rightarrow bW (\rightarrow jj)$ and $t \rightarrow \tilde{t}_1 \tilde{\chi}_1^0$ followed by $\tilde{t}_1 \rightarrow b \tilde{\chi}_1^\pm (\rightarrow \ell \nu \tilde{\chi}_1^0)$, the signature is $b\bar{b} \ell \nu jj + E_T$, the same as in the standard model, but where the E_T includes the momentum of the $\tilde{\chi}_1^0$. The lepton+jets channel has a large number of events, so a kinematic analysis can be performed on the event sample. Due to the mass of the $\tilde{\chi}_1^0$ and the intermediate sparticles in the decay chain, the jets from the SUSY decay are significantly softer. This difference is exploited as the basis of the search.

The cuts listed in Table X are optimized for acceptance of the SUSY decay and rejection of W +jets background. A likelihood function is computed for each

TABLE X. Selection criteria for the CDF search for top decaying into stop in the signature of one lepton (ℓ), E_T , and three jets including at least one b tag, where $\ell = e$ or μ . The quantity $|\cos \theta^*|$ is the polar angle of a jet in the rest frame of the ℓ , E_T , and jets. ΔR_i is the distance between a jet i and the next-nearest jet in $\eta - \phi$ space. The jets are ordered in E_T , so $E_T^1 > E_T^2 > E_T^3$.

Quantity	CDF cuts
$\int \mathcal{L} dt$	110 pb^{-1}
E_T^ℓ	$> 20 \text{ GeV}$
E_T	$> 45 \text{ GeV}$
$M_T(\ell E_T)$	$> 40 \text{ GeV}$
$p_T(\ell E_T)$	$> 50 \text{ GeV}$
$E_T^{1,2}$	$> 20 \text{ GeV}, \eta < 2.0$
E_T^3	$> 15 \text{ GeV}, \eta < 2.0$
$ \cos \theta^* _{1,2,3}$	$< 0.9, 0.8, 0.7$
$\Delta R_{1,2,3}$	≥ 0.9
Number of SVX b tags	≥ 1 for $E_T^j > 15 \text{ GeV}$

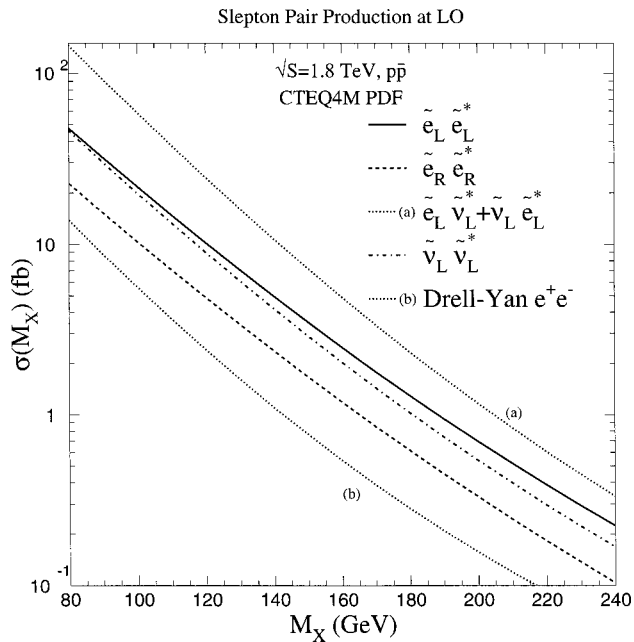


FIG. 15. Production cross sections for sleptons vs slepton mass at the Tevatron. The Drell-Yan cross section for producing e^+e^- (curve b) is plotted as a function of $M_{e^+e^-}=2M_X$. On this scale, the Drell-Yan peak ($Z \rightarrow e^+e^-$) would appear at $M_X=45$ GeV.

event reflecting the probability that the jets with the second- and third-highest E_T in the event are consistent with the stiffer standard-model distribution (as compared to the SUSY distribution). The distribution of this likelihood function shows a significant separation of these two hypotheses. After applying the cuts listed in Table X, nine events remain, all of which fall outside of the SUSY signal region. For stop masses between 80 and 150 GeV and chargino masses between 50 and 135 GeV, a $BR(t \rightarrow \tilde{t}_1 \tilde{\chi}_1^0) = 50\%$ is excluded at the 95% C.L., provided that $M_{\tilde{\chi}_1^0} = 20$ GeV. Because $M_{\tilde{\chi}_1^0}$ is fixed in this manner, it is not related to $M_{\tilde{\chi}_1^\pm}$ as in supergravity. At present, only this one example is available (for a value of $M_{\tilde{\chi}_1^0}$ already excluded by LEP); more statistics will significantly improve it.

The most robust Tevatron limit on top squarks comes from pair production with the decay $\tilde{t} \rightarrow c \tilde{\chi}_1^0$. The relative reach of the Tevatron and LEP is illustrated in Fig. 13. The Tevatron limit (labeled $D\emptyset$) extends to stop masses of 90 GeV, provided that the splitting between the stop and lightest-superpartner mass is greater than about 40 GeV. This limit depends only on the assumption $BR(\tilde{t} \rightarrow c \tilde{\chi}_1^0) = 1$. The LEP limit depends moderately on the details of the stop left-right mixing. A stop mass of below about 71–77 GeV can be excluded as long as the mass splitting is greater than about 10 GeV (Schmitt, 1998; Asai *et al.*, 1997).

D. Sleptons

At hadron colliders, sleptons can be directly pair produced through their electroweak couplings to the γ , Z ,

and W bosons. Figure 15 shows the cross sections as a function of the corresponding slepton mass compared to the differential Drell-Yan pair-production cross section, $d\sigma_{D-Y}/dQ$, where $Q=2M_X$. The rate for slepton pair production is at most a few tens or hundreds of fb at the Tevatron, and so far neither collaboration has presented results on searches for sleptons in the supergravity or RIPS framework (we describe limits in gauge-mediated models later).

A (stable) charged slepton is not a viable lightest-superpartner candidate, so the decays $\tilde{\ell}_{L,R}^\pm \rightarrow \ell^\pm \tilde{\chi}_i^0$ or $\tilde{\ell}_L^\pm \rightarrow \nu \tilde{\chi}_i^\pm$ are expected. The sneutrino, instead, can be the lightest superpartner, or it can decay invisibly $\tilde{\nu} \rightarrow \nu \tilde{\chi}_1^0$ or visibly $\tilde{\nu} \rightarrow \tilde{\chi}_i^\pm \ell^\mp$. If $m_{\tilde{\nu}} < m_{\tilde{\chi}} < M_{\tilde{\chi}_1^0}$, then the decay $\tilde{\ell} \rightarrow \ell' \nu' \tilde{\nu}$ (or $\tilde{\ell} \rightarrow q \bar{q} \tilde{\nu}$) is possible. Promising signatures are (i) $e^+e^-, \mu^+\mu^-, \tau^+\tau^-$ plus E_T (Baer, Chen *et al.*, 1994), (ii) $e\mu, e\tau, \mu\tau$ plus E_T , and (iii) e, μ , or τ + jets plus E_T (or jets plus E_T). Although charged slepton production can lead to charged leptons in the final state, there is no guarantee.

The major background to same-flavor lepton pairs is Drell-Yan pair production, with fake E_T from mismeasurement of the lepton or jets in the event. Most of this background can be removed by vetoing on a dilepton mass window around the Z mass, by requiring significant $E_T (\geq 25$ GeV), and by vetoing events with the E_T pointing in ϕ along one of the leptons or a jet. Top-quark production is also a major background to a slepton heavier than the lighter gaugino, as it produces dilepton events that have real E_T (Baer *et al.*, 1994). Untangling a few heavy-slepton events from top events would be difficult at the present low level of statistics.

Inclusive searches have the advantage of a larger acceptance than searches in exclusive channels. A unique signature of slepton production directly or in cascade decays would be the apparent violation of lepton universality. If the sleptons are not degenerate, both the production and decays of the sleptons will favor one or two leptons over the others, resulting in an imbalance in the detected $e/\mu/\tau$ ratios in SUSY-enhanced channels. The dominant backgrounds to inclusive leptons come from heavy flavor production (e.g., b quarks), and (single) W and Z boson production (Abe *et al.*, 1995b). Because sparticles are produced in pairs, it may be possible to discriminate against standard-model backgrounds by requiring the identification of a part of the decay of the second sparticle. Examples of channels that may have enhanced SUSY contributions over standard-model backgrounds (and hence possibly apparent lepton universality violation) are those that have, in addition to the lepton, a γ , W , Z , additional lepton, or third-generation particle.

The relative importance of slepton production to other sparticle production processes is much larger at LEP than at the Tevatron. The present LEP data exclude selectrons below about 75 GeV, provided the mass difference between the selectron and lightest superpartner is greater than 10 GeV. The limits on smuons and especially staus are less stringent (Schmitt, 1998).

E. Charged Higgs bosons

Even though Higgs bosons are not sparticles, the discovery of a charged Higgs boson would be considered *indirect* evidence for supersymmetry.³⁷ If it is light enough, the charged Higgs boson H^\pm can be produced in the decay of the top quark $t \rightarrow bH^+$ (Godbole and Roy, 1991; Guchait and Roy, 1997). At tree level, the branching fraction for this decay depends on the charged Higgs-boson mass and $\tan\beta$. When kinematically allowed, this branching ratio is larger than 50% for $\tan\beta$ less than approximately 0.7 or greater than approximately 50, and completely dominates for very small or very large values of $\tan\beta$. However, as discussed in Sec. II.A, values of $\tan\beta \leq 0.6-0.7$ or above 60 would be associated with large top or bottom Yukawa couplings, which will become infinite at scales not far above the TeV scale. In general, at reasonably small values of $\tan\beta$, the charged Higgs boson decays $H^+ \rightarrow c\bar{s}$; at large $\tan\beta$ it instead decays $H^+ \rightarrow \tau^+ \nu_\tau$.

CDF has searched for the decay $t \rightarrow bH^+$ using both direct (Abe *et al.*, 1994d; Abe *et al.*, 1997b) and indirect (Bevensee, 1997) methods. [See also Jessop, 1994. This analysis uses 4.2 pb^{-1} from the 1989 run and a signature of a hadronically decaying $\tau + \geq 1 \text{ jet} + E_T$.] Direct searches look for an excess over standard-model expectations of events with τ leptons from the charged Higgs-boson decay $H^+ \rightarrow \tau^+ \nu_\tau$ (dominant for large $\tan\beta$). On the other hand, indirect searches are “disappearance” experiments, relying on the fact that decays into the charged Higgs-boson mode will deplete the standard-model decays $t \rightarrow bW$, decreasing the number of events in the dilepton and lepton+jets channels.

The CDF direct search at large $\tan\beta$ uses two sets of cuts, listed in Table XI, to search for an excess of τ 's in $t\bar{t}$ events. The first set selects a sample containing a τ that decays hadronically, an SVX b -tagged jet, E_T and objects indicating activity from the second top decay: a second jet and a third jet or lepton. As M_{H^\pm} approaches m_t , the b produced in the top decay $t \rightarrow bH$ becomes less energetic, causing a reduced efficiency for the jet and b -tagging requirements. To maintain efficiency in this region, a second set of cuts accepts events that have two high- E_T τ 's and E_T .

The signature for hadronically decaying τ 's is a narrow jet associated with one or three tracks, with no other tracks nearby. Typically the τ tracks are required to be within a cone of opening angle 10° with no other tracks within 30° . Fake rates, measured as the probability that a generic jet is identified as a τ , are approximately 1% or less. These fake rates are too high to identify τ 's in a sample dominated by QCD. However, if another selection criterion is added that further purifies the sample, τ 's can be identified with a good signal-to-background ratio. For example, hadronic decays of the τ

³⁷If $M_{H^\pm} \lesssim 300 \text{ GeV}$, then there must exist extra light-matter fields beyond the standard-model to partially cancel the H^\pm contribution to $\text{BR}(b \rightarrow s\gamma)$.

TABLE XI. Selection criteria for the CDF direct search for $t \rightarrow bH^\pm (\rightarrow \tau\nu)$ in 100 pb^{-1} of data. The τ 's are identified in their hadronic decay modes as one or three isolated, high- p_T tracks. Events are accepted if they pass the cuts in either analysis path. The E_T of a τ candidate is the E_T of the corresponding cluster in the calorimeter.

Quantity	CDF
Analysis path 1:	
E_T^τ	$> 20 \text{ GeV}$
E_T	$> 30 \text{ GeV}$
E_T^j , SVX tagged	$> 15 \text{ GeV}$
E_T^l	$> 10 \text{ GeV}$
Additional object	e, μ, τ or 3rd jet with $E_T > 10 \text{ GeV}$
Analysis path 2:	
$E_T^{\tau_1}, E_T^{\tau_2}$	$> 30 \text{ GeV}$
$\Delta\phi(\tau_1, \tau_2)$	$< 160^\circ$
E_T	$> 30 \text{ GeV}$

are observed in (i) monojet ($W \rightarrow \tau\nu$), (ii) lepton, E_T and jet ($Z \rightarrow \tau\tau$), and (iii) the lepton+jets top-quark samples (Gallinaro, 1996; Hohlmann, 1997).

The CDF direct search for $t\bar{t}$ events with one or two charged Higgs bosons decaying to τ leptons sets limits by two methods. In the first method, a $t\bar{t}$ production cross section and a SUSY model (M_{H^\pm} and $\tan\beta$) is assumed and the number of expected τ events is computed. If the number expected is too large to be consistent with the observed number at the 95% C.L., the SUSY model is excluded for that $t\bar{t}$ cross section. This method excludes a charged Higgs boson with mass less than about 150 GeV (100 GeV) if $\tan\beta$ is greater than approximately 100 (50) and the top cross section³⁸ is 7.5 pb, as shown in Fig. 16(a).

The second method combines the observation of $t \rightarrow bW$ decays into leptons (e or μ) and jets with the number of τ decays from the direct search. This has the advantage that a top production cross section does not need to be assumed. The lepton+jets sample defines a top production cross section which, in turn, through the SUSY model, predicts the number of τ events expected. If the number is too large to be consistent with the ob-

³⁸The reader should be aware that there are subtleties in analyses that assume cross sections. The CDF experiment normalizes all cross sections to its measured proton-antiproton cross sections, rather than to a hard process such as W production. The CDF total cross section, in the judgment of one of the authors (HF), is most likely 10% too high, and thus all cross sections (in particular, the top cross section) are too high. For analyses that compare different channels internally this has no effect, but for analyses that compare to theoretical predictions the reader should be careful. The $D\bar{D}$ experiment normalizes to a weighted mean of the CDF and E710 values for the total cross section, which is 2.4% lower than the CDF value.

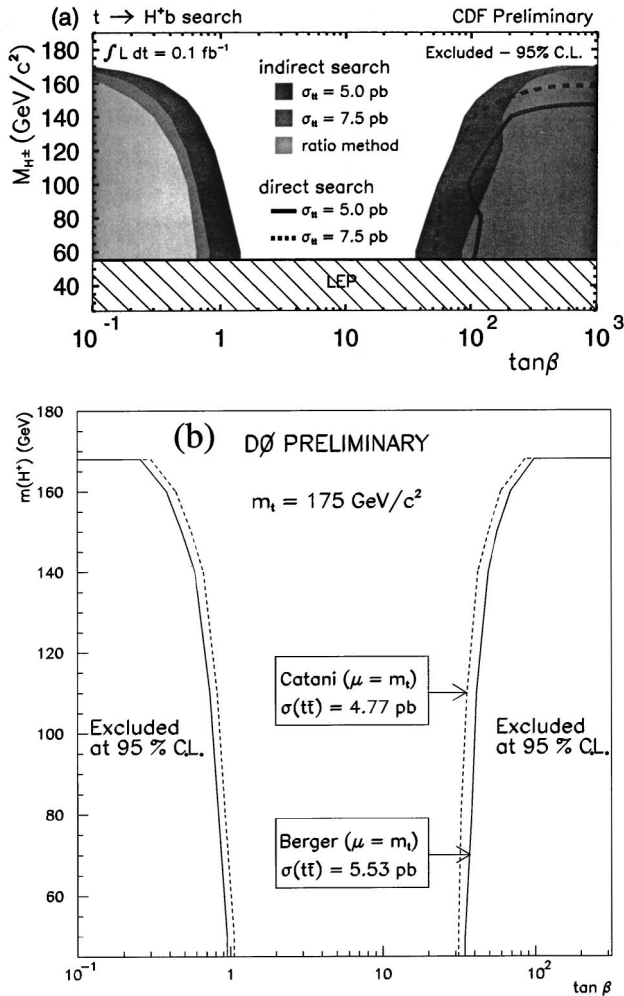


FIG. 16. Limits from searches for charged Higgs-boson decays of the top quark in $t\bar{t}$ events. (a) Exclusion space for the CDF search. The shaded regions are from the indirect searches. For the regions labeled $\sigma_{t\bar{t}}=5.0$ and 7.5 pb, a top production cross section is assumed and points are excluded if the predicted SUSY decays have depleted the standard-model channels to an extent that they are inconsistent with the data. The “ratio method” is an indirect method comparing the number of lepton+jets events to the number of dilepton events, and no top cross section is assumed. The region excluded with solid lines at high $\tan\beta$ is from a direct search for events where one or both top quarks decay to $bH^+(\rightarrow\tau^+\nu)$ and information from the standard-model channels is ignored. (b) The results of a DØ indirect search for a charged Higgs boson assuming $m_t=175$ GeV and a $t\bar{t}$ production cross section of 5.53 pb and 4.77 pb. This limit is based on the full Run-I DØ data sample.

servation, the model is excluded. The limits set by this method are presented in detail elsewhere (Abe *et al.*, 1997b). Qualitatively, the limits are similar to those set by the indirect method (discussed below).

At small $\tan\beta$, a direct search is difficult since the charged Higgs boson decays into two jets. Instead, only the indirect method is applied. This method can also be used for large- $\tan\beta$ searches. The observed numbers of dilepton and lepton+jets events are consistent (at the 95% C.L.) with a minimum production and decay rate in

the standard-model. For an assumed $t\bar{t}$ cross section (and a charged Higgs-boson mass and $\tan\beta$), a simulation of the expected mixture of standard-model and charged Higgs-boson decays predicts a number of events in the standard-model channels. At some points in the parameter space, the decays to charged Higgs bosons are more pronounced. If the number expected in a standard-model channel is not consistent with the rate defined by the data, the assumed values are excluded. This method provides the limit displayed in Fig. 16(a). The cross section of 5 pb is the expected cross section for a top mass of 175 GeV; the curves using 7.5 pb show the sensitivity of the limit to the assumed top cross section. Also shown in the figure is how the limit in the region of large $\tan\beta$ can be extended using the assumptions of the indirect method. In this region the possibility that a τ decay produces a high- p_T lepton is included.

The area in Fig. 16(a) labeled “ratio method” is the exclusion region for an indirect search that does not make an assumption for the $t\bar{t}$ cross section. If charged Higgs-boson decays were competing with standard-model decays, the ratio of dilepton events to lepton+jets events would decrease, regardless of the $t\bar{t}$ cross section. This occurs because the lepton+jets yield is proportional to the standard-model branching ratio, while the dilepton yield is proportional to the branching ratio squared. For each SUSY parameter point, the lepton+jets sample can be used to infer a top cross section which, in turn, predicts a number of dilepton events. The point is excluded if the prediction is inconsistent with the dilepton data. Although this method excludes less parameter space, it is important since the $t\bar{t}$ cross section may be enhanced by SUSY mechanisms such as $\bar{g}\rightarrow t\bar{t}$ (Mrenna and Kane, 1996). At present, this method only excludes values of $\tan\beta\leq 0.7$, which are not of much interest according to present theoretical bias.

DØ has also searched for a charged Higgs boson lighter than the top quark using the indirect method (Abachi *et al.*, 1997c). The analysis compares the number of events observed in the lepton+jets channel to the number predicted assuming a theoretical $t\bar{t}$ production cross section. The limits depend on the mass of the charged Higgs boson, $\tan\beta$, and the top-quark mass m_t . Table XII shows the selection criteria used in the search. Figure 16(b) shows the excluded region.

Recent studies have shown that quantum SUSY effects (supersymmetry QCD and electroweak radiative corrections) to the decay mode $t\rightarrow bH^+$ (with subsequent decays into τ 's) may be important and should be considered in future analyses (Guasch *et al.*, 1995; Coarasa *et al.*, 1998; Guasch and Sola, 1998; Sola, 1998).

In conclusion, Tevatron data can probe charged Higgs-boson masses as large as m_t for very large or very small $\tan\beta$. However, for values of $\tan\beta$ compatible with a perturbative description of the MSSM up to scales near M_{GUT} , the masses that can be probed are of the order of 100 GeV. In contrast, the LEP search for charged Higgs-boson pair production in a generic two-doublet extension of the standard model can exclude a

TABLE XII. Selection criteria of the $D\bar{O}$ search for a charged Higgs boson produced in top-quark decays. In addition, events are vetoed if the \vec{E}_T is aligned in ϕ within 25° of a muon or if the muons in a μ event with a μ -tagged jet have a good fit to the decay $Z \rightarrow \mu\mu$. The neutrino is reconstructed from the lepton and the \vec{E}_T using a W mass constraint and selecting the lowest p_z solution. H_T is the scalar sum of the jet E_T . Aplanarity is 3/2 times the smallest eigenvalue of the tensor: $M^{ab} = \Sigma p_i^a p_i^b / \Sigma p_i^2$ where the sum is over the jets, lepton, and neutrino.

Quantity	$D\bar{O}$ topological	$D\bar{O}$ tagged
E_T threshold on leptons	20 GeV	20 GeV
Max η for leptons	2 (e) 1.7 (μ)	2 (e) 1.7 (μ)
Number of jets	4	3
jet E_T threshold	15 GeV	20 GeV
\vec{E}_T	25 GeV (e) 20 (μ)	20 GeV
H_T	180 GeV	110 GeV
Sum of lepton E_T and \vec{E}_T	60 GeV	N.A.
Aplanarity	0.065	0.04
$ \eta_W $	2.0	N.A.
μ -tagged jets	veto	require

charged Higgs-boson mass below about 52 GeV for any reasonable $\tan\beta$ (Barate *et al.*, 1998; Hinchliffe, 1998). In the MSSM, the charged Higgs-boson mass will typically be beyond the reach of LEP.

F. Neutral Higgs bosons

Within the MSSM, the main production channels for the lightest CP -even Higgs boson h at the Tevatron are the same as for a standard-model Higgs boson, Wh or Zh production (Stange *et al.*, 1994). The cross sections behave in such a way that these channels are relevant for large values of the CP -odd mass M_A (the standard-model limit) or for small M_A and small $\tan\beta$. The heavy CP -even Higgs boson H will become relevant for searches at an upgraded Tevatron through ZH , WH production, in some region of parameter space, complementary to the one relevant for the light CP -even Higgs-boson searches. In addition, the enhancement of the bottom Yukawa coupling in the large- $\tan\beta$ regime can render the production processes $hb\bar{b}$, $Ab\bar{b}$, and $Hb\bar{b}$ useful to perform searches in a large region of parameter space (Dai *et al.*, 1996).

Both collaborations have searched for a neutral Higgs boson in the mode $q\bar{q}' \rightarrow W^* \rightarrow W(\rightarrow e\nu, \mu\nu)h(\rightarrow b\bar{b})$. $D\bar{O}$ has searched in 100 pb^{-1} of data using a data sample containing a lepton, \vec{E}_T and two jets (Abachi *et al.*, 1997b). One of the jets must have a muon associated with it for b tagging. The cuts are listed in Table XIII. The detection efficiency is in the range 2–5%, not including the branching ratio of the W . The b tag alone has an efficiency of 10–15%. Twenty-seven events pass the selection criteria; 25.5 ± 3 events are expected from Wjj and $t\bar{t}$. The limits shown in Fig. 17 are set by a

TABLE XIII. Selection criteria of Tevatron searches for the associated production of a neutral Higgs boson and a W or Z , and the Higgs boson decays to $b\bar{b}$.

Quantity	CDF	$D\bar{O}$
$WH \rightarrow \ell \nu b\bar{b}$		
$E_T^e (E_T^\mu)$	>25(20) GeV	>20(20) GeV
$\vec{E}_T e (\mu)$	>25(20) GeV	>20(20) GeV
E_T^{j1}, E_T^{j2}	>15 GeV	>15 GeV
b tagging	one SVX tag	one μ tag
$(W, Z)H \rightarrow jjb\bar{b}$		
Quantity	CDF	
E_T^{j1-4}	>15 GeV	
b tagging	2 SVX tags	
$P_T(b\bar{b})$	>50 GeV	

simple event-counting method and by fitting the $b\bar{b}$ dijet mass spectrum.

CDF has recently completed a similar search for the same decay mode using 109 pb^{-1} of data (Abe *et al.*, 1997c). All events must have one SVX b tag. These events are split into single-tagged (one SVX tag) and double-tagged samples [two SVX tags or one SVX and one lepton (e or μ) tag]. Efficiencies for the single-tagged events, not including the W branching ratio, are in the range 3–5%; the tag by itself contributes a 25% efficiency. The 36 single-tagged events or six double-

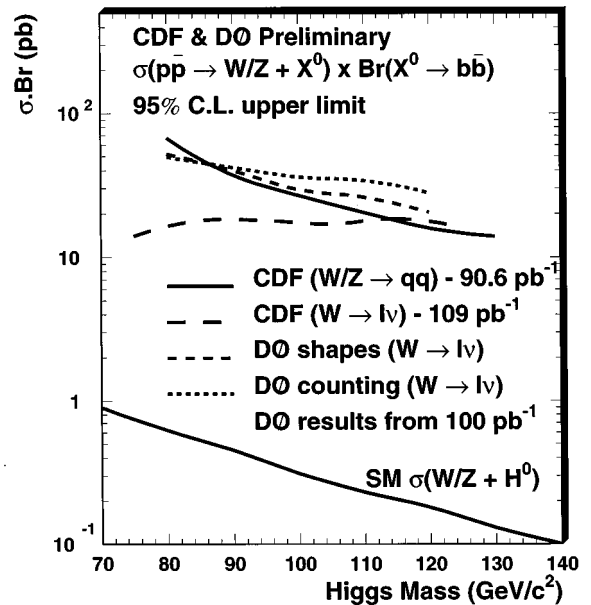


FIG. 17. Limits from CDF and $D\bar{O}$ for the associated production of a neutral Higgs boson and a W or Z boson. The CDF limits are shown for the final states of $\ell \nu b\bar{b}$ and $jjb\bar{b}$, and the $D\bar{O}$ limit is for the final-state $\ell \nu b\bar{b}$. The limit is set using a simple counting method and by fitting the $b\bar{b}$ spectrum (“shapes”). The predicted standard-model cross section \times branching ratio is also shown for reference (lower solid line).

TABLE XIV. Selection criteria for the $D\bar{O}$ search for a Higgs boson produced in association with a hadronically decaying W , and which decays to two photons.

Quantity	$D\bar{O}$
E_T threshold on photons	1 above 20 GeV, 1 above 15
$ \eta $ on photons	<1.1 or $1.5 < \eta < 2.25$
E_T threshold jets	1 above 20 GeV, 1 above 15
$ \eta $ on jets	<2
vector sum of photon E_T	<10 GeV
vector sum of jet E_T	<10 GeV

tagged events are consistent with the 30 ± 5 (3.0 ± 0.6) expected from the standard-model W +jets and $t\bar{t}$. Both the single- and double-tagged dijet mass distributions are fit simultaneously to set the limits shown in Fig. 17.

The process $q\bar{q} \rightarrow Z^* \rightarrow Zh$ occurs at a comparable rate to the W^* process. CDF has searched for both associated production processes assuming $W/Z \rightarrow jj$ (Valls, 1997). The event selection criteria are listed in Table XIII. In 91 pb^{-1} of data, 589 events remain, consistent with the expectation from QCD heavy-flavor production and fake tags. To set limits, the $b\bar{b}$ dijet mass spectrum is fit. Also shown in Fig. 17 is the standard-model production cross section for Wh and Zh as a function of the Higgs boson mass. The present experimental limits are roughly two orders of magnitude away from the predicted cross section. However, Run II will provide at least 20 times the data and a substantially improved efficiency. This plus the possibilities of looking at other decay modes (i.e., $Zh \rightarrow \nu b \bar{b}$) holds promise for Higgs physics at the Tevatron (Mrenna and Kane, 1994; Mrenna, 1997b).

$D\bar{O}$ has also searched for a fermio-phobic Higgs boson, i.e., one with suppressed couplings to fermions (Abachi *et al.*, 1997d). For a light neutral Higgs boson, the decay through a virtual W loop to a $\gamma\gamma$ final state can be dominant (Stange *et al.*, 1994a). Events are selected containing two photons with $E_T > 20$ and 15 GeV, and two jets with $E_T > 20$ and 15 GeV (see Table XIV). No evidence of a resonance is seen in the mass distribution of the two photons, and $D\bar{O}$ excludes, at a 95% C.L., such Higgs bosons with masses less than 81 GeV. The branching fraction for $h \rightarrow \gamma\gamma$ is taken from Stange *et al.* (1994a).

At present, none of the Tevatron limits on neutral Higgs-boson production exclude any theoretically favored regions of MSSM parameter space. For large m_A , LEP data can exclude a standard-model-like Higgs boson with mass below about 90 GeV. For small m_A and intermediate or large values of $\tan\beta$, LEP excludes masses below about 75 GeV from hA production (Hinchliffe, 1998; Treille, 1998).

G. R -parity violation and a short-lived lightest superpartner

Allowing for R -parity violation (RPV) in the MSSM opens a host of possibilities at the Tevatron. Either considering baryon-number-violating operators (UDD) or

TABLE XV. Selection criteria of the CDF search for R -parity-violating processes using 105 pb^{-1} of data.

Quantity	CDF
$E_T^{e_1}, E_T^{e_2}$	>15 GeV, $ \eta < 1.1$
$Q_{e_1} + Q_{e_2}$	± 2
$E_T^{j_1}, E_T^{j_2}$	>15 GeV, $ \eta < 2.4$
$S = \mathbf{E}_T / \sqrt{\sum E_i}$	<5 GeV/2

lepton-number-violating ones (LLE and LQD), there are many resonant and nonresonant particle production mechanisms and subsequent decay processes which have been analyzed in the literature (Dimopoulos, Ezmailzadeh, *et al.*, 1990; Dreiner and Ross, 1991; Roy, 1992; Barger *et al.*, 1994; Baer, Kao, and Tata, 1995; Guchait and Roy, 1996; Kalinowski *et al.*, 1997) and which certainly deserve detailed experimental studies. In this section we restrict ourselves to the experimental analyses performed so far.

The possible excess of HERA events at large Q^2 has triggered interest in studying the consequences of the interaction of a light squark (preferably a top or charm squark) with an electron and a d quark (Choudhury and Raychaudhuri, 1997). If the gluino were heavier than this squark, then gluino pair production at the Tevatron and the decay $\tilde{g} \rightarrow \bar{c}\tilde{c}_L$ through R -conserving couplings, followed by the RPV decay $\tilde{c}_L \rightarrow e^+d$, would yield the signature of two electrons and four jets. If the RPV decay $\tilde{c}_L \rightarrow e^+d$ is allowed through the coupling λ'_{121} , then from the structure of the R -parity-violating Lagrangian [Eq. (24)] it follows that $\tilde{s}_L \rightarrow \nu_e d$, $\tilde{d}_R \rightarrow e^-c$, and $\tilde{d}_R \rightarrow \nu_e s$ are also allowed. If $m_{\tilde{c}_L} \approx m_{\tilde{s}_L}$ (which is guaranteed) $\approx m_{\tilde{d}_R}$ (which is probable), then the gluino decays equally to $\tilde{c}_L\bar{c}$, $\tilde{s}_L\bar{s}$, and $\tilde{d}_R\bar{d}$ (+H.c.) final states. Assuming that only R -parity-violating decays occur, then 1/2 of gluino decays produce a charged lepton. Therefore $\tilde{g}\tilde{g}$ production produces like-sign dileptons 1/8 of the time. The requirement of only R -parity-violating decays demands $M_{\tilde{\chi}_1^0} > m_{\tilde{Q}}$.

CDF has performed a search (Chertok, 1998) for an R -parity-violating squark with the signature of two like-sign electrons and two jets. In 105 pb^{-1} of Run Ia and Ib data, no events remain after all cuts are applied (see Table XV). Varying the masses of the SUSY particles does not alter the acceptance significantly, since they are heavy enough for the decay products to easily pass the E_T thresholds. Because of this, the limit on the cross section \times branching ratio is approximately constant at 0.19 pb. For $m_{\tilde{c}_L} = 200$ GeV, this excludes $M_{\tilde{g}} < 230$ GeV, assuming $\text{BR}(\tilde{g}\tilde{g} \rightarrow e^\pm e^\pm X) = 1/8$.

Allowing for possible R -parity-conserving squark decays, the decay $\tilde{Q} \rightarrow q\tilde{\chi}_1^0$ is possible, where $\tilde{\chi}_1^0$ is the lightest superpartner. Since the lightest superpartner has no R -parity-conserving decays kinematically accessible, the R -parity-violating decay $\tilde{\chi}_1^0 \rightarrow c\bar{d}e^\pm$ occurs through a virtual charm or down squark, while $\tilde{\chi}_1^0 \rightarrow d\bar{s}\nu$ occurs through a virtual strange or down squark. The exact

branching ratio for $\tilde{\chi}_1^0 \rightarrow e^\pm + X$ depends on sparticle masses and the mixing of the neutralinos. For the analysis, five squark masses are assumed to be degenerate and any squark pair can lead to like-sign dielectron events, since $\tilde{\chi}_1^0$ is a Majorana particle. Squark masses less than 210 GeV are excluded if the mass of the $\tilde{\chi}_1^0$ is more than half of the squark mass and the gluino is heavy. For lighter $\tilde{\chi}_1^0$, the three-body decay of the $\tilde{\chi}_1^0$ can produce electrons that are too soft to satisfy selection criteria.

In all sparticle searches, the LEP results have considered the possibility of R -parity-violating decays. In most cases, the previously stated LEP results apply equally well to this scenario (Schmitt, 1998).

H. R -parity violation and long-lived heavy charged sparticles

If R -parity is violated, and the lightest superpartner is charged, it can manifest itself as a long-lived charged particle (see Sec. II.D) in a collider detector. The particle can be identified by measuring the dE/dx energy loss as it passes through the CDF silicon vertex and central trackery chamber detectors. For a given momentum, a heavy particle has a slower velocity and hence a greater energy loss than a relativistic particle ($\beta \approx 1$). If the particle is weakly interacting or massive enough to suppress showering kinematically, it will penetrate the detectors and be triggered on and reconstructed as a muon with too much energy loss. A result using part of the Run I data has been presented by CDF (Maeshima, 1997) and is updated with the full data set here. In 90 pb^{-1} of inclusive muon triggers ($p_T > 30 \text{ GeV}$), CDF searches for particles with ionization consistent with $\beta\gamma < 0.6$ and finds 12 events depositing more than twice the energy expected from a minimum ionizing muon. This is consistent with the number of events expected from muons that overlap with other tracks to fake a large dE/dx signal.

The CDF method could be used in the future to exclude some SUSY scenarios with R -parity violation. For example, the lightest tau slepton could be the lightest superpartner. Its production rate through R -parity-conserving couplings can be determined from Fig. 15. If λ_{333} is the only large RPV coupling, the decay $\tilde{\tau} \rightarrow \tau\nu_\tau$ can occur with a lifetime fixed by λ_{333} and $m_{\tilde{\tau}}$ (see Sec. II.D). For small enough λ_{333} , this decay can occur outside the tracker, leading to the desired signal if the $\tilde{\tau}$ is traveling slowly enough.

LEP data exclude long-lived (lifetime greater than a microsecond) charged particles in the mass range of 45–90 GeV. In the MSSM, a lower limit of about 82 GeV can be derived for smuons and staus. Long-lived charginos are excluded for masses below about 90 GeV (Schmitt, 1998; Ackerstaff *et al.*, 1998).

I. Photon and E_T signatures

1. An unexpected turn: The CDF $e\bar{e}\gamma\gamma E_T$ event

Supersymmetry has so many parameters that the full range of its allowed signatures may be hard to predict.

$e\bar{e}\gamma\gamma E_T$ Candidate Event

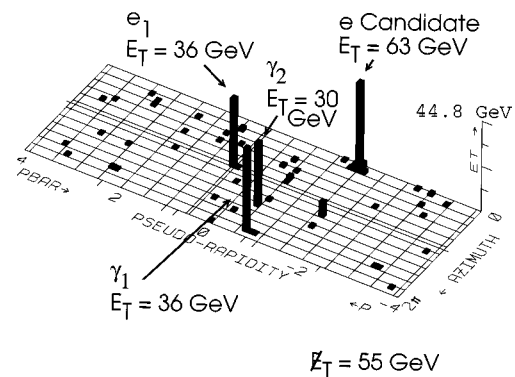


FIG. 18. The very unusual CDF event containing two “electrons,” two “photons,” and missing E_T . The display is the calorimeter cylinder unrolled into a plane. The towers represent energy deposition, with the height of the tower proportional to E_T .

In April 1995, the CDF experiment recorded an event with a very unusual topology (Park, 1996) which may have SUSY interpretations. It had four electromagnetic clusters, which passed the typical cuts for two electrons and two photons, and E_T . A display of the event is shown in Fig. 18.

The electron in the central region of the detector is well isolated and is associated with a track that has a p_T in good agreement with the e^- hypothesis. The two photons are also well isolated and have no associated tracks. The “electron” at large η is more difficult to identify positively. The associated track should only cross a part of the inner central tracking chamber where the occupancy is too high to find the track. Hence, its charge cannot be determined. The vertex time-projection chamber, a wire chamber surrounding the SVX but inside the central tracking chamber, measuring in the $r-z$ view, has a track at the correct η for the electron hypothesis. The path through the cluster and the event vertex can be searched for tracks in the SVX, and this analysis is underway. The probability that the event could be produced in the standard model, including the probability that one or more of the objects is fake, is being estimated. Possible sources include: (i) standard-model $WW\gamma\gamma$ events, (ii) an event that is part real and part fake, such as a $WW\gamma$ event with an additional jet which fakes a photon, (iii) a cosmic-ray interaction and a physics event occurring in the beam crossing, or (iv) two physics events occurring in the same beam crossing. The preliminary results indicate that the number of expected $e\bar{e}\gamma\gamma E_T$ events is many orders of magnitude less than one. However, the data set was derived from over three trillion collisions, and the probability of *all* signatures which would be considered “rare” must be estimated (an impossible task) to determine the significance of one event.

There have been two main proposals for a possible SUSY explanation of the event: the gravitino lightest-

superpartner and the Higgsino lightest-superpartner models [for non-SUSY explanations, see Bhattacharyya and Mohapatra (1997) and Rosner (1997), for example]. Both proposals also suggest other signatures that should be expected within these models and that are presented in the following. The Tevatron collaborations have completed some of these searches, which are also discussed below.

2. Gauge-mediated low-energy SUSY breaking: Gravitino lightest superpartner

The CDF analysis of the above event reminded theorists of low-energy SUSY-breaking models (Ambrosanio *et al.*, 1996a; Dimopoulos *et al.*, 1996; Dimopoulos, Dine, Raby, and Thomas, 1997; Dimopoulos, Thomas, and Wells, 1997a, 1997b; Ellis, Lopez, and Nanopoulos, 1997) which had long ago lost favor to supergravity models. In these models the (usually ignored) gravitino (\tilde{G}) is very light and becomes the lightest superpartner. The lightest standard-model superpartner becomes the next-to-lightest supersymmetric particle (NLSP), which is unstable and decays into its standard-model partner plus the Goldstino component of the gravitino (Fayet, 1977, 1979; Casalbuoni *et al.*, 1988). In the simplest gauge-mediated models, the squarks are heavy and the gauginos obey the unification relationship in Eq. (11). Generically the NLSP can be a neutralino or a slepton (most plausibly a right-handed slepton and, due to the larger Yukawa coupling, a $\tilde{\tau}$). If the scale of SUSY breaking is not far above the electroweak scale (\leq a few thousand TeV), the NLSP will decay within the detector, leading to distinctive signatures as displaced vertices or heavy charged sleptons decaying into leptons, possibly with a kink to a minimum ionizing track (Dimopoulos *et al.*, 1996; Dimopoulos, Dine, Raby, and Thomas, 1997; Dimopoulos, Thomas, and Wells, 1997a, 1997b; Dimopoulos, Dine, Raby, Thomas, and Wells, 1997b).

If a gaugino-like neutralino with a short lifetime is the NLSP, all sparticles decay down to $\tilde{\chi}_1^0$ which then decays to a photon and E_T . The production of $\tilde{\chi}_2^0\tilde{\chi}_1^\pm$, $\tilde{\chi}_1^+\tilde{\chi}_1^-$, and $\tilde{\chi}_R^+\tilde{\chi}_R^-$ pairs, followed by cascade decays, leads to the final states $WZ\gamma\gamma+E_T$, $W\ell^+\ell^-\gamma\gamma+E_T$, $WW\gamma\gamma+E_T$, and $\ell^+\ell^-\gamma\gamma+E_T$, all with comparable rates (Dimopoulos, Thomas, and Wells, 1997a, 1997b). A logical starting place for searches is in the inclusive two-photon-and- E_T channel (Ambrosanio *et al.*, 1996b). In particular, the CDF event can be interpreted as either $\tilde{e}\tilde{e}^*$ production (Dimopoulos *et al.*, 1996; Dimopoulos, Dine, Raby, and Thomas 1997; Ellis, Lopez, and Nanopoulos, 1997), followed by $\tilde{e}\rightarrow e\tilde{\chi}_1^0$ or $\tilde{\chi}_1^+\tilde{\chi}_1^-$ production (Ellis, Lopez, and Nanopoulos, 1997), followed by $\tilde{\chi}_1^-\rightarrow e^-\tilde{\nu}_e\tilde{\chi}_1^0$. If the coupling between the gravitino and matter is large enough, then the lightest neutralino can decay $\tilde{\chi}_1^0\rightarrow\gamma\tilde{G}$ inside a collider detector, yielding the desired signature of $e^+e^-\gamma\gamma E_T$. However, it follows that if one adjusts the parameters of the model to explain the multilepton-plus-photons CDF event, then a very large rate of multijet-plus-multileptons-plus-

photon(s) events is to be expected (Ambrosanio *et al.*, 1996b; Baer, Brhlik, *et al.*, 1997).

Signatures of photons+ E_T can point towards models of low-energy SUSY breaking, but there are other possible signatures in these models (Dicus *et al.*, 1997a, 1997b; Dimopoulos, Dine, Thomas, and Wells, 1997). If the NLSP is a neutralino which is mainly Higgsino-like, then $\tilde{\chi}_1^0$ decays to the lightest Higgs boson (or the heavy CP -even or the CP -odd neutral Higgs bosons if they are sufficiently light) plus a gravitino. The Higgs boson will subsequently decay into $b\bar{b}$. Hence the signature of four b jets, which reconstruct the lightest Higgs-boson mass in pairs, plus E_T is possible. If the NLSP is a right-handed slepton, then the decay $\tilde{\chi}\rightarrow\ell\tilde{G}$ occurs, yielding lepton pairs and E_T as final signature of slepton pair production. The dilepton signature will suffer from large irreducible backgrounds, but the production and decay of heavier sparticles can give spectacular signals. For example, the pair production of a left-handed slepton which cascade-decays into a right-handed slepton and a neutralino can yield six leptons+ E_T in the final state. Also, since the NLSP slepton can be $\tilde{\tau}_R$, signatures with many τ leptons are possible.

If any of the above signatures were observed experimentally, a measurement of the decay length of the NLSP would provide information about the scale of supersymmetry breaking. However, the scale of SUSY breaking might be sufficiently large that a NLSP slepton would penetrate the calorimeter and decay outside the detector. In this case, heavy charged particle pair production, possibly appearing as “muons,” without missing energy could be a manifestation of gauge-mediated low-energy SUSY-breaking models.

3. Higgsino lightest superpartner

The Higgsino lightest-superpartner model (Ambrosanio *et al.*, 1996a) involves a region of MSSM parameter space in which the $\tilde{\chi}_2^0$ is photino-like and the $\tilde{\chi}_1^0$ is Higgsino-like, so the radiative decay $\tilde{\chi}_2^0\rightarrow\gamma\tilde{\chi}_1^0$ dominates over other $\tilde{\chi}_2^0$ decay modes [see, for example, Eq. (5); Haber, Kane, and Quirós, 1986a, 1986b]. The event can again be interpreted as (i) $\tilde{e}\tilde{e}^*$ production, but with $\tilde{e}\rightarrow e\tilde{\chi}_2^0$, or (ii) $\tilde{\chi}_1^+\tilde{\chi}_1^-$ production, with $\tilde{\chi}_1^-\rightarrow e^-\tilde{\nu}_e\tilde{\chi}_2^0$, and the subsequent radiative decay of the $\tilde{\chi}_2^0$ yielding the observed signature.

In these models, photons arise only from the decay of $\tilde{\chi}_2^0$. Other signatures involving two photons might come from the process $\tilde{\nu}\tilde{\nu}^*\rightarrow\nu\tilde{\nu}\tilde{\chi}_2^0\tilde{\chi}_2^0$, but there is no guarantee that the $\tilde{\nu}$ is light enough to produce a substantial signal. Because the $\tilde{\chi}_2^0$ is photino-like, direct $\tilde{\chi}_2^0\tilde{\chi}_2^0$ production is not large. In this model, the dominant neutralino and chargino production processes are $\tilde{\chi}_1^+\tilde{\chi}_1^-$, $\tilde{\chi}_1^0\tilde{\chi}_3^0$ and $\tilde{\chi}_1^\pm\tilde{\chi}_1^\pm$, $\tilde{\chi}_1^\pm\tilde{\chi}_3^0$. None of these involve the direct production of $\tilde{\chi}_2^0$. Typically, the decay $\tilde{\chi}_3^0\rightarrow Z^*\tilde{\chi}_1^0$ occurs, yielding no photon. One of the next largest processes is $\tilde{\chi}_1^\pm\tilde{\chi}_2^0$, which would produce a trilepton signature in supergravity models, but can produce $\ell\gamma E_T$ or

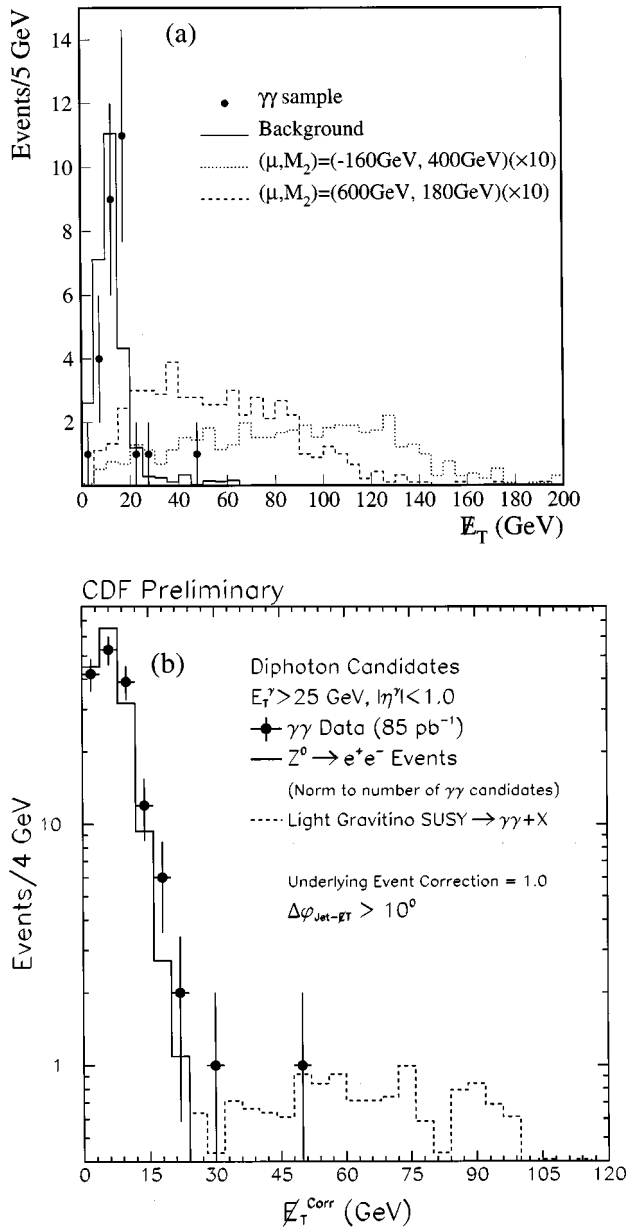


FIG. 19. The E_T spectra in the searches for events with two photons and E_T : (a) The DØ results, where one photon has $E_T > 25$ GeV and the other has $E_T > 12$ GeV (Abachi *et al.*, 1997e). The points are the data. The solid line is the estimated background from dijet events and direct photon events. The dotted and dashed lines are predicted distributions ($\times 10$) from gauge-mediated models using the parameters listed and $M_1 \approx 2M_2$. (b) The CDF results for events with two central photons and $E_T > 25$ GeV. Events which have any jet with $E_T > 10$ GeV pointing within 10 degrees in azimuth of the E_T are removed. The solid histogram shows the resolution from the $Z \rightarrow e^+e^-$ control sample. The dashed line shows the expected distribution from all SUSY production in a model (Ambrosanio *et al.*, 1996b) with $M_2 = 225$ GeV, $\mu = 300$ GeV, $\tan \beta = 1.5$, and $M_{\tilde{Q}} = 300$ GeV.

$jj\gamma E_T$ signatures in the Higgsino lightest-superpartner model.

If the stop is light, this discussion changes, because the $\tilde{\chi}_1^\pm$ can decay $\tilde{\chi}_1^\pm \rightarrow b\tilde{t}_1$, followed by $\tilde{t}_1 \rightarrow c\tilde{\chi}_1^0$. The sig-

TABLE XVI. Selection criteria for $\gamma\gamma + E_T + X$ searches.

Quantity	DØ	CDF
$E_T^{\gamma_1}, E_T^{\gamma_2}$	$> 20, 12$ GeV	$> 25, 25$ GeV
$ \eta^\gamma $	< 1.2 or between 1.5 and 2.0	< 1.1
E_T	> 25 GeV	> 35 GeV
$\Delta\phi$ between	N.A.	$> 10^\circ$
E_T and nearest jet		

nature is then a rather distinct $\gamma bc E_T$. However, such a light stop would appear in top decays, depleting the observed standard-model decays to a potentially unacceptable level. This is only true, though, if there are no other sources of top-quark production from SUSY, which there obviously can be. Surprisingly, such models can be constructed in accord with the present SUSY limits (Mrenna and Kane, 1996). If the gluinos are heavy enough so that $\tilde{g} \rightarrow t\tilde{t}_1^*$ or $\rightarrow t\tilde{t}_1$, and gluino production is further fed by squark decay $\tilde{Q} \rightarrow q\tilde{g}$, then one can compensate for the lost top quarks in SUSY decay modes. This leads to more sources of $\gamma bc E_T$ events than just $\tilde{\chi}_1^\pm \tilde{\chi}_2^0$ events, as well as other signatures.

4. Inclusive two-photons-and- E_T signatures

The generic $\gamma\gamma E_T + X$ signature has no significant background from real photons. The main backgrounds are caused by jets and electrons faking photons. The standard-model production of $W(\rightarrow e\nu)\gamma$ plus jets can fake some of the signatures if the electron is misidentified as a photon. These events have an E_T spectrum typical of W events, peaked at about $M_W/2 \approx 40$ GeV, with a long tail to high E_T . The dominant instrumental background, however, is from dijet and γ +jet production, where the large production cross section overcomes the small probability ($\approx 10^{-4} - 10^{-3}$) that a jet fakes a photon.

Figure 19 shows the E_T distributions from DØ (a) and CDF (b) diphoton events (Culbertson, 1998; Abachi *et al.*, 1997e) after imposing the selection criteria given in Table XVI. The DØ histogram contains fewer events because the trigger included $E_T > 14$ GeV while the CDF trigger had no E_T requirement. For the DØ analysis, the shape of the E_T spectra agrees well with backgrounds containing two electromagneticlike clusters, where at least one of the two clusters fails the photon selection criteria. Two events satisfy all selection criteria, with a predicted background, dominated by jets faking photons, of 2.3 ± 0.9 events. For the CDF analysis, the shape of the E_T distribution is in good agreement with the resolution of the $Z \rightarrow e^+e^-$ control sample. The event on the tail in E_T is the " $ee\gamma\gamma E_T$ " event. If the source of this event is an anomalously large $WW\gamma\gamma$ production cross section that yields one event in $\mathcal{L}\gamma\gamma E_T$, CDF would expect dozens of events with two photons and four jets. However, the jet multiplicity spectrum in diphoton events is well modeled by an exponential, and there are no diphoton events with three or four jets. As

TABLE XVII. Summary of the 85 pb^{-1} data sample for the CDF $\gamma b \cancel{E}_T$ search. Limits are set using all cuts that result in two events.

Quantity	Cut	Cumulative number of events
E_T^γ , ID cuts	$>25 \text{ GeV}$	511335
SVX b -tag	≥ 1	1487
E_T^b , $ \eta < 2.0$	$>30 \text{ GeV}$	1175
E_T	$>20 \text{ GeV}$	98
$E_T, \Delta\phi(\gamma - \cancel{E}_T) < 2.93$	$>40 \text{ GeV}$	2

mentioned before, events with diphotons, jets, and \cancel{E}_T can be signatures of gauge-mediated low-energy supersymmetry-breaking models.

$D\bar{O}$ presents limits (Abachi *et al.*, 1997) in the framework of the Gravitino lightest-superpartner scenario by considering neutralino and chargino pair production. Assuming $M_2 \approx 2M_1$ and large values of $m_{\tilde{Q}}$, the signatures are a function of only M_2 , μ , and $\tan\beta$. Event rates are predicted using PYTHIA (Sjöstrand, 1994; Mrenna, 1997a). Approximately 50% of events have two photons that would pass the kinematic cuts. Approximately 33% of those events pass all cuts for a very good total efficiency in the range 15–26%. Figure 20 shows the limit on the cross section for $\tilde{\chi}_1^\pm \tilde{\chi}_1^\pm$ and $\tilde{\chi}_1^\pm \tilde{\chi}_2^0$ production as a function of the $\tilde{\chi}_1^\pm$ mass when $|\mu|$ is large and thus the $\tilde{\chi}_1^\pm$ mass is approximately twice the $\tilde{\chi}_1^0$ mass. The figure also shows, more generally, the excluded region in the M_2 - μ plane ($\mu < 0$ gives larger $\tilde{\chi}_1^\pm, \tilde{\chi}_2^0 - \tilde{\chi}_1^0$ mass splittings, small $|\mu|$ means $\tilde{\chi}_1^\pm, \tilde{\chi}_1^0$, and $\tilde{\chi}_2^0$ are more Higgsino-like), along with a prediction for the region that might explain the CDF $ee\gamma\gamma\cancel{E}_T$ event as chargino pair production. The latter explanation requires $100 \text{ GeV} < M_{\tilde{\chi}_1^\pm} < 150 \text{ GeV}$ with $M_{\tilde{\chi}_1^0} < 0.6M_{\tilde{\chi}_1^\pm}$ to produce one event with a reasonable probability (Ellis, Lopez, and Nanopoulos, 1997).

As can be seen from Fig. 20, the cross-section limit is typically 0.24 pb for either $\tilde{\chi}_1^+ \tilde{\chi}_1^-$ or $\tilde{\chi}_1^\pm \tilde{\chi}_2^0$ production. By combining all chargino and neutralino pair-production processes, a $\tilde{\chi}_1^\pm$ with mass below 150 GeV is excluded. Hence, to keep the chargino interpretation of the $ee\gamma\gamma\cancel{E}_T$ event, it is necessary to expand on the analysis of Ellis, Lopez, and Nanopoulos (1997). The chargino mass limit is much higher than in supergravity models, because of the 100% branching fraction for the decay $\tilde{\chi}_1^0 \rightarrow \gamma\tilde{G}$ and the high detectability of the photon and \cancel{E}_T . The result eliminates the possibility of observing signatures of this particular model at LEP200. The \cancel{E}_T cut needed to control QCD backgrounds makes the analysis sensitive to the mass splittings between $\tilde{\chi}_1^0$ and $\tilde{\chi}_1^\pm$ or $\tilde{\chi}_2^0$. However, the simplest models predict unification mass relations between the gauginos, which thus gives acceptable mass splittings.

$D\bar{O}$ also has a limit on the cross section for $\tilde{e}\tilde{e}^* \rightarrow e^-e^+\tilde{\chi}_2^0\tilde{\chi}_2^0, \tilde{\nu}\tilde{\nu}^* \rightarrow \nu\bar{\nu}\tilde{\chi}_2^0\tilde{\chi}_2^0$, and $\tilde{\chi}_2^0\tilde{\chi}_2^0 \rightarrow \gamma\gamma\tilde{\chi}_1^+\tilde{\chi}_1^-$ using the same analysis as for the gravitino lightest-superpartner search. Such signatures might also be ex-

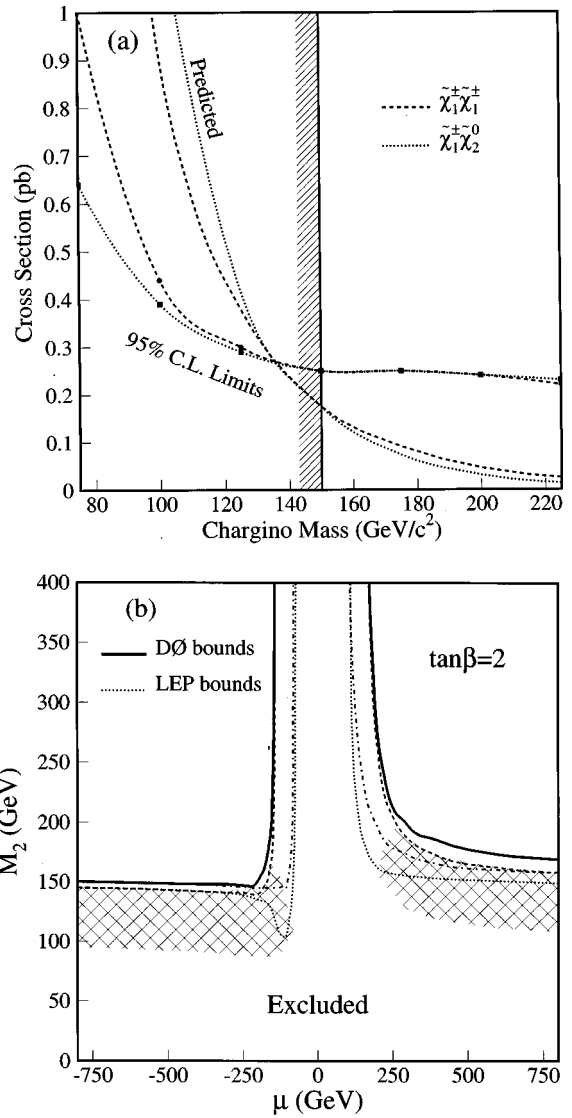


FIG. 20. Limits from the $D\bar{O}$ search for events with two photons and \cancel{E}_T : (a) The $D\bar{O}$ cross-section limit on $\tilde{\chi}_1^\pm \tilde{\chi}_1^\pm$ and $\tilde{\chi}_1^\pm \tilde{\chi}_2^0$ production, assuming $M_{\tilde{\chi}_1^\pm} \approx 2M_{\tilde{\chi}_1^0}$ and $\text{BR}(\tilde{\chi}_1^0 \rightarrow \gamma\tilde{G}) = 100\%$. The upper dotted curve is the cross section from PYTHIA and the lower dotted curve is the limit from the $D\bar{O}$ collaboration on $\tilde{\chi}_1^\pm \tilde{\chi}_2^0$ production (Abachi *et al.*, 1997e). The upper and lower dashed curves are the limits on $\tilde{\chi}_1^\pm \tilde{\chi}_1^\mp$ production from PYTHIA and the $D\bar{O}$ Collaboration, respectively. The vertical line marks the lower limit on the chargino mass considering all chargino and neutralino pair production and all values of μ . (b) The limits on the parameters M_2 and μ in gauge-mediated models based on PYTHIA for $\tan\beta=2$ and $M_{\tilde{Q}}=800 \text{ GeV}$ (Abachi *et al.*, 1997e). The hatched area is the region proposed (Ellis, Lopez, and Nanopoulos, 1997) to explain the CDF $ee\gamma\gamma\cancel{E}_T$ event. The solid line shows the $D\bar{O}$ bounds. The long-dashed and dash-dotted lines show contours of $M_{\tilde{\chi}_1^\pm}=150 \text{ GeV}$ and $M_{\tilde{\chi}_1^0}=75 \text{ GeV}$, respectively. The dotted lines show an interpretation of preliminary LEP results at an energy of 161 GeV.

pected in Higgsino lightest-superpartner models. The limit on the cross section for such processes is about 0.35 pb for $M_{\tilde{\chi}_2^0} - M_{\tilde{\chi}_1^0} > 30 \text{ GeV}$, which is close to the maximum cross section predicted in these models.

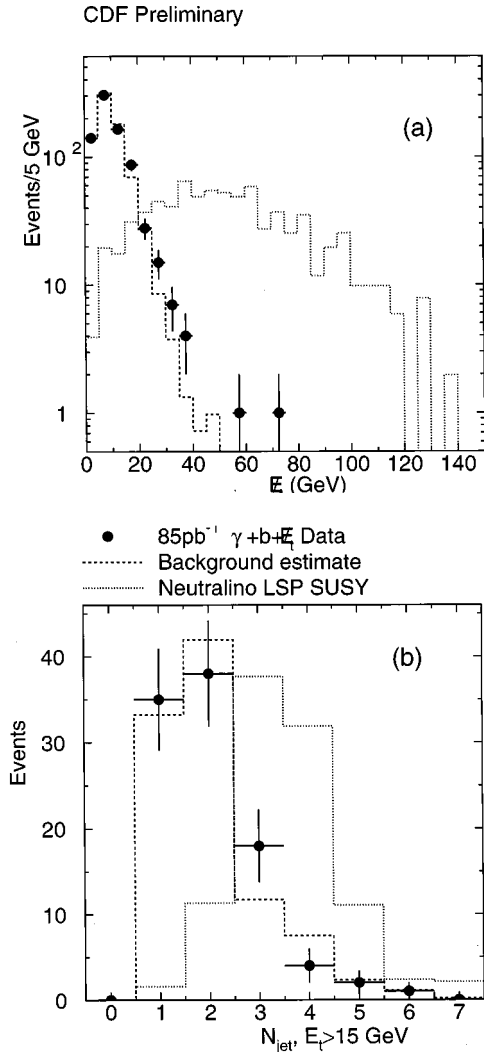


FIG. 21. CDF results from the search for the signature $b\gamma E_T$ in a scenario where $\tilde{\chi}_2^0 \rightarrow \gamma\tilde{\chi}_1^0$ and the stop is light: (a) The E_T distribution, and (b) the jet multiplicity distribution with $E_T > 15$ GeV in events with a photon and a SVX b tag. The jet multiplicity histogram is made by requiring $E_T > 20$ GeV. The SUSY model is normalized to the area of the data histogram, scaling by a factor of 100 for the E_T histogram and a factor of 10 for the n_{jet} histogram. The SUSY model has a Higgsino lightest superpartner (Mrenna and Kane, 1996) generated with PYTHIA 6.1.

Provided that a $\tilde{\chi}_1^0$ NLSP decays to a photon and a gravitino lightest superpartner well within the detector, Tevatron data can exclude a chargino mass of about 150 GeV. The LEP data are used to derive a comparable limit (Schmitt, 1988). For both the Tevatron and LEP, strong limits are lacking for the case of a heavy, Higgsino-like lightest superpartner because of the small production rate and significant backgrounds.

5. Single photon, heavy flavor, and E_T

CDF has searched for the signature $\gamma bc E_T$, as predicted in Higgsino lightest-superpartner models with a light stop (Mrenna and Kane, 1996). The data sample of

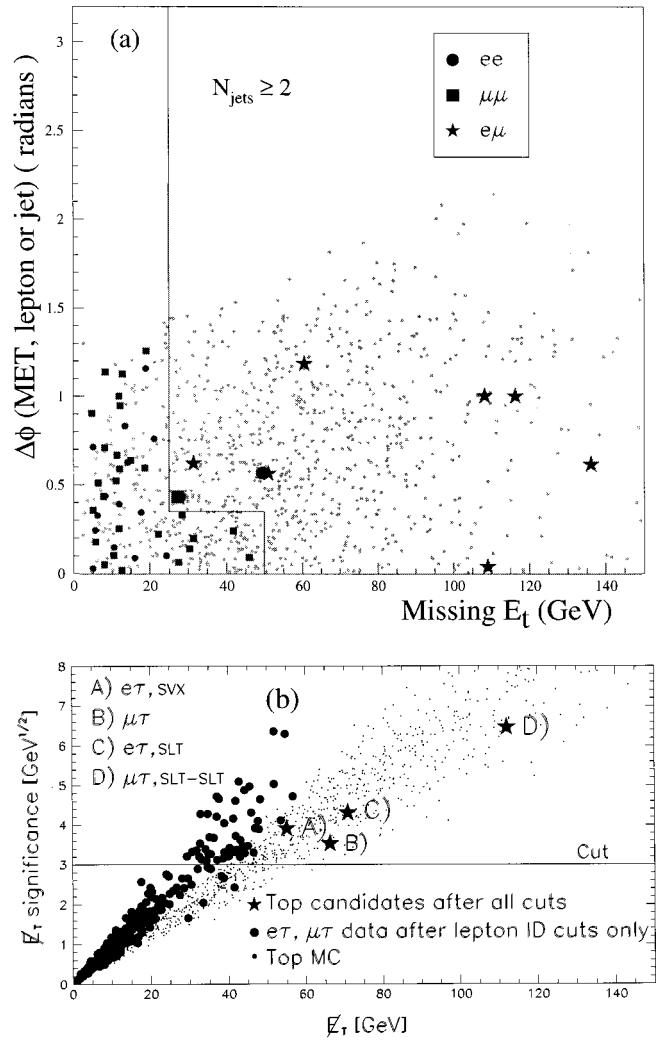


FIG. 22. Data from the CDF searches for dileptons in $t\bar{t}$ events: (a) Scatterplot of the angle $\Delta\phi(E_T, \ell/j)$ between the corrected E_T and the closest lepton or jet vs corrected E_T for the ee , $\mu\mu$, and $e\mu$ candidate events, compared with the expected distributions for $t\bar{t}$ and background. Background and top contributions are *not* normalized to the expected number of events. (b) The distribution of E_T significance vs E_T for events with a primary lepton and a tau candidate (the slopes of the data and background are different, because the background is dominated by QCD) in the CDF data compared with the $t\bar{t}$ Monte Carlo. Three of the four final candidate events (stars) have b -tagged jets.

85 pb^{-1} contains events with an isolated photon with $E_T^{\gamma} > 25$ GeV and a jet with an SVX b tag (see Table XVII). The E_T spectrum of these events can be seen in Fig. 21. After requiring $E_T > 20$ GeV, 98 events remain (Culbertson, 1998).

The estimated background to the 98 events is $77 \pm 23 \pm 20$ events. The shape is consistent with background. About 60% of the background is due to jets faking photons, 13% to real photons and fake b tags, and the remainder to standard-model $\gamma b\bar{b}$ and $\gamma c\bar{c}$ production; all of these sources require fake E_T . When the E_T cut is increased to 40 GeV, two events remain. Calculating a

TABLE XVIII. Typical final states from sparticle decay, assuming $\tilde{\chi}^0, \tilde{\chi}^\pm, \tilde{\nu}, \tilde{p} < \tilde{Q} (\neq \tilde{t}, \tilde{b}), \tilde{g}$. HLSP denotes models with a Higgsino lightest superpartner and GLSP denotes models with a Gravitino lightest superpartner. Event signatures from sparticle pair production can be constructed by combining two decays.

Particle	Intermediate state	Final state	Comment
$\tilde{\chi}_i^0$		$\rightarrow \mathbf{E}_T$	
		$\rightarrow \cancel{\ell} \mathbf{E}_T$	
		$\rightarrow jj \mathbf{E}_T$	
		$\rightarrow \gamma \mathbf{E}_T$	HLSP, GLSP
	$\rightarrow t \tilde{t}^*$	$\rightarrow b W \bar{c} \mathbf{E}_T$	$m_{\tilde{t}} < m_b + M_{\tilde{\chi}_1^\pm}$
	...	$\rightarrow b W \bar{b} \mathbf{E}_T$	
$\tilde{\chi}_i^\pm$		$\rightarrow \cancel{\ell} \mathbf{E}_T$	
		$\rightarrow jj \mathbf{E}_T$	
		$\rightarrow \cancel{\ell} \gamma \mathbf{E}_T$	HLSP, GLSP
		$\rightarrow jj \gamma \mathbf{E}_T$	HLSP, GLSP
	$\rightarrow b \tilde{t}^*$	$\rightarrow b \bar{c} \mathbf{E}_T$	$m_{\tilde{t}} < m_b + M_{\tilde{\chi}_1^\pm}$
	...	$\rightarrow b \bar{b} \mathbf{E}_T$	
$\tilde{\nu}$	$\rightarrow \cancel{\ell} \tilde{\chi}_1^0$	$\rightarrow \cancel{\ell} \mathbf{E}_T$	
	$\rightarrow \cancel{\ell} \tilde{\chi}_2^0$	$\rightarrow \cancel{\ell} \mathbf{E}_T$	
	...	$\rightarrow \cancel{\ell} \cancel{\ell}' \mathbf{E}_T$	
	...	$\rightarrow \cancel{\ell} jj \mathbf{E}_T$	
		$\rightarrow \cancel{\ell} \gamma \mathbf{E}_T$	HLSP, GLSP
	$\rightarrow \nu \tilde{\chi}_1^\pm$	$\rightarrow \cancel{\ell} \mathbf{E}_T$	
\tilde{t}	$\rightarrow \nu \tilde{\chi}_1^0$	$\rightarrow \mathbf{E}_T$	
	$\rightarrow \nu \tilde{\chi}_2^0$	$\rightarrow \mathbf{E}_T$	
	...	$\rightarrow \cancel{\ell}' \cancel{\ell}' \mathbf{E}_T$	
	...	$\rightarrow jj \mathbf{E}_T$	
		$\rightarrow \gamma \mathbf{E}_T$	HLSP, GLSP
	$\rightarrow \cancel{\ell} \tilde{\chi}_1^\pm$	$\rightarrow \cancel{\ell} \mathbf{E}_T$	
\tilde{b}	$\rightarrow c \tilde{\chi}_1^0$	$\rightarrow c \mathbf{E}_T$	$m_{\tilde{t}} < m_b + M_{\tilde{\chi}_1^\pm}$
	$\rightarrow b \tilde{\chi}_1^\pm$	$\rightarrow b \mathbf{E}_T$	
	...	$\rightarrow b jj \mathbf{E}_T$	
	$\rightarrow t \tilde{\chi}_1^0$	$\rightarrow b W \mathbf{E}_T$	$M_{\tilde{t}} > m_t + M_{\tilde{\chi}_1^0}$
	$\rightarrow \tilde{b} W$	$\rightarrow b W \mathbf{E}_T$	
	...	$\rightarrow b \cancel{\ell} \mathbf{E}_T$	
\tilde{g}	...	$\rightarrow b jj \mathbf{E}_T$	
	$\rightarrow t \tilde{t}^*$	$\rightarrow b W \bar{c} \mathbf{E}_T$	$m_{\tilde{t}} < m_b + M_{\tilde{\chi}_1^\pm}$
	$\rightarrow b \tilde{b}^*$	$\rightarrow b \bar{b} \mathbf{E}_T$	
	$\rightarrow jj \tilde{\chi}_1^0$	$\rightarrow jj \mathbf{E}_T$	
	$\rightarrow jj \tilde{\chi}_2^0$	$\rightarrow jj \mathbf{E}_T$	
	...	$\rightarrow jj \cancel{\ell} \mathbf{E}_T$	
\tilde{Q}	$\rightarrow j \tilde{\chi}_1^0$	$\rightarrow j \mathbf{E}_T$	
	$\rightarrow j \tilde{\chi}_2^0$	$\rightarrow j \mathbf{E}_T$	
	...	$\rightarrow j \cancel{\ell} \mathbf{E}_T$	
	...	$\rightarrow jj \mathbf{E}_T$	
	$\rightarrow j \tilde{\chi}_1^\pm$	$\rightarrow j \cancel{\ell} \mathbf{E}_T$	
	...	$\rightarrow jjj \mathbf{E}_T$	
\tilde{g}	...	$\rightarrow j b \bar{c} \mathbf{E}_T$	$m_{\tilde{t}} < m_b + M_{\tilde{\chi}_1^\pm}$
	$\rightarrow j \tilde{g}$	$\rightarrow jjj \mathbf{E}_T$	HLSP, GLSP
	$\rightarrow j \tilde{Q}$	$\rightarrow jj \mathbf{E}_T$	
	$\rightarrow t \tilde{t}^*$	$\rightarrow b W \bar{c} \mathbf{E}_T$	$m_{\tilde{t}} < m_b + M_{\tilde{\chi}_1^\pm}$
	$\rightarrow b \tilde{b}^*$	$\rightarrow b \bar{b} \mathbf{E}_T$	
	$\rightarrow jj \tilde{\chi}_1^0$	$\rightarrow jj \mathbf{E}_T$	
\tilde{g}	$\rightarrow jj \tilde{\chi}_2^0$	$\rightarrow jj \mathbf{E}_T$	
	...	$\rightarrow jj \cancel{\ell} \mathbf{E}_T$	
	...	$\rightarrow jjj \mathbf{E}_T$	
	$\rightarrow jj \tilde{\chi}_1^\pm$	$\rightarrow jj \cancel{\ell} \mathbf{E}_T$	
	...	$\rightarrow jjj \mathbf{E}_T$	
	...	$\rightarrow jj b \bar{c} \mathbf{E}_T$	
\tilde{g}	$\rightarrow t \tilde{t} \tilde{\chi}_1^0$	$\rightarrow b W \bar{b} W \mathbf{E}_T$	
	$\rightarrow t \tilde{b} \tilde{\chi}_1^\pm$	$\rightarrow b W \bar{b} \mathbf{E}_T$	
	...	$\rightarrow b W \bar{b} jj \mathbf{E}_T$	

TABLE XVIII. (Continued).

Particle	Intermediate state	Final state	Comment
\tilde{t}	$\rightarrow \tilde{t} W$	$\rightarrow c W \mathbf{E}_T$	$m_{\tilde{t}} < m_b + M_{\tilde{\chi}_1^\pm}$
	...	$\rightarrow b \cancel{W} \mathbf{E}_T$	
	...	$\rightarrow b jj W \mathbf{E}_T$	
\tilde{Q}	$\rightarrow j \tilde{\chi}_1^0$	$\rightarrow j \mathbf{E}_T$	
	$\rightarrow j \tilde{\chi}_2^0$	$\rightarrow j \mathbf{E}_T$	
	...	$\rightarrow j \cancel{\ell} \mathbf{E}_T$	
	...	$\rightarrow jj \mathbf{E}_T$	
	$\rightarrow j \tilde{\chi}_1^\pm$	$\rightarrow j \cancel{\ell} \mathbf{E}_T$	
	...	$\rightarrow jjj \mathbf{E}_T$	
\tilde{g}	...	$\rightarrow j b \bar{c} \mathbf{E}_T$	$m_{\tilde{t}} < m_b + M_{\tilde{\chi}_1^\pm}$
	$\rightarrow j \tilde{g}$	$\rightarrow jjj \mathbf{E}_T$	HLSP, GLSP
	$\rightarrow j \tilde{Q}$	$\rightarrow jj \mathbf{E}_T$	
	$\rightarrow t \tilde{t}^*$	$\rightarrow b W \bar{c} \mathbf{E}_T$	$m_{\tilde{t}} < m_b + M_{\tilde{\chi}_1^\pm}$
	$\rightarrow b \tilde{b}^*$	$\rightarrow b \bar{b} \mathbf{E}_T$	
	$\rightarrow jj \tilde{\chi}_1^0$	$\rightarrow jj \mathbf{E}_T$	
\tilde{g}	$\rightarrow jj \tilde{\chi}_2^0$	$\rightarrow jj \mathbf{E}_T$	
	...	$\rightarrow jj \cancel{\ell} \mathbf{E}_T$	
	...	$\rightarrow jjj \mathbf{E}_T$	
	$\rightarrow jj \tilde{\chi}_1^\pm$	$\rightarrow jj \cancel{\ell} \mathbf{E}_T$	
	...	$\rightarrow jjj \mathbf{E}_T$	
	...	$\rightarrow jj b \bar{c} \mathbf{E}_T$	
\tilde{g}	$\rightarrow t \tilde{t} \tilde{\chi}_1^0$	$\rightarrow b W \bar{b} W \mathbf{E}_T$	
	$\rightarrow t \tilde{b} \tilde{\chi}_1^\pm$	$\rightarrow b W \bar{b} \mathbf{E}_T$	
	...	$\rightarrow b W \bar{b} jj \mathbf{E}_T$	

95% confidence limit, more than 6.43 events of anomalous production in this topology are excluded.

The efficiency in the limits is derived from a “baseline” model with $M_{\tilde{\chi}_1^0} = 40$ GeV, $M_{\tilde{\chi}_2^0} = 70$ GeV, $m_{\tilde{t}_1} = 60$ GeV, $m_{\tilde{Q}} = 250$ GeV, and $M_{\tilde{g}} = 225$ GeV.³⁹ The distribution of the number of jets in the data is shown in Fig. 21 compared to that expected from backgrounds and the SUSY model (scaled $\times 10$). There are more jets expected in the SUSY model than the data indicate because of the hard kinematics of squark and gluino decays. The baseline model predicts a total efficiency \times branching ratio of 1.5%, resulting in 6.65 events expected, so this model is excluded (at the 95% C.L.). This result does not rule out the Higgsino lightest-superpartner model in general, only one version with a fairly light mass spectrum. A more general limit can be set by holding the lighter sparticle masses constant and varying the squark and gluino masses. In this case squarks and gluinos less than 200 GeV and 225 GeV, respectively, are excluded.

J. Other anomalies: Top dilepton events

There are other anomalies in the current data beyond the “ $ee\gamma\gamma\mathbf{E}_T$ ” event. These are, so far, either single,

³⁹This analysis predates LEP results which exclude this example.

TABLE XIX. Examples of R -parity-conserving SUSY signatures at the Tevatron: Jets+ E_T . Not all signatures are listed—we have (somewhat arbitrarily) restricted the list. We assume that the lightest superpartner is the $\tilde{\chi}_1^0$. Note that \tilde{Q} decays give one or three jets, \tilde{g} decays give two, four, or six jets, and the $\tilde{\chi}_i^\pm$, $\tilde{\chi}_i^0$, $\tilde{\nu}$, and \tilde{t} decays give an even number of jets.

R -parity-conserving Signatures: Jets+ E_T		
Signature	Production	Decay
jE_T	$\tilde{Q}\tilde{\chi}_1^0$	$\tilde{Q}\rightarrow q\tilde{\chi}_1^0$
jjE_T	$\tilde{Q}\tilde{Q}^*$	$\tilde{Q}\rightarrow q\tilde{\chi}_1^0; \tilde{Q}^*\rightarrow\bar{q}\tilde{\chi}_1^0$
	$\tilde{\chi}_1^\pm\tilde{\chi}_1^0$	$\tilde{\chi}_1^\pm\rightarrow q\bar{q}\tilde{\chi}_1^0$
	$\tilde{t}\tilde{t}^*$	$\tilde{t}\rightarrow c\tilde{\chi}_1^0$
$jjjE_T$	$\tilde{Q}\tilde{\chi}_1^0$	$\tilde{Q}\rightarrow q\tilde{\chi}_1^\pm, \tilde{\chi}_1^\pm\rightarrow q\bar{q}\tilde{\chi}_1^0$
	$\tilde{Q}\tilde{g}$	$\tilde{Q}\rightarrow q\tilde{\chi}_1^0; \tilde{g}\rightarrow q\bar{q}\tilde{\chi}_1^0$
$jjjjE_T$	$\tilde{Q}\tilde{Q}^*$	$\tilde{Q}\rightarrow q\tilde{\chi}_1^0; \tilde{Q}^*\rightarrow q\tilde{\chi}_1^\pm\rightarrow q(q\bar{q}\tilde{\chi}_1^0)$
	$\tilde{g}\tilde{g}$	$\tilde{g}\rightarrow q\bar{q}\tilde{\chi}_1^0$
$5jE_T$	$\tilde{Q}\tilde{g}$	$\tilde{Q}\rightarrow q\tilde{\chi}_1^\pm\rightarrow q(q\bar{q}\tilde{\chi}_1^0); \tilde{g}\rightarrow q\bar{q}\tilde{\chi}_1^0$
$6jE_T$	$\tilde{Q}\tilde{Q}^*$	$\tilde{Q}\rightarrow q\tilde{\chi}_1^\pm\rightarrow q(q\bar{q}\tilde{\chi}_1^0)$
	$\tilde{g}\tilde{g}$	$\tilde{g}\rightarrow q\bar{q}\tilde{\chi}_1^0; \tilde{g}\rightarrow q\tilde{Q}\rightarrow q(q\tilde{\chi}_1^\pm\rightarrow q(q\bar{q}\tilde{\chi}_1^0))$
$>6jE_T$	$\tilde{Q}\tilde{g}$	$\tilde{Q}\rightarrow q\tilde{\chi}_1^\pm\rightarrow q(q\bar{q}\tilde{\chi}_1^0); \tilde{g}\rightarrow q\tilde{Q}\rightarrow q(q\tilde{\chi}_1^\pm\rightarrow q(q\bar{q}\tilde{\chi}_1^0))$
	$\tilde{g}\tilde{g}$	$\tilde{g}\rightarrow\tilde{t}\tilde{t}\rightarrow(Wb)(\tilde{\chi}_1^\pm b)\rightarrow(jjb)(jjb\tilde{\chi}_1^0); \tilde{g}\rightarrow q\bar{q}\tilde{\chi}_1^0$

rare events or discrepancies on the tails of distributions where statistics are low and backgrounds difficult to calculate. In addition, there is the problem of calculating probabilities for “anomalies” *a posteriori*. The expected number of events in any one channel from SUSY is usually small with the present integrated luminosity. New physics will most likely show up as a few events on the tails of standard-model distributions. Since there are many potential SUSY signatures, one can only follow a strategy of systematically analyzing all high-mass channels and looking for discrepancies on the tails of distributions. The single events such as the “ $ee\gamma\gamma E_T$ ” event have been useful as “guideposts” indicating promising new channels, such as the γbjE_T channel described above. It is still possible that a sensible picture of these events will emerge from the Run-I data when a complete survey of all channels is completed using both detectors. At the very least, this is an important exercise for preparing the Run-II analyses.

As discussed earlier, the signature of dileptons+2 jets+ E_T is a promising SUSY search channel (see Sec. IV.B.2). However, such events would also be a background to the standard-model top-quark search using dileptons. The consistency of this dilepton sample with that expected from $\tilde{t}\tilde{t}$ production has been the subject of intense investigation. There are a number of peculiarities, none by themselves statistically significant at a level required to claim new physics. However, there are several events that have low probabilities of being from top

TABLE XX. Examples of R -parity-conserving SUSY signatures at the Tevatron: b tags+jets+ E_T . We have shown only a few modes. The signatures change depending on the relative masses of the \tilde{b} , \tilde{t} , $\tilde{\chi}_1^\pm$, and $\tilde{\chi}_1^0$.

R -parity-conserving signatures: b quarks		
Signature	Production	Decay
bE_T	$\tilde{b}\tilde{\chi}_1^0$	$\tilde{b}\rightarrow b\tilde{\chi}_1^0$
bjE_T	$\tilde{b}\tilde{t}$	$\tilde{b}\rightarrow b\tilde{\chi}_1^0; \tilde{t}\rightarrow c\tilde{\chi}_1^0$
$bjjE_T$	$\tilde{b}\tilde{g}$	$\tilde{b}\rightarrow b\tilde{\chi}_1^0; \tilde{g}\rightarrow q\bar{q}\tilde{\chi}_1^0$
	$\tilde{t}\tilde{\chi}_1^0$	$\tilde{t}\rightarrow b\tilde{\chi}_1^\pm$
$bjjjE_T$	$\tilde{b}\tilde{b}$	$\tilde{b}\rightarrow b\tilde{\chi}_1^0; \tilde{b}\rightarrow\tilde{t}W, \tilde{t}\rightarrow c\tilde{\chi}_1^0$
	$\tilde{b}\tilde{t}$	$\tilde{b}\rightarrow b\tilde{g}, \tilde{g}\rightarrow q\bar{q}\tilde{\chi}_1^0; \tilde{t}\rightarrow c\tilde{\chi}_1^0$
$bjjj\dots E_T$	$\tilde{b}\tilde{b}$	$\tilde{b}\rightarrow b\tilde{g}\tilde{g}\rightarrow q\bar{q}\tilde{\chi}_1^0; \tilde{b}\rightarrow\tilde{t}W\tilde{t}\rightarrow c\tilde{\chi}_1^0$
$bbj\dots E_T$	$\tilde{b}\tilde{b}$	$\tilde{b}\rightarrow b\tilde{\chi}_1^0$
	$\tilde{t}\tilde{t}^*$	$\tilde{t}\rightarrow b\tilde{\chi}_1^\pm, \tilde{\chi}_1^\pm\rightarrow qq'\tilde{\chi}_1^0$
$bbbj\dots E_T$	$\tilde{g}\tilde{b}$	$\tilde{g}\rightarrow b\bar{b}\tilde{\chi}_1^0; \tilde{b}\rightarrow b\tilde{\chi}_1^0$
	$\tilde{g}\tilde{t}$	$\tilde{g}\rightarrow b\bar{b}\tilde{\chi}_1^0; \tilde{t}\rightarrow b\tilde{\chi}_1^\pm, \tilde{\chi}_1^\pm\rightarrow qq'\tilde{\chi}_1^0$
$bbbbj\dots E_T$	$\tilde{g}\tilde{g}$	$\tilde{g}\rightarrow b\bar{b}\tilde{\chi}_1^0$
bb/jjE_T	$\tilde{t}\tilde{t}$	$\tilde{t}\rightarrow b\tilde{\chi}_1^\pm, \tilde{\chi}_1^\pm\rightarrow e\nu\tilde{\chi}_1^0, \tilde{\chi}_1^\pm\rightarrow qq'\tilde{\chi}_1^0$
$bb/\ell E_T$	$\tilde{t}\tilde{t}$	$\tilde{t}\rightarrow b\tilde{\chi}_1^\pm, \tilde{\chi}_1^\pm\rightarrow e\nu\tilde{\chi}_1^0$

TABLE XXI. Examples of R -parity-conserving SUSY signatures at the Tevatron: leptons. We have shown only a few modes. Note that (for example) \tilde{e} decays can give no, one, or three (charged) leptons, and $\tilde{\nu}$ decays can give one or two leptons. The signatures will change depending on the relative masses of the sneutrinos and sleptons in the different generations. We have not shown explicitly the differences in the “left” and “right” slepton decays. The decays that single out the τ (for example, from the H^+) are omitted here. Decay modes involving neutralinos and charginos can be created by feed-down from squark and gluino decays. Gluino decays can lead to leptons with uncorrelated charges.

R -parity-conserving signatures: “generic” leptons		
Signature	Production	Decay
$\ell \mathbf{E}_T$	$\tilde{\nu}$	$\tilde{\nu} \rightarrow \nu \tilde{\chi}_1^0$
	$\tilde{\chi}_1^\pm \tilde{\chi}_2^0$	$\tilde{\chi}_1^\pm \rightarrow \nu \tilde{\chi}_1^0$; $\tilde{\chi}_2^0 \rightarrow \nu \tilde{\chi}_1^0$
$\ell \ell \mathbf{E}_T$	$\tilde{\chi}_1^\pm \tilde{\chi}_1^\pm$	$\tilde{\chi}_1^\pm \rightarrow \nu \tilde{\chi}_1^0$
	$\tilde{\chi}_2^0 \tilde{\chi}_2^0$	$\tilde{\chi}_2^0 \rightarrow \ell \ell \tilde{\chi}_1^0$; $\tilde{\chi}_2^0 \rightarrow \nu \tilde{\chi}_1^0$
	$\tilde{\nu} \tilde{\nu}$	$\tilde{\nu} \rightarrow \ell \tilde{\chi}_1^0$
$\ell \ell \ell \dots \mathbf{E}_T$	$\tilde{\chi}_1^\pm \tilde{\chi}_2^0$	$\tilde{\chi}_1^\pm \rightarrow \nu \tilde{\chi}_1^0$; $\tilde{\chi}_2^0 \rightarrow \ell \ell \tilde{\chi}_1^0$
	$\tilde{\chi}_2^0 \tilde{\chi}_2^0$	$\tilde{\chi}_2^0 \rightarrow \ell \ell \tilde{\chi}_1^0$; $\tilde{\chi}_2^0 \rightarrow \ell \ell \tilde{\chi}_1^0$
	$\tilde{\nu} \tilde{\nu}$	$\tilde{\nu} \rightarrow \ell \tilde{\chi}_2^0$, $\tilde{\chi}_2^0 \rightarrow \ell \ell \tilde{\chi}_1^0$
$\ell; 2$	$\tilde{\nu}$	$\tilde{\nu} \rightarrow \ell \tilde{\chi}_2^0$, $\tilde{\chi}_2^0 \rightarrow \ell \ell \tilde{\chi}_1^0$; $\tilde{\nu} \rightarrow \ell \tilde{\chi}_1^\pm$
$\ell j \dots \mathbf{E}_T$	$\tilde{\chi}_1^\pm \tilde{\chi}_2^0$	$\tilde{\chi}_1^\pm \rightarrow \nu \tilde{\chi}_1^0$; $\tilde{\chi}_2^0 \rightarrow q \bar{q} \tilde{\chi}_1^0$
	$\tilde{g} \tilde{g}$	$\tilde{g} \rightarrow q q' \ell \tilde{\chi}_1^\pm$; $\tilde{g} \rightarrow q \bar{q} \tilde{\chi}_1^0$
$\ell \ell j \dots \mathbf{E}_T$	$\tilde{\nu} \tilde{\nu}$	$\tilde{\nu} \rightarrow \ell \tilde{\chi}_1^0$; $\tilde{\nu} \rightarrow \nu \tilde{\chi}_1^\pm$ ($\rightarrow \nu \tilde{\chi}_1^0$)
	$\tilde{\chi}_1^\pm \tilde{\chi}_2^0$	$\tilde{\chi}_1^\pm \rightarrow q q' \tilde{\chi}_1^0$; $\tilde{\chi}_2^0 \rightarrow \ell \ell \tilde{\chi}_1^0$
	$\tilde{g} \tilde{g}$	$\tilde{g} \rightarrow q q' \tilde{\chi}_1^\pm$, $\tilde{\chi}_1^\pm \rightarrow \ell \nu \tilde{\chi}_1^0$
	$\tilde{t} \tilde{t}^*$	$\tilde{t} \rightarrow b \tilde{\chi}_1^\pm$, $\tilde{\chi}_1^\pm \rightarrow \ell \nu \tilde{\chi}_1^0$
$\ell \ell \ell \dots j \dots \mathbf{E}_T$	$\tilde{\chi}_1^\pm \tilde{\chi}_3^0$	$\tilde{\chi}_1^\pm \rightarrow \nu \tilde{\chi}_1^0$; $\tilde{\chi}_3^0 \rightarrow q \bar{q} \tilde{\chi}_2^0$ ($\rightarrow \ell \ell \tilde{\chi}_1^0$)
	$\tilde{g} \tilde{g}$	$\tilde{g} \rightarrow q q' \tilde{\chi}_1^\pm$; $\tilde{g} \rightarrow q \bar{q} \tilde{\chi}_2^0$

decay or any other standard-model process. This is well documented inside CDF (see also Barnet and Hall, 1996). Such events should be taken seriously as potential SUSY candidates.

The most interesting of the anomalous CDF events (Park, 1996; Hohlmann, 1997) is event 129 896 of run 67 581, which has *three* clean, isolated, high- p_T leptons, large \mathbf{E}_T , and a high- E_T jet. In addition, the most energetic of the leptons is a positron with $E_T \approx 200$ GeV, significantly larger than is typical for top events (0.06 ± 0.02 events are expected). The corrected \mathbf{E}_T is over 100 GeV, also large for top decay (0.6 ± 0.1 events are expected). The event contains a jet with $E_T \approx 100$ GeV; the total transverse energy plus \mathbf{E}_T is about 450 GeV. The other two leptons are an electron with $E_T = 27$ GeV and a muon (μ^-) with $p_T = 27$ GeV/ c . The invariant mass of the e^+e^- pair is 130 GeV, well away from M_Z ; the pair has very high p_T . In the standard-model top-quark analysis, the event is classified as a dilepton+two-jet event, because the lower E_T electron fails the fiducial cut by 4 mm and is thus defined to be a jet; however, the electron passes all other standard electron criteria and is a “golden” electron in all other

ways.⁴⁰ The kinematics of the event are unusual: the invariant mass $M_{e\mu j}$ is on the order of m_t , while the other hemisphere contains only the high- E_T positron. The three isolated leptons and the kinematics make the event unlikely to come from standard-model top production and decay. The event is a high-mass tripleton + \mathbf{E}_T event and is consequently a good SUSY candidate (Barnett and Hall, 1996).

Other discrepancies in the top dilepton sample involve the kinematics. Some of the anomalous behavior in the kinematics can be seen in Fig. 22(a), which shows \mathbf{E}_T versus $\Delta\phi$ between the \mathbf{E}_T and the nearest jet or lepton (Hohlmann, 1997; Abe *et al.*, 1997d). Also shown is the distribution expected from Monte Carlo $t\bar{t}$ events, but corresponding to 100 times the luminosity. There are several events out in regions less populated by top-quark events (one is the tripleton event). Figure 22(b) shows the distribution in \mathbf{E}_T significance (Hohlmann,

⁴⁰In the top-quark analysis, the fiducial volume was conservatively chosen to be the same as for the precision electroweak measurement of the ratio of W to Z cross sections. The 4-mm miss does not affect the electron identification.

TABLE XXII. Examples of R -parity-conserving SUSY signatures at the Tevatron: γ 's+ \mathbf{E}_T . In the gravitino lightest-superpartner scenario (GLSP), $\tilde{\chi}_1^0 \rightarrow \gamma\tilde{G}$ always occurs if the x_1^0 is the NLSP. If the decay has a long lifetime (LLG), one of the two $\tilde{\chi}_1^0$ may decay outside the detector. In the Higgsino lightest-superpartner scenario (HLSP), $\tilde{\chi}_2^0 \rightarrow \gamma\tilde{\chi}_1^0$ often occurs.

R -parity-conserving signatures: Photons			
Signature	Production	Decay	Comment
$\gamma\mathbf{E}_T$	$\tilde{\chi}_1^0\tilde{\chi}_1^0$	$\tilde{\chi}_1^0 \rightarrow \gamma\tilde{G}, \tilde{\chi}_1^0 \rightarrow \gamma\tilde{G}$	LLG
$\gamma j\mathbf{E}_T$	$\tilde{Q}\tilde{\chi}_1^0$	$\tilde{Q} \rightarrow q\tilde{\chi}_1^0, \tilde{\chi}_1^0 \rightarrow \gamma\tilde{G}$	LLG
$\gamma jj\mathbf{E}_T$	$\tilde{\chi}_1^+\tilde{\chi}_1^0$	$\tilde{\chi}_1^+ \rightarrow W\tilde{\chi}_1^0, \tilde{\chi}_1^0 \rightarrow \gamma\tilde{G}$	LLG
	$\tilde{\chi}_1^+\tilde{\chi}_2^0$	$\tilde{\chi}_1^+ \rightarrow q q' \tilde{\chi}_1^0, \tilde{\chi}_2^0 \rightarrow \gamma\tilde{\chi}_1^0$	HLSP
$\gamma jjj \dots \mathbf{E}_T$	$\tilde{g}\tilde{g}$	$\tilde{g} \rightarrow q\tilde{Q} \rightarrow q(q\tilde{\chi}_1^+ \rightarrow q(q\tilde{q}\tilde{\chi}_1^0))$	LLG
	$\tilde{Q}\tilde{g}$	$\tilde{Q} \rightarrow q\tilde{\chi}_1^0; \tilde{g} \rightarrow q\tilde{q}\tilde{\chi}_2^0, \tilde{\chi}_2^0 \rightarrow \gamma\tilde{\chi}_1^0$	HLSP
$\gamma b\mathbf{E}_T$	$\tilde{\chi}_1^+\tilde{\chi}_2^0$	$\tilde{\chi}_1^+ \rightarrow \tilde{t}b, \tilde{t} \rightarrow c\tilde{\chi}_1^0; \tilde{\chi}_2^0 \rightarrow \gamma\tilde{\chi}_1^0$	HLSP
$\gamma \ell\mathbf{E}_T$	$\tilde{\chi}_1^+\tilde{\chi}_1^0$	$\tilde{\chi}_1^+ \rightarrow e\nu\tilde{\chi}_1^0, \tilde{\chi}_1^0 \rightarrow \gamma\tilde{g}$	LLG
	$\tilde{\chi}_1^+\tilde{\chi}_2^0$	$\tilde{\chi}_1^+ \rightarrow e\nu\tilde{\chi}_1^0; \tilde{\chi}_2^0 \rightarrow \gamma\tilde{\chi}_1^0$	HLSP
	$\tilde{e}\tilde{\nu}$	$\tilde{e} \rightarrow e\tilde{\chi}_2^0, \tilde{\chi}_2^0 \rightarrow \gamma\tilde{\chi}_1^0; \tilde{\nu} \rightarrow \nu\tilde{\chi}_1^0$	HLSP
$\gamma \ell jj \dots \mathbf{E}_T$	$\tilde{g}\tilde{g}$	$\tilde{g} \rightarrow q q' \tilde{\chi}_1^+ (\rightarrow e\nu\tilde{\chi}_1^0); \tilde{g} \rightarrow q\tilde{q}\tilde{\chi}_2^0, \tilde{\chi}_2^0 \rightarrow \gamma\tilde{\chi}_1^0$	HLSP
$\gamma \ell \ell \mathbf{E}_T$	$\tilde{\chi}_2^0\tilde{\chi}_2^0$	$\tilde{\chi}_2^0 \rightarrow ee\tilde{\chi}_1^0; \tilde{\chi}_2^0 \rightarrow \gamma\tilde{\chi}_1^0$	HLSP
$\gamma \ell \ell jj \dots \mathbf{E}_T$	$\tilde{g}\tilde{g}$	$\tilde{g} \rightarrow q\tilde{q}\tilde{\chi}_2^0, \tilde{\chi}_2^0 \rightarrow ee\tilde{\chi}_1^0, \tilde{\chi}_2^0 \rightarrow \gamma\tilde{\chi}_1^0$	HLSP
$\gamma \gamma jj \dots \mathbf{E}_T$	$\tilde{\chi}_1^+\tilde{\chi}_2^0$	$\tilde{\chi}_1^+ \rightarrow q q' \tilde{\chi}_1^0; \tilde{\chi}_2^0 \rightarrow q\tilde{q}\tilde{\chi}_1^0, \tilde{\chi}_1^0 \rightarrow \gamma\tilde{G}$	GLSP
$\gamma \gamma \ell jj \dots \mathbf{E}_T$	$\tilde{\chi}_1^+\tilde{\chi}_2^0$	$\tilde{\chi}_1^+ \rightarrow e\nu\tilde{\chi}_1^0; \tilde{\chi}_2^0 \rightarrow q\tilde{q}\tilde{\chi}_1^0, \tilde{\chi}_1^0 \rightarrow \gamma\tilde{G}$	GLSP
$\gamma \gamma \ell \ell jj \dots \mathbf{E}_T$	$\tilde{e}\tilde{e}$	$\tilde{e} \rightarrow e\tilde{\chi}_1^0, \tilde{\chi}_1^0 \rightarrow \gamma\tilde{G}$	GLSP
	$\tilde{\chi}_1^+\tilde{\chi}_1^+$	$\tilde{\chi}_1^+ \rightarrow e\nu\tilde{\chi}_2^0, \tilde{\chi}_2^0 \rightarrow \gamma\tilde{\chi}_1^0$	HLSP

1997) versus \mathbf{E}_T for the CDF tau-lepton top sample. None of these latter discrepancies is at a significant statistical level; these will be channels of great interest in Run II.

V. CONCLUSIONS

As can be seen from Table I, there has been a large effort in SUSY searches at the Tevatron. However, given the wide range of possible experimental signatures in the minimal supersymmetric extension of the standard model, there is still work in progress and much to be done. Many Run-I analyses are under way.

Our quantitative conclusions on Run I are reflected in the figures and tables of this review. Here we shall add a few more general qualitative observations:

- (1) A systematic exploration of signatures and channels is just starting. In addition, the detectors have not yet been exploited fully; for example, better c tagging and dijet resolution to investigate final states with reconstructed W and Z bosons may be possible. These tools will allow the study of new channels.
- (2) There are some events involving leptons and/or photons that are provocative and that can be “guideposts” for Run II and further Run-I analyses.

- (3) There is a substantial need for theorists and experimentalists to work together to understand better how to derive and present limits from the Tevatron. We should move on parallel paths toward more “model-independent” predictions and limits (e.g., presenting plots of cross section versus experimentally measured quantities like thresholds) and confront specific models in ways that allow the two experiments to compare results.
- (4) The analyses so far are luminosity limited: the reach of the searches is just entering the interesting regions.

In Run II, two upgraded detectors at the Tevatron will collect more data at a higher energy of 2 TeV. The nominal integrated luminosity is 2 fb^{-1} , with a possible extension to 10 or even 30 fb^{-1} . The production cross sections for heavy sparticles will increase significantly with the higher energy. Chargino and neutralino searches, as well as squark and gluino searches, will cover a wide range of SUSY parameter space in Run II. And, finally, by extending Run II up to an integrated luminosity of about 20 fb^{-1} and combining search channels, the Tevatron can perform a crucial test of the MSSM Higgs-boson sector.

The experience gained from Run-I analyses will greatly increase the quality of the Run-II searches (Ami-

dei *et al.*, 1996a; Amundson, *et al.*, 1997). New triggering capabilities will open up previously inaccessible channels, particularly those involving τ 's and heavy flavor. Increased b -tagging efficiency and E_T resolution will enhance many analyses. A factor of 20 or more data combined with improved detector capabilities makes the next run at the Tevatron an exciting prospect.

ACKNOWLEDGMENTS

The authors would like to thank the following people for useful discussions and comments: H. Baer, A. Beretvas, J. Berryhill, B. Bevensee, S. Blessing, A. Boehnlein, D. Chakraborty, P. H. Chankowski, M. Chertok, D. Claes, R. Demina, J. Done, E. Flattum, C. Grosse-Pilcher, J. D. Hobbs, M. Hohlmann, T. Kamon, S. Lamme, A. L. Lyon, D. Norman, M. Paterno, S. Pokorski, J. Qian, A. Savoy-Navarro, H. C. Shankar, M. Spira, D. Stuart, B. Tannenbaum, X. Tata, D. Toback, C. E. M. Wagner, N. Whiteman, P. Wilson, and P. M. Zerwas. Part of this manuscript was completed at the Aspen Center for Physics.

APPENDIX: DECAY MODES AND SIGNATURES OF SUPERSYMMETRY

Table XVIII lists typical decay modes of supersymmetric particles. Tables XIX, XX, XXI, and XXII list experimental signatures and examples of supersymmetric decays that could lead to the signatures.

REFERENCES

- Abachi, S., *et al.* (DØ Collaboration) 1994, Nucl. Instrum. Methods Phys. Res. A **338**, 185, and references therein.
- Abachi, S., *et al.* (DØ Collaboration), 1995a, Phys. Rev. Lett. **74**, 2632.
- Abachi, S., *et al.* (DØ Collaboration), 1995b, Phys. Lett. B **357**, 500.
- Abachi, S., *et al.* (DØ Collaboration), 1995c, Phys. Rev. D **52**, 4877.
- Abachi, S., *et al.* (DØ Collaboration), 1995d, Phys. Rev. Lett. **75**, 618.
- Abachi, S., *et al.* (DØ Collaboration), 1996a, Phys. Rev. Lett. **76**, 2228.
- Abachi, S., *et al.* (DØ Collaboration), 1996b, Phys. Rev. Lett. **76**, 2222.
- Abachi, S., *et al.* (DØ Collaboration), 1996c, FERMILAB-PUB-96/449-E, hep-ex/9612009 [added in proof, Phys. Rev. D **57** (1998) 589].
- Abachi, S., *et al.* (DØ Collaboration), 1997a, FERMILAB-CONF-97/357-E [added in proof, FERMILAB PUB-98/402e, hep-ex/9902013].
- Abachi, S., *et al.* (DØ Collaboration), 1997b, in *Proceedings of the 28th International Conference on High Energy Physics*, edited by Z. Ajduk and A. K. Wroblewski (World Scientific, Singapore), p. 1469.
- Abachi, S., *et al.* (DØ Collaboration), 1997c, FERMILAB-CONF-97/386-E. [added in proof, FERMILAB PUB-99/029-E, hep-ex/9902028].
- Abachi, S., *et al.* (DØ Collaboration), 1997d, FERMILAB-CONF-97/325-E [added in proof, Phys. Rev. Lett. **15**, 2244].
- Abachi, S., *et al.* (DØ Collaboration), 1997e, FERMILAB-PUB-97/273-E [added in proof, Phys. Rev. Lett. **80** (1998), 442].
- Abbott, B., *et al.* (DØ Collaboration), 1997a, FERMILAB PUB-97/201-E, hep-ex/9705015 [added in proof, Phys. Rev. Lett. **80**, 1591].
- Abbott, B., *et al.* (DØ Collaboration), 1997b, in *Proceedings of the International Europhysics Conference on High Energy Physics*, Jerusalem, edited by D. Lellonch, G. Mikenberg, and E. Rabinović (Springer, Berlin).
- Abe, F., *et al.* (CDF Collaboration), 1988, Nucl. Instrum. Methods Phys. Res. A **271**, 387.
- Abe, F., *et al.* (CDF Collaboration), 1992, Phys. Rev. D **45**, 1448.
- Abe, F., *et al.* (CDF Collaboration), 1994a, Phys. Rev. D **50**, 2966.
- Abe, F., *et al.* (CDF Collaboration), 1994b, Phys. Rev. Lett. **75**, 11.
- Abe, F., *et al.* (CDF Collaboration), 1994c, Phys. Rev. D **50**, 2996.
- Abe, F., *et al.* (CDF Collaboration), 1994d, Phys. Rev. Lett. **72**, 1977.
- Abe, F., *et al.* (CDF Collaboration), 1994e, Phys. Rev. Lett. **73**, 2667.
- Abe, F., *et al.* (CDF Collaboration), 1995a, Phys. Rev. Lett. **74**, 2626.
- Abe, F., *et al.* (CDF Collaboration), 1995b, Phys. Rev. D **52**, 2624.
- Abe, F., *et al.* (CDF Collaboration), 1996a, Phys. Rev. Lett. **76**, 4307.
- Abe, F., *et al.* (CDF Collaboration), 1996b, Phys. Rev. Lett. **76**, 2006.
- Abe, F., *et al.* (CDF Collaboration), 1996c, Phys. Rev. D **54**, 735.
- Abe, F., *et al.* (CDF Collaboration), 1997a, Phys. Rev. D **56**, R1357.
- Abe, F., *et al.* (CDF Collaboration), 1997b, Phys. Rev. D **54**, 357.
- Abe, F., *et al.* (CDF Collaboration), 1997c, Phys. Rev. Lett. **79**, 3819.
- Abe, F., *et al.* (CDF Collaboration), 1997d, Phys. Rev. Lett. , **79**, 3585.
- Ackerstaff, K., *et al.* (OPAL Collaboration), 1998, Phys. Lett. B **433**, 195.
- Alvarez-Guamé, U., J. Polchinski, and M. B. Wise, 1983, Nucl. Phys. B **221**, 495.
- Amaldi, S., W. de Boer, and H. Fürstenau, 1991, Phys. Lett. B **260**, 447.
- Ambrosanio, S., G. L. Kane, G. D. Kribs, S. P. Martin, and S. Mrenna, 1996a, Phys. Rev. Lett. **76**, 3498.
- Ambrosanio, S., G. L. Kane, G. D. Kribs, S. P. Martin, and S. Mrenna, 1996b, Phys. Rev. D **54**, 5395.
- Amidei, D., *et al.* (CDF Collaboration), 1994, Nucl. Instrum. Methods Phys. Res. A **350**, 73.
- Amidei, D., *et al.*, 1996a, "Future Electroweak Physics at the Fermilab Tevatron: Report of the TeV-2000 Study Group," FERMILAB-PUB-96/082.
- Amidei, D., *et al.*, 1996b, "Report of the TeV 2000 Study Group: Light Higgs Physics," FERMILAB-PUB-96/046.

- Amundson, J., *et al.*, 1997, in *New Directions for High-Energy Physics*, edited by D. Cassel, L. Gennari, and R. Siemann (SLAC, Stanford), p. 644.
- Anderson, F., G. D. Castaño, and A. Riotto, 1997, *Phys. Rev. D* **55**, 2950.
- Anselmo, R., L. Cifarelli, A. Peterman, and A. Zichichi, 1991, *Nuovo Cimento A* **104**, 1817.
- Arnowitz, R., A. Chamseddine, and P. Nath, 1984, *Applied N=1 Supergravity* (World Scientific, Singapore).
- Asai, S., F. Cerutti, P. Gris, and W. Orejudos (LEP2-SUSY working group), 1997, LEP2-SUSYWG/97-02.1.
- Azzi, P. (CDF Collaboration), in *'97 Electroweak Interactions and United Theories: Proceedings of the XXXIInd Rencontres de Moriond*, edited by J. Tran Thanh Van (Editions Frontières, Paris), p. 49.
- Baer, H., M. Brhlik, C. Chen, and X. Tata, 1997, *Phys. Rev. D* **55**, 4463.
- Baer, H., C. Chen, M. Drees, F. Paige, and X. Tata, 1997, *Phys. Rev. Lett.* **79**, 986.
- Baer, H., C. Chen, C. Kao, and X. Tata, 1995, *Phys. Rev. D* **52**, 1565.
- Baer, H., C. Chen, F. Paige, and X. Tata, 1994, *Phys. Rev. D* **49**, 3283.
- Baer, H., C. Chen, F. Paige, and X. Tata, 1996, *Phys. Rev. D* **54**, 5866.
- Baer, H., M. Drees, R. Godbole, J. Gunion, and X. Tata, 1991, *Phys. Rev. D* **44**, 725.
- Baer, H., K. Hagiwara, and X. Tata, 1987, *Phys. Rev. D* **35**, 1598.
- Baer, H., C. Kao, and X. Tata, 1993a, *Phys. Rev. D* **48**, 2978.
- Baer, H., C. Kao, and X. Tata, 1993b, *Phys. Rev. D* **48**, 5175.
- Baer, H., C. Kao, and X. Tata, 1995, *Phys. Rev. D* **51**, 2180.
- Baer, H., F. Paige, S. Protopopescu, and X. Tata, 1986, Brookhaven National Laboratory Report No. 38304.
- Baer, H., J. Sender, and X. Tata, 1994, *Phys. Rev. D* **50**, 4517.
- Baer, H., and X. Tata, 1993, *Phys. Rev. D* **47**, 2739.
- Baer, H., X. Tata, and J. Woodside, 1989, *Phys. Rev. Lett.* **63**, 352.
- Baer, H., X. Tata, and J. Woodside, 1990, *Phys. Rev. D* **41**, 906.
- Baer, H., X. Tata, and J. Woodside, 1991, *Phys. Rev. D* **44**, 207.
- Bagger, J. A., 1996, *QCD and Beyond: Proceedings of the Theoretical Advanced Study Institute in Elementary Particle Physics (TASI '95)*, edited by D. E. Soper (World Scientific, Singapore), p. 109.
- Bagger, J. A., S. Dimopoulos, and E. Masso, 1985, *Phys. Rev. Lett.* **55**, 920.
- Bagger, J. A., K. Matchev, and D. Pierce, 1995, *Phys. Lett. B* **348**, 443.
- Barate, R., *et al.* (ALEPH Collaboration), 1997, *Z. Phys. C* **76**, 1.
- Barate, R., *et al.* (ALEPH Collaboration), 1998, *Phys. Lett. B* **418**, 419.
- Barbieri, R., 1988, *Riv. Nuovo Cimento* **11**, 1.
- Barbieri, R., N. Cabbibo, L. Maiani, and S. Petrarca, 1983, *Phys. Lett.* **127B**, 458.
- Barbieri, R., F. Caravaglios, M. Frigeni, and M. Mangano, 1991, *Nucl. Phys. B* **367**, 28.
- Barbieri, R., M. Ciafaloni, and A. Strumia, 1995, *Nucl. Phys. B* **442**, 461.
- Barbieri, R., M. Frigeni, and F. Caravaglios, 1991, *Phys. Lett. B* **258**, 167.
- Barbieri, R., and G. F. Giudice, 1988, *Nucl. Phys. B* **306**, 63.
- Barbieri, R., and L. Maiani, 1989, *Nucl. Phys. B* **243**, 129.
- Bardeen, W. A., M. Carena, T. Clark, K. Sasaki, and C. E. M. Wagner, 1992, *Nucl. Phys. B* **396**, 33.
- Bardeen, W. A., M. Carena, S. Pokorski, and C. E. M. Wagner, 1994, *Phys. Lett. B* **320**, 110.
- Barger, V., M. S. Berger, and P. Ohmann, 1993, *Phys. Rev. D* **47**, 1093.
- Barger, V., M. S. Berger, P. Ohmann, and R. J. N. Phillips, 1994, *Phys. Rev. D* **50**, 4299.
- Barger, V., W. Y. Keung, and R. J. N. Phillips, 1985, *Phys. Rev. Lett.* **55**, 166.
- Barnett, R. M., J. Gunion, and H. Haber, 1993, *Phys. Lett. B* **315**, 349.
- Barnett, R. M., and L. J. Hall, 1996, *Phys. Rev. Lett.* **77**, 3506.
- Bastero-Gil, M., and J. Mercader, 1995, *Nucl. Phys. B* **450**, 21.
- Beenakker, W., R. Hopker, and M. Spira, 1996, preprint hep-ph/9611232.
- Beenakker, W., R. Hopker, M. Spira, and P. M. Zerwas, 1996a, *Z. Phys. C* **69**, 163.
- Beenakker, W., R. Hopker, M. Spira, and P. M. Zerwas, 1996b, *Phys. Rev. Lett.* **74**, 2905.
- Beenakker, W., R. Hopker, M. Spira, and P. M. Zerwas, 1996c, *Nucl. Phys. B* **492**, 51.
- Beenakker, W., M. Kramer, T. Plehn, M. Spira, and P. M. Zerwas, 1998, *Nucl. Phys. B* **515**, 3.
- Berends, F. B., H. Kuijff, B. Tausk, and W. T. Giele, 1991, *Nucl. Phys. B* **357**, 32.
- Bevensee, B. (CDF Collaboration), 1997, in *Quantum Effects in the Minimal Supersymmetric Standard Model: 1st Conference Proceedings* Barcelona, Spain, 1997, edited by J. Sola (World Scientific, Singapore).
- Bhattacharyya, G., 1997, in *Proceedings of the Workshop on Physics beyond the Standard Model: Beyond the Desert, Accelerator and Nonaccelerator Approaches*, Tengenrsee, Germany, June 1997, edited by H. V. Klapdor-Kleingrothaus (Institute of Physics, Bristol), p. 194.
- Bhattacharyya, G., and R. N. Mohapatra, 1997, *Phys. Rev. D* **54**, 4204.
- Brignole, A., J. Ellis, G. Ridolfi, and F. Zwirner, 1991, *Phys. Lett. B* **271**, 123.
- Brun, R., and F. Carminati, 1993, CERN Program Library Long Writeup W5013.
- Carena, M., P. Chankowski, M. Olechowski, S. Pokorski, and C. E. M. Wagner, 1997, *Nucl. Phys. B* **491**, 103.
- Carena, M., P. Chankowski, S. Pokorski, and C. E. M. Wagner, 1998, *Phys. Lett. B* **441**, 205.
- Carena, M., J. R. Espinosa, M. Quirós, and C. E. M. Wagner, 1995, *Phys. Lett. B* **335**, 209.
- Carena, M., M. Olechowski, S. Pokorski, and C. E. M. Wagner, 1994a, *Nucl. Phys. B* **419**, 213.
- Carena, M., M. Olechowski, S. Pokorski, and C. E. M. Wagner, 1994b, *Nucl. Phys. B* **426**, 269.
- Carena, M., S. Pokorski, and C. E. M. Wagner, 1993, *Nucl. Phys. B* **406**, 59.
- Carena, M., S. Pokorski, and C. E. M. Wagner, 1998, *Phys. Lett. B* **430**, 281.
- Carena, M., M. Quirós, and C. E. M. Wagner, 1996, *Nucl. Phys. B* **461**, 407.
- Carena, M., and C. E. M. Wagner, 1994a, in *Proceedings of the 2nd IFT Workshop on Yukawa Couplings and the Origins of Mass*, Gainesville, 1994, edited by P. Ramond (International Press, Cambridge), p. 60.

- Carena, M., and C. E. M. Wagner, 1994b, in *Proceedings of the 2nd IFT Workshop on Yukawa Couplings and the Origins of Mass*, Gainesville 1994, edited by P. Ramond (International Press, Cambridge), p. 85.
- Carena, M. and C. E. M. Wagner, 1995, Nucl. Phys. B **452**, 45.
- Carena, M., P. Zerwas, and the Higgs Physics Working Group, 1996, *Proceedings of Workshop on Physics at LEP2, Vol. 1*, edited by G. Altarelli, T. Sjöstrand, and F. Zwirner, CERN “Yellow” Report No. 96-01.
- Casalbuoni, R., S. de Curtis, D. Dominici, F. Feruglio, and R. Gatto, 1988, Phys. Lett. B **215**, 313.
- Casas, J. A., J. R. Espinosa, M. Quirós, and A. Riotto, 1995, Nucl. Phys. B **436**, 3.
- Chankowski, P., Z. Pluciennik, and S. Pokorski, 1995a, Nucl. Phys. B **439**, 23.
- Chankowski, P., Z. Pluciennik, S. Pokorski, and C. Vayonakis, 1995b, Phys. Lett. B **358**, 264.
- Chertok, M. (CDF Collaboration), 1998, in *Proceedings of the 29th International Conference on High-Energy Physics (ICHEP '98)* (World Scientific, Singapore).
- Choudhury, D., and S. Raychaudhuri, 1997, Phys. Rev. D **56**, 1778.
- Coarasa, J., D. Garcia, J. Guasch, R. Jimenez, and J. Sola, 1998, Eur. Phys. J. C **2**, 373.
- Culbertson, R. L. (CDF and DØ Collaboration), 1998, Nucl. Phys. B, Proc. Suppl. **62**, 47.
- Dai, J., J. F. Gunion, and R. Vega, 1993, Phys. Rev. Lett. **71**, 2699.
- Dai, J., J. F. Gunion, and R. Vega, 1996, Phys. Lett. B **387**, 801.
- Dawson, S., 1996, in *Techniques and Concepts of High-Energy Physics IX: Proceedings, NATO Advanced Study Institute*, 1996, St. Croix, Virgin Islands, NATO-ASI Series B, No. 365, edited by T. Ferbel (Plenum, New York), p. 33.
- Dawson, S., E. Eichten, and C. Quigg, 1985, Phys. Rev. D **31**, 1581, and references on particular signatures given in the following sections.
- Diaz, M. A., 1997a, in *Proceedings of the International Workshop on Quantum Effects in the Minimal Supersymmetric Standard Model*, Barcelona, Spain, edited by J. Sola (World Scientific, Singapore), p. 333, and references therein.
- Diaz, M. A., 1997b, in *Proceedings of the International Europhysics Conference on High-Energy Physics (HEP '97)*, Jerusalem, Israel, edited by D. Lellouch, G. Mikenberg, and E. Rabinović (Springer, Berlin), p. 895.
- Dicus, D., B. Dutta, and S. Nandi, 1997a, Phys. Rev. Lett. **78**, 3055.
- Dicus, D., B. Dutta, and S. Nandi, 1997b, Phys. Rev. D **56**, 5748.
- Diehl, E., C. Kolda, G. L. Kane, and J. D. Wells, 1995, Phys. Rev. D **52**, 4223.
- Dimopoulos, S., M. Dine, S. Raby, and S. Thomas, 1996, Phys. Rev. Lett. **76**, 3494.
- Dimopoulos, S., M. Dine, S. Raby, and S. Thomas, 1997, Phys. Rev. D **55**, 1372.
- Dimopoulos, S., M. Dine, S. Raby, S. Thomas, and J. Wells, 1997, Nucl. Phys. B, Proc. Suppl. **52A**, 38.
- Dimopoulos, S., R. Esmailzadeh, L. J. Hall, and G. D. Starkman, 1990, Phys. Rev. D **41**, 2099.
- Dimopoulos, S., and H. Georgi, 1981, Nucl. Phys. B **193**, 150.
- Dimopoulos, S., S. Raby, and F. Wilczek, 1981, Phys. Rev. D **24**, 1681.
- Dimopoulos, S., S. Thomas, and J. Wells, 1997a, Phys. Rev. D **54**, 3283.
- Dimopoulos, S., S. Thomas, and J. Wells, 1997b, Nucl. Phys. B **488**, 39.
- Dine, M., 1996, in *Supersymmetry Phenomenology (with a Broad Brush)*, lectures given at the Theoretical Advanced Study Institute in Elementary Particle Physics (TASI '96), Boulder, p. 813.
- Dine, M., A. E. Nelson, and Y. Shirman, 1995a, Phys. Rev. D **51**, 1362.
- Dine, M., A. E. Nelson, and Y. Shirman, 1995b, Phys. Rev. D **53**, 2658.
- Done, J. (CDF Collaboration), 1996, in *Proceedings of 1996 Divisional Meeting of the Division of Particles and Fields of the APS*, Minneapolis, edited by H. Heller, J. K. Nelson, and D. Reeder (World Scientific, Singapore), p. 171.
- Drees, M., and S. P. Martin, 1996, in *Electroweak Symmetry Breaking and New Physics at the TeV Scale*, edited by T. L. Barklow, S. Dawson, H. Haber, and J. L. Sigrist (World Scientific, Singapore), p. 146.
- Drees, M., and M. Nojiri, 1992, Phys. Rev. D **45**, 2482.
- Dreiner, H., 1998, in *Perspectives on Supersymmetry*, edited by G. L. Kane (World Scientific, Singapore), p. 462.
- Dreiner, H., and G. Ross, 1991, Nucl. Phys. B **365**, 597.
- Ellis, J., E. Enqvist, D. V. Nanopoulos, and F. Zwirner, 1986, Mod. Phys. Lett. A **1**, 57.
- Ellis, J., J. S. Hagelin, D. V. Nanopoulos, K. Olive, and M. Srednicki, 1984, Nucl. Phys. B **238**, 453.
- Ellis, J., S. Kelley, and D. V. Nanopoulos, 1991, Phys. Lett. B **260**, 131.
- Ellis, J., J. L. Lopez, and D. V. Nanopoulos, 1997, Phys. Lett. B **394**, 354.
- Ellis, J., G. Ridolfi, and F. Zwirner, 1991a, Phys. Lett. B **257**, 83.
- Ellis, J., G. Ridolfi, and F. Zwirner, 1991b, Phys. Lett. B **262**, 477.
- Englert, F., and R. Brout, 1964, Phys. Rev. Lett. **13**, 321.
- Faraggi, A., and B. Grinstein, 1994, Nucl. Phys. B **422**, 3.
- Farrar, G. R., 1984, Phys. Rev. Lett. **53**, 1029.
- Farrar, G. R., 1995, preprint hep-ph/9508291.
- Farrar, G. R., 1997, Nucl. Phys. B, Proc. Suppl. **62**, 485, and references therein.
- Farrar, G. R., and P. Fayet, 1978, Phys. Lett. **76B**, 575.
- Farrar, G. R., and A. Masiero, 1994, hep-ph/9410401.
- Fayet, P., 1975, Nucl. Phys. B **90**, 104.
- Fayet, P., 1977, Phys. Lett. **70B**, 461.
- Fayet, P., 1979, Phys. Lett. **84B**, 416.
- Ferrara, S., J. Iliopoulos, and B. Zumino, 1974, Nucl. Phys. B **77**, 413.
- Flaugher, B., and K. Meier, 1990, in *Research Directions for the Decode: Proceedings of the 1990 Summer Study on High Energy Physics in the 1990s*, edited by E. L. Berger (World Scientific, Singapore), p. 129.
- Gallinaro, M., 1996, Ph.D. thesis (University of Rome).
- Gervais, J. L., and B. Sakita, 1971, Nucl. Phys. B **34**, 632.
- Glashow, S., 1961, Nucl. Phys. **20**, 579.
- Godbole, R. M., and D. P. Roy, 1991, Phys. Rev. D **43**, 3640.
- Gol'fand, Y., and E. Likhtam, 1971, Pis'ma Zh. Eksp. Teor. Fiz. **13**, 452 [JETP Lett. **13**, 323 (1971)].
- Grivaz, J.-F., 1998, in *Perspectives on Supersymmetry*, edited by G. L. Kane (World Scientific, Singapore), p. 179.
- Guasch, J., R. Jimenez, and J. Sola, 1995, Phys. Lett. B **360**, 47.
- Guasch, J., and J. Sola, 1998, Phys. Lett. B **416**, 353.
- Guchait, M., and D. P. Roy, 1996, Phys. Rev. D **54**, 3276.
- Guchait, M., and D. P. Roy, 1997, Phys. Rev. D **55**, 7263.

- Gunion, J. F., H. E. Haber, G. L. Kane, and S. Dawson, 1990, *The Higgs Hunter's Guide* (Addison-Wesley, Reading, Massachusetts).
- Guralnik, G. S., C. R. Hagen, and T. W. Kibble, 1964, *Phys. Rev. Lett.* **13**, 585.
- Haber, H. E., and R. Hempfling, 1991, *Phys. Rev. Lett.* **66**, 1815.
- Haber, H. E., R. Hempfling, and A. H. Hoang, 1997, *Z. Phys. C* **75**, 539.
- Haber, H. E., and G. L. Kane, 1985, *Phys. Rep.* **117**, 75.
- Haber, H. E., G. L. Kane, and M. Quirós, 1986a, *Phys. Lett.* **160B**, 297.
- Haber, H. E., G. L. Kane, and M. Quirós, 1986b, *Nucl. Phys. B* **273**, 333.
- Hall, L., R. Rattazzi, and U. Sarid, 1994, *Phys. Rev. D* **50**, 7048.
- Hempfling, R., 1994, *Phys. Rev. D* **49**, 6168.
- Hempfling, R., and A. Hoang, 1994, *Phys. Lett. B* **331**, 99.
- Higgs, P. W., 1964, *Phys. Rev. Lett.* **12**, 132.
- Higgs, P. W., 1966, *Phys. Rev.* **145**, 1156.
- Hill, C. T., 1981, *Phys. Rev. D* **24**, 691.
- Hill, C. T., C. Leung, and S. Rao, 1985, *Nucl. Phys. B* **262**, 517.
- Hinchliffe, I., 1998, *Eur. Phys. J. C* **3**, 244.
- Hohlmann, M., 1997, Ph.D. thesis (University of Chicago).
- Ibañez, L., and G. G. Ross, 1981, *Phys. Lett.* **105B**, 439.
- Iliopoulos, J., and B. Zumino, 1974, *Nucl. Phys. B* **76**, 310.
- Janot, P., 1997, in *Perspectives on Higgs Physics II*, edited by G. L. Kane (World Scientific, Singapore).
- Jessop, C., 1994, Ph.D. thesis (Harvard University).
- Kalinowski, J., R. Ruckl, H. Spiesberger, and P. M. Zerwas, 1997, *Phys. Lett. B* **414**, 297.
- Kamon, T., J. Lopez, P. McIntyre, and J. T. White, 1994, *Phys. Rev. D* **50**, 5676.
- Kim, S., S. Kuhlmann, and W. M. Yao, 1996, in *Proceedings of the 1996 DPF/DPB Summer Study on New Directions for High Energy Physics*, Snowmass, Colorado, edited by D. G. Cassel, L. Trindle Gennari, and R. H. Siemann (SLAC, Stanford), p. 610.
- Kodaira, J., Y. Yasui, and K. Sasaki, 1994, *Phys. Rev. D* **50**, 7035.
- Kolda, C., 1998, *Nucl. Phys. B, Proc. Suppl.* **62**, 266.
- Langacker, P., and M. X. Luo, 1991, *Phys. Rev. D* **44**, 817.
- Langacker, P., and N. Polonsky, 1993, *Phys. Rev. D* **47**, 4028.
- Langacker, P., and N. Polonsky, 1994, *Phys. Rev. D* **49**, 1454.
- Langacker, P., and N. Polonsky, 1995, *Phys. Rev. D* **52**, 3082.
- Lopez, J., D. Nanopoulos, G. Park, X. Wang, and A. Zichichi, 1994, *Phys. Rev. D* **50**, 2164.
- Lopez, J., D. Nanopoulos, X. Wang, and A. Zichichi, 1993, *Phys. Rev. D* **48**, 2062.
- Lopez, J., D. Nanopoulos, X. Wang, and A. Zichichi, 1995, *Phys. Rev. D* **52**, 142.
- Lykken, J., 1996, in *Introduction to SUSY*, lectures given at the Theoretical Advanced Study Institute in Elementary Particle Physics, Boulder (TASI '96), hep-ph/9612114.
- Maeshima, K. (CDF Collaboration), 1997, in *Proceedings of the 28th International Conference on High Energy Physics*, edited by Z. Ajduk and A. K. Wroblewski (World Scientific, Singapore), p. 1434.
- Maiani, L., 1980, in *Proceedings of the Gif-sur-Yvette Summer School*, edited by R. Barloutand, J. F. Cavaignac, and D. Nanopoulos (Institut National de Physique Nucléaire et de Physique des Particules, Paris).
- Marchesini, G., and B. R. Webber, 1988a, *Nucl. Phys. B* **238**, 1.
- Marchesini, G., and B. R. Webber, 1988b, *Nucl. Phys. B* **310**, 461.
- Martin, S., 1997, in *Perspectives on Supersymmetry*, edited by G. L. Kane (World Scientific, Singapore), p. 1, Secs. 6 and 7.
- Matalliotakis, D., and H. P. Nilles, 1995, *Nucl. Phys. B* **435**, 115.
- Misiak, M., S. Pokorski, and J. Rosiek, 1997, in *Heavy Flavors II*, Advanced Series on Directions in High-Energy Physics, No. 15, edited by A. J. Buras, and M. Lindner (World Scientific, Singapore).
- Mohapatra, R., 1986, *Unification and Supersymmetry* (Springer, Berlin).
- Mrenna, S., 1997a, *Comput. Phys. Commun.* **101**, 232.
- Mrenna, S., 1997b, in *Perspectives on Higgs Physics*, II, edited by G. L. Kane (World Scientific, Singapore).
- Mrenna, S., and G. L. Kane, 1994, preprint hep-ph/9406337.
- Mrenna, S., and G. L. Kane, 1996, *Phys. Rev. Lett.* **77**, 3502.
- Mrenna, S., G. L. Kane, G. D. Kribs, and J. D. Wells, 1996, *Phys. Rev. D* **53**, 1168.
- Nath, P., and R. Arnowitt, 1987, *Mod. Phys. Lett. A* **2**, 331.
- Neveu, A., and J. H. Schwarz, 1971, *Nucl. Phys. B* **31**, 86.
- Nilles, H.-P., 1984, *Phys. Rep.* **110**, 1.
- Okada, Y., M. Yamaguchi, and T. Yanagida, 1991a, *Phys. Lett. B* **262**, 54.
- Okada, Y., M. Yamaguchi, and T. Yanagida, 1991b, *Prog. Theor. Phys.* **85**, 1.
- Olechowski, M., and S. Pokorski, 1995, *Phys. Lett. B* **344**, 201.
- Paige, F., and S. D. Protopopescu, 1986, in *Supercollider Physics: Proceedings of the Oregon Workshop on Super High Energy Physics*, 1985, edited by D. E. Soper (World Scientific, Singapore), p. 41.
- Park, S. (CDF Collaboration), 1996, in *Proceedings of the 10th Topical Workshop on Proton-Antiproton Collider Physics*, AIP Conf. Proc. No. 357, edited by R. Raja and J. Yoh (AIP, Woodbury, New York), p. 240.
- Peoples, J., 1996, letter of January, 1996.
- Pomarol, A., and N. Polonsky, 1994, *Phys. Rev. Lett.* **73**, 2292.
- Raby, S., 1997, *Phys. Rev. D* **56**, 2852.
- Ramond, P., 1971, *Phys. Rev. D* **3**, 2415.
- Rosner, J. L., 1997, *Phys. Rev. D* **55**, 3143.
- Roy, D. P., 1992, *Phys. Lett. B* **283**, 270.
- Salam, A., 1968, in *Elementary Particle Theory*, edited by N. Svartholm (Wiley, New York), p. 367.
- Schmitt, M., 1998, *Eur. Phys. J. C* **3**, 752.
- Sjöstrand, T., 1994, *Comput. Phys. Commun.* **82**, 74.
- Sola, J., 1998, *Nucl. Phys. B, Proc. Suppl.* **66**, 100–103.
- Stange, A., W. Marciano, and S. Willenbrock, 1994a, *Phys. Rev. D* **49**, 2.
- Stange, A., W. Marciano, and S. Willenbrock, 1994b, *Phys. Rev. D* **49**, 1354.
- Stange, A., W. Marciano, and S. Willenbrock, 1994c, *Phys. Rev. D* **50**, 4491.
- Tata, X., 1996, in *QCD and Beyond: Proceedings of the Theoretical Advanced Study Institute in Elementary Particle Physics (TASI '95)*, edited by D. E. Soper (World Scientific, Singapore), p. 163; and Ref. 3 therein.
- Tata, X., 1997, in *Proceedings of the 9th Jorge Andre Swieca Summer School: Particles and Fields*, 1997, Campos do Jordao, Brazil, edited by J. C. A. Barata, A. P. C. Malbouisson, and S. F. Novaes (World Scientific, Singapore), p. 404.
- 't Hooft, G., 1980, in *Recent Developments in Gauge Theories*, edited by G. 't Hooft *et al.* (Plenum, New York), p. 101.

- Treille, D., 1998, plenary talk on searches at LEP, International Conference on High Energy Physics '98 (ICHEP98), Vancouver.
- Valls, J. A. (CDF Collaboration), 1997, in '97 *QCD and High Energy Hadronic Interactions: Proceedings 32nd Rencontres de Moriond*, Les Arcs, edited by Y. Giraud-Heraud and J. Tran Thanh Van (Editions Frontières, Paris), p. 59.
- Veltman, M., 1981, *Acta Phys. Pol. B* **12**, 473.
- Volkov, D., and V. Akulov, 1973, *Phys. Lett.* **46B**, 109.
- Wagner, C. E. M., 1998, *Phys. Lett. B* **441**, 205.
- Wang, J., 1994, Ph.D. thesis (University of Chicago).
- Weinberg, S., 1967, *Phys. Rev. Lett.* **19**, 1264.
- Wess, J., and J. Bagger, 1983, *Supersymmetry and Supergravity* (Princeton University, Princeton).
- Wess, J., and B. Zumino, 1974a, *Nucl. Phys. B* **78**, 39.
- Wess, J., and B. Zumino, 1974b, *Phys. Lett.* **49B**, 52.
- West, P., 1986, *Introduction to Supersymmetry and Supergravity* (World Scientific, Singapore).
- Wilson, K., 1979, as quoted by L. Susskind, *Phys. Rev. D* **20**, 2619.
- Wilson, P. (CDF Collaboration), 1997, in *Proceedings of Les Rencontres de Physique de La Vallée D'Aosta: Results and Perspectives in Particle Physics*, La Thuile, Italy, 1997, edited by M. Greco, Frascati Physics Series No. 9, p. 627.
- Witten, E., 1981, *Nucl. Phys. B* **188**, 513.
- Yao, W. M., 1996, in *Proceedings of the 1996 DPF/DPB Summer Study on New Directions for High Energy Physics* (Snowmass '96), Snowmass, Colorado, edited by D. G. Cassel, L. Trindle-Gennari, and R. H. Siemann (SLAC, Stanford), p. 619.
- Zhu, Q., 1994, Ph.D. thesis (New York University).